

Immunochemistry of mycolic acid antigens in tuberculosis

Vanessa Valerie Roberts

MSc with specialization in Biochemistry

In the Department of Biochemistry
Faculty of Natural and Agricultural Sciences
University of Pretoria

December 2008



I declare that the thesis/dissertation that I hereby submit for the degree in Biochemistry at the University of Pretoria has not previously been submitted by me for degree purposes at any other university.

SIGNATURE: DATE:

Acknowledgements

I would humbly like to thank the following individuals and organizations for their support towards the completion of my MSc. Degree.

Prof J. A. Verschoor, my supervisor, for his guidance and support throughout the duration of the project and writing of the dissertation. For his positive criticism, patience, and consideration on all the ideas and questions I have taxed him with. For always being approachable on any subject.

Dr L. A. Pilcher, my co-supervisor, for assisting with all the chemistry related obstacles of the project as well as creating the opportunity for me to take part and enjoy chemistry discussion groups. For giving guidance on both an academic and personal front.

Dr G. Sekanka, co-supervisor and best friend, for always being there when I needed her most on both a professional and personal level. For never having a dull moment, and especially for her constant encouragement and guidance.

A very special thanks to **Mrs Sandra van Wyngaard** for introducing me to all the biochemical techniques I know and providing a helping hand at any given time. For sharing of her wisdom, friendship, and being someone I could always confide in.

I would also like to thank the **BIA team** for their continuous support and advice as well as **Mr E. Palmer** for his technical assistance in the NMR analysis.

My sincere thanks to the **NRF** for providing the funding which made these studies possible.

Last, but not least, I would like to give my gratitude to every member of **my family** for their love, encouragement, guidance and understanding through all the years of study. To my **friends** for their moral support and understanding and to **Chris**, for his unconditional love and support in every aspect of my life. Thank you.

Table of contents

Acknowledgements	ii
Table of contents	iii
List of figures and tables	viii
List of Abbreviations	x
Summary.....	xiii
Opsomming.....	xv
Chapter 1: Introduction	1
1.1 Etiology of Tuberculosis	1
1.2 Impact of the TB-HIV synergism on world health	2
1.3 Current diagnostics for TB	5
1.3.1 Microbiology.....	5
1.3.2 Molecular diagnostics	6
1.3.3 Phage based tests.....	7
1.3.4 Immunodiagnostics	7
1.3.4.1 Tests based on the cellular immune response.....	7
1.3.4.2 Tests based on the humoral immune response.....	8
1.4 The mycobacterial cell envelope	10
1.4.1 Protein antigens of the <i>M. tb</i> cell wall	12
1.4.2 Glycolipid and lipid antigens of the <i>M. tb</i> cell wall.....	13
1.4.2.1 Acyl trehaloses	13
1.4.2.2 Trehalose dimycolate.....	14
1.4.2.3 Mycolic acid.....	14
1.5. Mycolic acid structure and biological activity.....	15
1.5.1 Mycolic acid structure elucidation.....	15
1.5.2 Distribution of MA subclasses.....	16
1.5.3 Conformation of MA	17
1.5.4 Fine structure of MA defines its biological activity	18

1.6 The structural relatedness between MA and cholesterol	21
<u>Chapter 2: Investigation of the cholesterol nature of mycolic acid using serum antibodies</u>	<u>25</u>
2.1 Introduction.....	25
2.2 Hypothesis.....	27
2.3 Materials	27
2.3.1 Source of sera.....	27
2.3.2 List of reagents and buffers.....	28
2.4 Methods.....	30
2.4.1 Liposome preparation	30
2.4.2 Specificity of serum binding to MA and cholesterol.....	31
2.4.3 Measuring ACHA binding to cholesterol and MA containing liposomes.....	32
2.4.3.1 <i>CELIA</i> using cholesterol liposomes	32
2.4.3.2 <i>CELIA</i> using MA liposomes	32
2.4.4 Using the CELIA assay to assess the nature of the cross-reactive antibody to MA from a TB negative control serum.....	33
2.4.5 Measuring antibody binding from a pooled TB positive patient serum to cholesterol and MA containing liposomes in a CELIA assay	33
2.5 Results	34
2.5.1 Apparent molecular mimicry between MA and cholesterol	34
2.5.2 Specificity of anti-cholesterol antibodies in TB negative control serum.....	35
2.5.2.1 <i>Inhibition of ACHA with cholesterol containing liposomes</i>	35
2.5.2.2 <i>Inhibition of ACHA with MA containing liposomes</i>	37
2.5.3 Nature of the cross-reactive antibody to MA from a TB negative control serum	38
2.5.4 Specificity of antibodies recognising MA in TB positive patient sera	40
2.6 Discussion.....	42
<u>Chapter 3: Analysis of antibody binding to MA liposomes immobilized on a resonant mirror biosensor surface.....</u>	<u>46</u>
3.1 Introduction.....	46

3.2 Hypothesis.....	48
3.3 Materials	49
3.3.1 Source of sera.....	49
3.3.2 List of reagents.....	49
3.3.2.1 <i>Chemicals obtained from Saarchem, a division of Merck, South Africa (unless stated otherwise)</i>	49
3.3.2.2 <i>Chemicals obtained from Sigma, a division of Aldrich, Germany</i>	49
3.3.2.3 <i>Chemicals obtained from other sources</i>	50
3.3.3 List of buffers.....	50
3.4 Methods.....	53
3.4.1 Isolation of IgG from a TB positive and TB negative serum using Protein A Sepharose	53
3.4.2 Removal of glycerol from IgG samples for biosensor and ELISA analysis....	55
3.4.3 SDS-polyacrylamide gel electrophoresis (PAGE) of isolated IgG and depleted serum fractions.....	55
3.4.4 Preparation of MA containing liposomes for biosensor analysis	56
3.4.5 Detection of anti-MA antibody (IgG) with IAsys affinity biosensor	56
3.4.6 Regeneration of non-derivatized cuvettes.....	57
3.5 Results	57
3.5.1 Isolation of IgG from a TB positive and TB negative serum using Protein A Sepharose	57
3.5.2 Biological activity of isolated and purified IgG in ELISA	59
3.5.3 Biological activity of the isolated IgG fractions to MA/PC liposomes measured on a resonant mirror biosensor.....	60
3.5.4 Analysing the inhibition of IgG accumulation onto immobilized MA after pre-incubation with MA/ PC or PC liposomes.....	61
3.6 Discussion.....	63
<u>Chapter 4: Immunochemical analysis of MA subclasses from <i>Mycobacterium tuberculosis</i></u>.....	<u>67</u>
4.1 Introduction.....	67
4.2 Hypothesis.....	69

4.3 Materials	69
4.3.1 Source of sera.....	69
4.3.2 List of reagents and buffers.....	70
4.3.2.1 <i>Chemicals obtained from Saarchem, a division of Merck, South Africa..</i>	70
4.3.2.2 <i>Chemicals obtained from Sigma, Aldrich, Germany ..</i>	71
4.3.2.3 <i>Chemicals obtained from BDH chemicals, England ..</i>	71
4.3.2.4 <i>Other ..</i>	71
4.4 Methods.....	72
4.4.1 Quality considerations	72
4.4.2 Methyl-esterification of MA	73
4.4.2.1 <i>NMR analysis of unesterified MA before methylation</i>	73
4.4.2.2 <i>NMR analysis of the methyl ester of the natural MA mixture (ME-MA) ..</i>	73
4.4.2.3 <i>Calculation to determine the percentage of each subclass present.....</i>	74
4.4.3 Separation of MA subclasses.....	75
4.4.4 Hydrolysis and purification of mycolic acid.....	75
4.4.5 NMR analysis of the separated and purified MA subclasses.....	76
4.4.5.1 <i>NMR analysis of purified α-MA.....</i>	76
4.4.5.2 <i>NMR analysis of purified MeO-MA</i>	76
4.4.5.3 <i>NMR analysis of purified Ket-MA.....</i>	77
4.4.6 Immunological analysis of the natural mixture and separated subclasses of MA	77
4.4.6.1 <i>Coating MAs onto ELISA plates</i>	77
4.4.6.2 <i>ELISA of sera to MA subclasses</i>	78
4.5 Results: Separation and purification of MA subclasses	79
4.5.1.1 Methyl-esterification of MA and separation into the three subclasses	79
4.5.1.2 Hydrolysis and purification of each MA subclass	81
4.5.2 Results: Immunochemical analysis of the purified MA subclasses.....	84
4.5.2.1 Investigation of the free and ME-MA in PBS and hexane	84
4.5.2.2 Antigenicity of MA subclasses when coated from PBS	86
4.5.2.3 Antigenicity of MA subclasses when coated from hexane.....	88
4.6 Discussion.....	89



<u>Chapter 5: General Discussion</u>	<u>92</u>
Conclusion	101
<u>Appendix.....</u>	<u>103</u>
<u>References.....</u>	<u>110</u>

List of figures and tables

Figure 1.1: The estimated incidence of TB during the year 2005	3
Figure 1.2: A new theoretical model for the cell wall	11
Figure 1.3: The structure of the diacyl sulphoglycolipid from <i>M. tb</i>	14
Figure 1.4: General structure of MA	15
Figure 1.5: The most abundant α -, MeO- and Ket-MA subclasses found in <i>M. tb</i>	17
Figure 1.6: Possible arrangement of MA subclasses in the cell envelope of <i>M. tuberculosis</i>	18
Figure 1.7: A hypothetical model of CD1 antigen presentation of mycolic acid	20
Figure 1.8: A predicted folded conformation for MeO-MA representing a possible molecular mimicry with cholesterol	23
Figure 2.1: An example of a MA (MeO-MA) with the “mero” chain folded to interact with the alpha-branch resulting in four hydrocarbon stretches juxtaposed and the polar groups in close proximity.	26
Figure 2.2: The acetylated and methylated α -MA ester.	29
Figure 2.3: Specificity of MA recognition by serum antibodies in ELISA.	35
Figure 2.4: Cholesterol liposomes inhibit the ELISA signal of a TB negative control serum using a CELIA assay	36
Figure 2.5: Determining whether ACHA in TB negative serum cross-react with MA containing liposomes in the CELIA assay	38
Figure 2.6: The nature of the antibodies found in TB negative control serum recognizing MA	40
Figure 2.7: Anti-MA antibodies from TB positive sera do not cross-react with cholesterol containing liposomes in the CELIA assay	41
Figure 3.1: The possible arrangement of MA/ phosphatidylcholine (MA/ PC) liposomes on the modified surface of the IAsys Affinity resonant mirror biosensor	47
Figure 3.2: Non-reduced SDS-PAGE gel indicating the purity of the protein A purified human IgG fraction compared with a standard mouse IgG sample	58

Figure 3.3: Response of serum and isolated IgG fractions to MA and cholesterol in ELISA	59
Figure 3.4: Response of isolated IgG from a TB positive patient and a pooled TB negative serum to MA / PC liposomes on a resonant mirror biosensor	61
Figure 3.5: Percentage inhibition of IgG binding to immobilized MA/ PC liposomes after a pre-incubation of IgG samples with MA/ PC or PC only (empty) liposomes on a resonant mirror biosensor	62
Table 3.1: Summary of ELISA and biosensor results for the TB positive and TB negative sera and IgG fractions	63
Table 4.1: NMR analysis of the whole MA sample before esterification and separation as well as the separated, hydrolysed and purified MA subclasses from <i>M. tb</i> (the 0% indicates that the signals were below the limit of detection in the proton NMR spectra)	80
Figure 4.1: Quantitative analysis of TLC separation of the natural MA mixture A) TLC of the methyl ester of the MA mixture from <i>M. tb</i> B) Versadoc analysis of the spots from which the volume for each spot was given as a % of the total	81
Figure 4.2: Purification of MA after the demethylation process	82
Figure 4.3: Proton NMR of MeO-MA	83
Figure 4.5: Comparison of different coating solutions on antibody recognition of MA and ME-MA in ELISA.	85
Figure 4.6: Antigenicity of MA subclasses when coated from PBS as determined by ELISA.	86
Figure 4.7: The effect of serum dilution in ELISA on antibody binding signals to MAs	87
Figure 4.8: Antigenicity of MA subclasses when coated from hexane as determined in ELISA	89

List of Abbreviations

ACHA	Human anti-cholesterol antibodies
AFB	Acid fast bacilli
AIDS	Acquired immune deficiency syndrome
α-MA	Alpha mycolic acid
AMAME	Acetylated and methylated alpha-mycolic acid ester
AmB	Amphotericin B
APC	Antigen presenting cell
ART	Anti-retroviral therapy
ATCC	American type culture collection
ATPase	Adenosine triphosphatase
BCG	Bacille Calmette-Guérin
CD1b	Cluster of Differentiation 1-b
CD4	Cluster of differentiation four
CD8⁺	Cluster of differentiation eight positive
CELIA	Competitive Enzyme Linked Inhibition Assay
Chol	Cholesterol
CPC	Cetyl pyridinium chloride
DAT	Diacyl trehalose
ddd	Double distilled deionised
DMPC	Dimeristoylphosphatidylcholine
DNA	Deoxyribose nucleic acid
DOTS	Directly Observed Treatment Short Course
DTH	Delayed-type hypersensitivity
ELISA	Enzyme-Linked ImmunoSorbent Assay
Enoyl-ACP	Enoyl acyl carrier protein
FDA	United States of America Food and Drug Administration
HAART	Highly active anti-retroviral therapy
HIV	Human immunodeficiency virus

IgG	Immunoglobulin subclass G
INF-γ	Interferon-gamma
INH	Isoniazid
IRD	Immune reconstitution disease
IreP28	Iron-regulated protein-28
kDa	Kilo Daltons
Ket-MA	Keto mycolic acid
LAM	Lipoarabinomannan
LDL	Low density lipoprotein
LRP	Luciferase reporter phages
MA	Mycolic acid
MAC	<i>Mycobacterium avium</i> complex
MARTI	Mycolic acid Antibody Real Time Inhibition
MCP	Monocyte chemotactic protein
MDR	Multidrug resistance
ME-MA	Methyl ester of mycolic acid
MeO-MA	Methoxy mycolic acid
MHC	Major histocompatibility complex
MOM	Mycobacterial outer Membrane
MRC	Medical Research Council
<i>M. tb</i>	<i>Mycobacterium tuberculosis</i>
MW	Molecular weight
NAA	Nucleic amplification
NMR	Nuclear Magnetic Resonance spectroscopy
NTM	Non-tuberculosis mycobacteria
OPD	O-phenylenediamine dihydrochloride
PAGE	Polyacrylamide gel electrophoresis
PAT	Polyacyl trehaloses
PBS	Phosphate buffered saline
PC	Phosphatidylcholine
PNA	Peptide nucleic acids

PPD	Protein purified derivative
PTLC	Preparative thin layer chromatography
SAS	Statistical Analysis System
SLB	Supported lipid bilayer
SDS	Sodium dodecyl sulfate
TAT	Triacyl trehalose
TB	Tuberculosis
T cell	Thymus derived lymphocyte
TCR	T cell receptor
TBGL	Tuberculous glycolipid antigen
TDM	Trehalose dimycolate
TEMED	N,N,N',N'-Tetramethylethylenediamine
TLC	Thin layer chromatography
TNF-α	Tumor necrosis factor-alpha
Tris	Tris(hydroxymethyl) aminomethane
TST	Tuberculin skin test
VLDL	Very low density lipoprotein
WHO	World Health Organisation
XDR	Extensively drug resistant

Summary

Tuberculosis (TB) is a collective name for the bacterial infection, which is caused by members of the *Mycobacterium tuberculosis* (*M. tb*) complex and can infect the lungs (pulmonary) as well as the kidneys, lymph nodes, bones and joints (extra-pulmonary). The re-emergence of drug-resistant strains and the HIV epidemic are among the main reasons for the resurgence of TB and there is a need for new drugs and diagnostic assays which are rapid and sensitive. Serodiagnostic assays have the potential of being rapid, inexpensive and relatively non-invasive. The most abundant antigen in the cell wall of *M. tb*, which has been analysed with ELISA and resonant mirror biosensor assays for use in serodiagnosis, is mycolic acid (MA). The sensitivity previously obtained in the ELISA assay was however inadequate for serodiagnostic purposes. It was believed that MA mimicked the structure of cholesterol, thereby causing anti-cholesterol human antibodies from TB negative sera to bind to MA and result in a large number of false positives. Within this work the apparent molecular mimicry between MA and cholesterol was investigated using a competitive enzyme linked inhibition assay (CELIA) assay. The results suggested that MA in liposomes resembled the liquid ordered arrangement of cholesterol in liposomes, rather than a direct mimicry of individual molecules. The nature of the antibody from TB negative patient sera binding to MA coated onto ELISA plates was also investigated. The results obtained from this study have not disproved the hypothesis of a cross-reactive anti-cholesterol antibody, but it would appear that the MA signal from TB negative serum was partially due to the binding of anti-MA antibodies. The presence of anti-MA antibodies in TB negative serum could have been the result of prior BCG vaccination, latent infection or due to constant immune stimulation from saprophytic mycobacteria. This creates the potential of using antibodies to MA to distinguish between latent TB infection and active disease. Furthermore, in order to overcome the low sensitivity of the ELISA assay due to high background signals from TB negative serum, members of our group previously developed a resonant mirror biosensor inhibition assay based on MA contained in liposomes. The biosensor measured mass accumulation and the identity of the binding molecules were unknown. It was

shown here that one of the serum components binding to the immobilised MA liposomes in the biosensor inhibition assay was immunoglobulin G antibodies. The specificity of both the ELISA and biosensor assays previously analysed using a natural mixture of MA however, remained poor, and in the search for a more specific antigen, this study investigated the potential of MA subclasses for TB serodiagnosis using ELISA. It was observed that the antibody binding signal to the MA subclasses depended on the polarity of the coating solution, for which hexane was the preferred solvent. Both the alpha- and keto-MA subclasses could better distinguish between a range of TB positive patient and TB negative sera compared with the natural mixture of MA. These results suggested that a particular subclass applied in the biosensor inhibition assay could enhance the test to reach the required sensitivity and specificity required for the serodiagnosis TB.

Opsomming

Tuberkulose (TB) is die bakteriese infeksie wat veroorsaak word deur lede van die *Mycobacterium tuberculosis* (*M. tb*) kompleks en infkteer die longe, asook die niere, bene en gewrigte. Die onlangse globale toename in TB word in deels toegeskryf tot die gesaamentlike her-verskyning van mikobakterië wat weerstandig is tot anti-TB middels en die HIV epidemie. Die her-verskyning van TB het gelei tot die behoefte vir nuwe diagnostieke toetse wat vinniger en meer sensitief is. n' Sero-diagnostiek het die vermoë om met min koste, vinnig resultate te verskaf sonder invallende metodes. Mikoolsuur (MA), is n' antigeen wat volop is in die sel wand van *M.tb*, en is reeds ondersoek met die ELISA asook die biosensor tegniek, vir die doeleinde van n' sero-diagnostiek. Die sensitiwiteit voorheen verkry met die ELISA toets deur die gebruik van mikoolsure, was egter ontoereikend vir sero-diagnose. Die rede vir die lae sensitiwiteit verkry met ELISA is beskryf tot n' ooreenkoms tussen die molekulêre struktuur van MA en cholesterol, wat kan lei tot die kruis-reaktiwiteit van anti-cholesterol teenliggame en wat die groot aantal false positiewe resultate verklaar. Dit is hier onderneem, om die skynbare molekulêre naaboetsing te ondersoek, met die gebruik van n' kompeterende inhibisie toets, genoem CELIA. Die resultate verkry stel voor dat MA in liposome rangskik op so n' manier dat dit die geordende vloeibare fase van cholesterol in liposome gelykstaan, en dat daar nie n' direkte nabootsing van struktuur tussen die individuele molekules is nie. Die eïnskappe van die leenliggaam in TB negatiewe serum wat MA op n' ELISA plaat herken, is ook ondersoek. Alhoewel die resultate verkry, nie die moontlikheid van n' kruis-reaktiewe anti-cholesterol teenliggaam weerlê nie, blyk dit hier dat die anti-MA sein van TB negatiewe serum in ELISA, in deels te beskryf is aan n' anti-MA teenliggaam. Die teenwoordigheid van n' anti-MA teenliggaam in TB negatiewe serum is moontlik die gevolg van n' vorige BCG vaksinasie, onderliggende infeksie of die gevolg van konstante immuun stimulasie deur saprofietiese bakterië. Hierdie verskynsel skep die geleentheid om anti-MA teenliggame te gebruik om onderskeid te tref tussen verborge TB en die aktiewe form van die siekte. Bykomend, lede van ons navorsings groep het onlangs n' biosensor inhibisie toets ontwikkel, gebasseer op MA in liposome, met die doel om die lae

sensitiwiteit van die ELISA te oorkom. Die biosensor meet egter net die verandering in opervlak digtheid en die aard van die molekules wat op die MA liposome akkumuleer, is onbekend. Dit is hier vasgestel dat IgG teenliggame een van die serum komponente is wat MA liposome in die biosensor inhibisie toets bind. Die ELISA en biosensor toetse wat van n' mengsel van mikoolsure gebruik maak, bly steeds te onsensitief vir die doeleinde van sero-diagnose en die enkele MA subklasse is hier met ELISA ondersoek. Dit is waargeneem dat die teenliggaam binding tot die MA subklasse afhanklik is van die polariteit van die oplosmiddel, waarvoor hekasaan die beste resultate verskaf. Beide die alfa- en keto-MA subklasse kon beter onderskeid tref tussen TB positiewe en TB negatiewe sera, in vergelyking met die mengsel van MA. Dus, hierdie resultate lei tot die gevolgtrekking dat die aanwending van n' enkele MA subklas in die biosensor inhibisie toets, die nodige sensitiwiteit en spesifisiteit sal verskaf vir die doel van n' TB serodiagnostiek.

Chapter 1: Introduction

1.1 Etiology of Tuberculosis

Tuberculosis (TB) has plagued civilisations throughout recorded history and has been known amongst other as “phthisis” and “consumption”(1). Franciscus Sylvius used the word “tubercle” to describe the characteristic nodules in lungs of TB patients in 1679 and from there came the name “tuberculosis” (2). The first formal demonstration that TB was contagious was made in 1865 by the French military surgeon, Jean-Antoine Villemin (3), but the causative organism, the non-motile and rod-shaped *Mycobacterium tuberculosis* (*M. tb*), was only isolated and cultured twenty years later (4). There are five mycobacterial species that belong to the *M. tb* complex and include *M. bovis*, *M. tb*, *M. africanum*, *M. microti* and *M. canettii* (5). Other non-tuberculosis mycobacteria (NTM), such as *M. avium*, *M. marinum* and *M. kansasii*, often cause TB-like diseases especially in immune compromised individuals (6).

Tuberculosis is characterised by symptoms of fever, weight loss and the development of a persistent cough (7). Two main forms of TB are recognised: pulmonary and extra-pulmonary TB. Pulmonary TB is the most prevalent form of the disease and is localised to the lung tissue and hilar lymph nodes, while extra-pulmonary TB is characterised by the infection of other regions of the body such as the kidneys, lymph nodes, bones, joints and skin (2). Extra-pulmonary TB represents only 20% of disease cases in HIV-sero-negative individuals, but is four times more prevalent in HIV-sero positive patients (8).

Transmission of *M. tb* has been shown to occur primarily through airborne bacilli usually found in what is known as droplet nuclei (9). Droplet nuclei are formed when organism-bearing particles are exhaled due to coughing, sneezing or speaking and which then vaporise to form a slow settling bacilli-containing particle. Most of the inhaled bacteria settle in the upper respiratory epithelium and are expelled through the ciliary action of the

mucosal system (2). The inhaled bacteria, which reach the respiratory bronchioli, infect resting alveolar macrophages and multiply slowly, with the simultaneous production of inflammatory cytokines and attraction of neutrophils (10). Only after 2-4 weeks after infection (11) do the circulating monocytes and lymphocytes (12) enter the site of infection. A granuloma (primary lesion) starts to form in order to contain the pathogen and prevent further growth and dissemination of the mycobacteria (13). Mature granulomas have been shown to consist of infected macrophages surrounded by mononuclear phagocytes, foamy macrophages, a mantle of lymphocytes and an outer fibrous wall (12). In most immuno-competent individuals the granuloma will eventually calcify or maintain a thick fibrous layer in which only a few mycobacteria can survive for decades without causing active TB (14). This persistent state of infection is known as latent tuberculosis in which no clinical signs of TB exists other than a positive result for the tuberculin skin test (TST) (15) or tuberculosis specific interferon-gamma (IFN- γ) test (16).

During active TB the granuloma fails to contain the mycobacterial infection and caseation of its core leads to the breakdown of the restricting wall and subsequent bacterial transmission (5). The development of TB is the result of the inability to contain the primary infection or due to reactivation of latent TB (11). The risk of developing active disease is highest in the first two years after infection and has been estimated to develop in about 10% of infected individuals (17). Reactivation of latent TB can occur due to extreme physical or psychological stress, malnutrition or due to a suppressed immune system (15).

1.2 Impact of the TB-HIV synergism on world health

Tuberculosis remains the leading infectious human disease with 8.8 million new cases being reported and 1.6 million lives being claimed annually (18). It has been estimated that one third of the world population is latently infected with *M. tb*. Although there has been a global decline in TB since 2002, it is still on the increase in Africa, the Eastern Mediterranean and South-East Asia regions (figure 1.1).

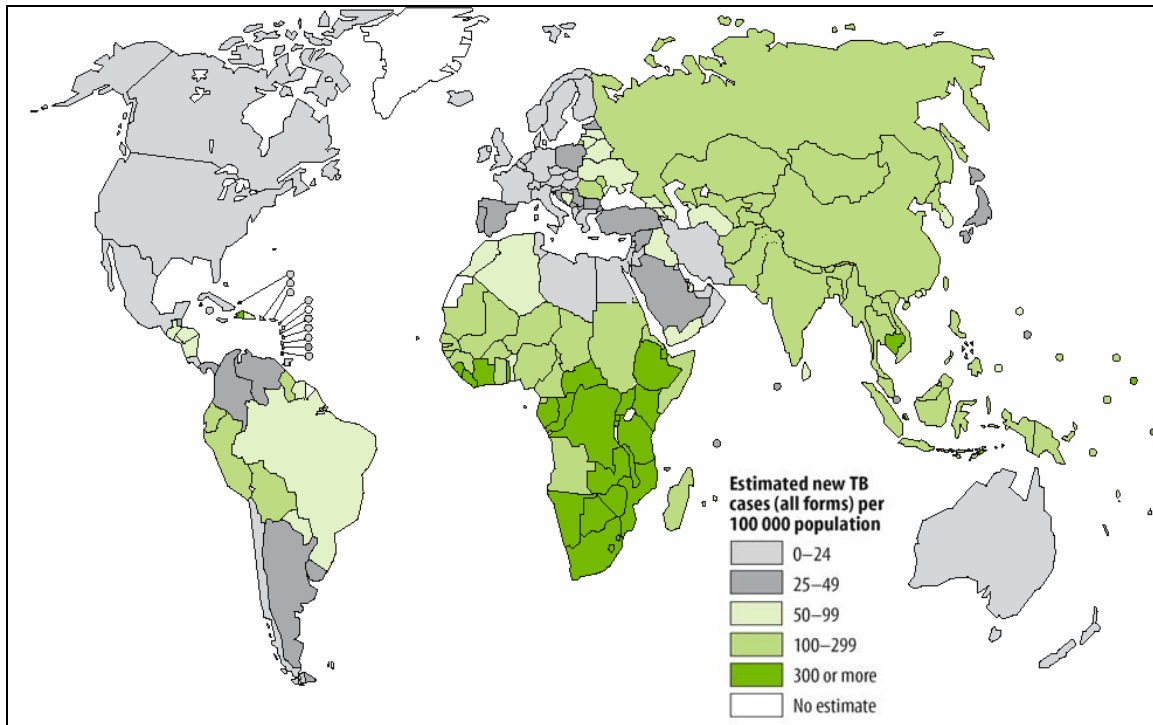


Figure 1.1: The estimated incidence of TB during the year 2005 (19).

Control strategies, such as DOTS (Directly Observed Treatment Short course) (20), were launched soon after the World Health Organization declared TB a global emergency (21). The targets set out by the TB control strategy were to detect 70% of new smear positive cases and to cure 85% of those. The inability to achieve the targets initially set out lead to the implementation of further strategies such as the Stop TB strategy, which aims at reducing TB prevalence to 50% by the year 2015, relative to the year 1990 (22).

The major constraints in the fight against TB include the development of multidrug-resistance and the HIV epidemic (23). The emergence of drug resistant strains has been attributed in part to improper prescriptions and the non-compliance of patients to TB treatment regimens (24,25). Multidrug-resistance (MDR) is defined as the resistance of *M. tb* to two of the first line drugs, isoniazid and rifampicin, while extensively drug resistant (XDR) TB is characterised by the resistance to two first line drugs as well as any of the second line drugs amikacin, kanamycin, or capreomycin (26). In 2006 there was an

outbreak of XDR-TB in South Africa which claimed the lives of 52 of the 53 TB patients within only 25 days (22). All of the deceased patients tested positive for HIV.

The co-infection of HIV increases the chance of developing TB from 5-10% in a lifetime to 5-15% within a year (22). People infected with HIV are particularly susceptible to TB, either by progression of primary infection or reactivation of latent *M. tb* infection (27). It has however been shown that HIV/AIDS co-infected individuals taking anti-retroviral therapy (ART), decreased the incidence of tuberculosis by 70-90% (28,29). It would thus appear that adequate distribution of ART within HIV prevalent areas strongly contributes to the reduction of the incidence of TB. There is however complications which have made this seemingly easy approach a daunting one.

First of all, the administration of highly active anti-retroviral therapy (HAART) in patients co-infected with *M. tb*, often results in immune reconstitution disease (IRD) (30). Immune reconstitution is the consequence of the restoration of the white blood cell count upon commencement with HAART. The host immune response becomes aware of previously “unmasked” infections and reacts vigorously, but without compensatory immunoregulatory mechanisms. In order to prevent the development of IRD, early detection and treatment of mycobacterial infections is essential.

The diagnosis of *M. tb* infection and disease in HIV/AIDS patients poses another complication. The culturing from sputum samples for diagnosis of TB is ineffective in HIV/AIDS patients, because of problems in producing adequate sputum samples (31). Furthermore, the immune cells expressing the cluster of differentiation four (CD4) marker is reduced, and the ability to form granulomas is impaired, making diagnosis by X-ray chest radiographs inaccurate (30,32). Many diagnostic tests, such as the tuberculosis specific INF- γ test, depend on active CD4 cells and are impaired in patients with advanced immune suppression (16).

The TB/ HIV synergism is apparent also at the molecular level in which HIV co-infection is accelerated concurrent with the development of TB (32). The increased replication of

the HIV virus is in part due to the release of tumour necrosis factor-alpha (TNF- α), which is a major cytokine produced during *M. tb* infection (33). Infection with *M. tb* has also been shown to cause the production of monocyte chemotactic protein (MCP), which results in increased transcriptional activity of the HIV virus (34).

Thus, the TB/ HIV synergism has created the requirement for rapid diagnostic TB tests, which are not influenced by the CD4 cell count and do not rely on mycobacterial culture and radiographic analysis.

1.3 Current diagnostics for TB

One of the major challenges in TB control is to be able to diagnose, predict and treat those who are latently infected before the onslaught of active disease (35). It has also become necessary to distinguish between *M. tb* and NTM infections which are more prevalent in immune-compromised individuals. Furthermore, with the increase in MDR- and XDR-TB, drug susceptibility testing is required to administer the correct treatment strategies. All of the above mentioned factors have emphasised the need for new or improved diagnostic assays in the fight against tuberculosis.

Among the current diagnostics available are the chest radiographs, which have been shown to have low diagnostic specificity (36). The limitation of radiographs is that the majority of pulmonary infections are unapparent in most HIV co-infected individuals (37). The culture and smear microscopy, molecular diagnostics and immunological methods are more relevant as diagnostic techniques in HIV-infected individuals and will be discussed in more detail here.

1.3.1 Microbiology

One of the first bacteriological evidences for the presence of mycobacteria is the staining of sputum smears. Staining can be done either with carbol fuchsin dye with subsequent destaining with acid alcohol, or the use of fluorescent auramine phenol (38). Microscopy is rapid and takes 1 day, but is only used for a preliminary confirmation of mycobacterial

infection (17). Although a positive smear stain for acid fast bacilli (AFB) is an indicator of advanced infectious disease (39), it requires the presence of between 5000-10,000 bacilli per ml sample, is not very sensitive and cannot distinguish between *M. tb* and NTM infections (40). In order to overcome the problem of species identification, peptide nucleic acids (PNA) have been developed (38). The PNA are composed of DNA with a peptide backbone and can be visualised using fluorescent labels. All of the smear tests however still lack sensitivity.

Currently the gold standard for TB diagnosis remains the culture of mycobacteria from either sputum or body fluid specimens (40), because it is one of the most sensitive (80-85%) and specific (98%) diagnostic methods that can discriminate between mycobacterial species and simultaneously determine the drug susceptibility (17). The limitations of the culture technique are that i) it is time consuming and can take up to 8 weeks to exclude active TB, ii) has reduced efficacy in children (17), and iii) is often a problem in HIV infected individuals who do not produce adequate sputum samples (31). Although culture methods have been improved to be able to give conclusive results within only 1-3 weeks, these systems require expensive laboratories that are problematic for low-income countries (41).

1.3.2 Molecular diagnostics

Molecular diagnostics were developed not for the purpose to replace conventional culture based tests, but rather to serve as complementary tools (40). Two commercially available nucleic acid amplifications (NAA) tests, the Amplified *Mycobacterium tuberculosis* Direct test (MTD test, Gen-Probe, San Diego, USA) and Cobas Amplicor *M. tuberculosis* assay (Roche Diagnostics, Mannheim, Germany) have been approved by the U.S. Food and Drug Administration (FDA) for the direct detection of mycobacteria in sputum samples. Initially these tests were only recommended for the use on smear positive samples, but an advanced Gen-Probe assay has now been approved for respiratory specimens regardless of smear status and has a reported sensitivity of 77-88% and specificity of 100% (40). The advantage of the molecular techniques is that they allow

direct detection and identification of *M. tb* with as little as 10 bacilli (17). New molecular techniques are constantly under investigation, which strive to obtain greater sensitivity and reduce the reaction time (42). One of the major drawbacks of the molecular techniques is that they still require the retrieval of specimen from the site of infection, which is particularly difficult in the case of extrapulmonary TB and in children (43).

1.3.3 Phage based tests

Phage based tests also depend on specimen retrieval, but do not require mycobacterial culture. These tests are based on the principal that *M. tb* complex specific phages multiply within live mycobacteria from a specimen and after 24-28 hours phage multiplication is measured (44). Phage replication is measured either as the production of light by luciferase reporter phages (LRP) or by the ability of progeny phages to form plaques on cultured plates of helper cells (45,46). The commercial phage tests currently available are the FASTPlaque[®] TB and PhageTek[®] MB assays and although the specificity is high (83-100%) and cost is low, the sensitivity of these assays remain inadequate (21-88%) to replace culture and microscopy analysis (41).

1.3.4 Immunodiagnosics

Immunological methods use specific humoral or cellular responses to infer the presence of infection or disease (43). Such immunological assays are attractive alternatives for diagnosis because they do not depend on the detection of mycobacteria and specimens from the site of infection and have the added potential to diagnose extrapulmonary TB (36).

1.3.4.1 Tests based on the cellular immune response

The tuberculin skin test is currently the most widely used method to indicate infection with *M. tb* (17). The TST assay is based on the fact that specific T cells sensitised during prior infection are recruited to antigen exposed skin where a delayed-type hypersensitivity (DTH) reaction develops. The skin reaction is usually measured 2-3 days

after administration of the test antigen (47). The current antigen mixture used for the TST test is the protein purified derivative (PPD). The PPD is prepared from culture filtrate of tubercle bacilli by protein precipitation and consists of small proteins, polysaccharides and lipids (48). A limitation of the TST test based on PPD is that it cannot distinguish between a previous vaccination with Bacille Calmette-Guérin (BCG), latent infection, and active disease (49). Furthermore, it has limited efficacy in HIV/AIDS patients and people vaccinated against yellow fever (17). The low specificity of the TST test is due to the use of antigens which are common to other mycobacteria. In an attempt to improve on the TST skin test, Lyashchenko *et al.* (50) investigated the use of a multi-antigen cocktail, which contained antigens specific for the *M. tb* complex. Specificity was greatly improved but the other limitations were not circumvented.

Another immunodiagnostic assay that is based on the cellular immune response to exposed antigen is the IFN- γ assay. One such test, the quantiFERON-TB gold assay (QTF-G, Cellestis) was approved by the FDA in 2004 for the detection of *M. tb* infection (51). The quantiFERON-TB Gold assay measures the amount of IFN- γ released after blood is incubated with synthetic antigens. The overall sensitivity of the IFN- γ assay ranges between 64-89% with specificity of 89% and is more sensitive than the TST test, but still cannot distinguish between active and latent tuberculosis (35). The INF- γ assay is however less affected by prior BCG vaccination (52,53) and shows higher sensitivity in children (54) and HIV-positive individuals when compared to the TST test (55).

1.3.4.2 Tests based on the humoral immune response

Serological tests based on detecting antibodies are promising in that they are rapid, simple, inexpensive and relatively non-invasive and have the potential to distinguish between latent infection and active disease (36). Serodiagnostic test are, however, affected by the immune status of the individual (56). Many different serological assays have been investigated, but none have managed to reach the required $> 80\%$ sensitivity and $> 95\%$ specificity set out by the World Health Organization (57). A problem that serological tests face is the heterogeneity between sera to the same antigens (50).

It was proposed that the use of multiple antigens could alleviate serum heterogeneity and increase sensitivity (36) and current serological tests have been developed based on single and multiple antigen mixtures of protein, lipids or a combination of both (50,58,59,60,61,62,63,64). Lipoarabinomannan (LAM) was one of the first non-protein antigens investigated for serodiagnosis of TB (65). A dipstick test has been developed based on detecting antibodies to LAM, called the Mycodot assay, but which has been shown to be ineffective in an HIV setting (66). In order to overcome the limitations posed by detecting serum antibodies, researchers have developed an assay based on direct detection of LAM in the urine of TB patients (67). Detection of the urine based LAM has shown to be very effective in an HIV setting, giving 80% sensitivity and 99% specificity (68) and appears to correspond to bacterial load, which could be used to monitor treatment progress.

Another promising serological test is based on a mixture of hydrophobic glycolipids, the tuberculous glycolipid antigen (TBGL) antigen (62). The sensitivity and specificity of the assay using the TBGL antigen has been shown to be 81% and 95.7% respectively and could diagnose active pulmonary and extrapulmonary TB. The TBGL based test could however not make the distinction between *M. tb* and opportunistic NTM infection, because it is not a species specific antigen (69). One way to circumvent mycobacterial cross-reactivity of the TBGL serodiagnostic test would be to combine it with the *M. avium* complex (MAC) specific test (70). The efficacy of these assays in a HIV burdened population has not yet been demonstrated.

Recently, the major mycobacterial cell wall lipid, MA has also been investigated for its potential in serodiagnosis of TB (64,71,72). Not only are MAs species specific (73), but they also differ from other mycobacterial lipids in that antibodies to MA have been shown to be maintained in HIV sero- positive individuals despite the severity of the disease (63). An Enzyme-Linked ImmunoSorbent Assay (ELISA) based on detecting antibodies to MA had limited sensitivity and specificity but was improved when using the methodology of a resonant mirror biosensor to detect antibodies (72). The sensitivity obtained with the biosensor assay using MA as antigen, was 86.7% and specificity was

76.9%. The biosensor assay has thus shown good potential as a serodiagnostic assay for TB in HIV burdened populations, but the affordability and reliability still has to be proven in low income and high TB incidence regions (72).

1.4 The mycobacterial cell envelope

The intracellular survival of *M. tb*, as with the other pathogenic mycobacteria, depends to a large extent on the unusual physiochemical properties of the mycobacterial cell surface (74). The impermeability of the cell envelope is thought to be one of the reasons behind drug resistance. The most effective drugs are those that inhibit synthesis of some of its components (75). Many of the cell envelope lipids, polysaccharides and proteins are species specific (76) and are also attractive targets for use in TB diagnostic assays. Although the absolute structure of the cell envelope is still unclear, it is known that the envelope is not a static entity, but rather a dynamic structure which is altered in response to growth phase and environmental conditions of the mycobacteria (77).

The mycobacterial cell envelope consists of three main layers: the cytoplasmic membrane, the cell wall and the capsule (78). The mycobacterial cytoplasmic membrane appears to resemble a typical bacterial membrane while the capsule, which appears to be limited to the pathogenic mycobacteria, contains polysaccharides and excreted proteins (79). Over the past thirty years much research has gone into establishing the structure of the cell wall and current models describe the cell wall as being asymmetric and to consist of an inner segment of MAs attached to a peptidoglycan-arabinogalactan scaffold and an outer segment of non-covalently associated lipids and proteins (80,81). However, recent evidence (82) confirms the indications of Imaeda *et al.* (83) and Klegermann *et al.* (84), that the outer layer of the cell wall is actually a lipid bilayer, referred to as the Mycobacterial outer Membrane (MOM). The outer membrane appears to be approximately 8 nm in diameter, which coincides with the size and presence of outer membrane proteins, such as porins (85). The previously identified extractable lipids of the cell wall, such as glycolipids and phospholipids (86,87,88), are thought to form the

basis for the MOM and to be tethered to the lower lying MA complex in an as yet unknown manner.

The most recent evidence of Hoffmann *et al.* (82) also shows the region representing the mycolate layer as being smaller in size than the currently predicted 9 nm (89,90). It has been shown that MAs can assume compact conformations in monolayers, approximately ± 3 nm in length (91,92), and it has been proposed that MAs also assume compact conformations in the cell wall of *M. tb* (61). It could be for this reason that the mycolate layer appears to be smaller than expected.

Based on the recent findings of an outer lipid bilayer and a smaller mycolate layer (82), I propose a new theoretical cell wall model for *M. tb* (figure 1.2), in which some subclasses of MA fold into compact conformations to form the thin and compact mycolate layer, while the remaining MAs extend into the MOM (containing extractable lipids, polysaccharides and proteins), to tether it to the rest of the cell wall. It is further proposed that the more deeply imbedded extractable lipids, such as TDM and TMM (87,93), are intercalated between the MAs below the MOM and do not form part of the outer lipid bilayer.

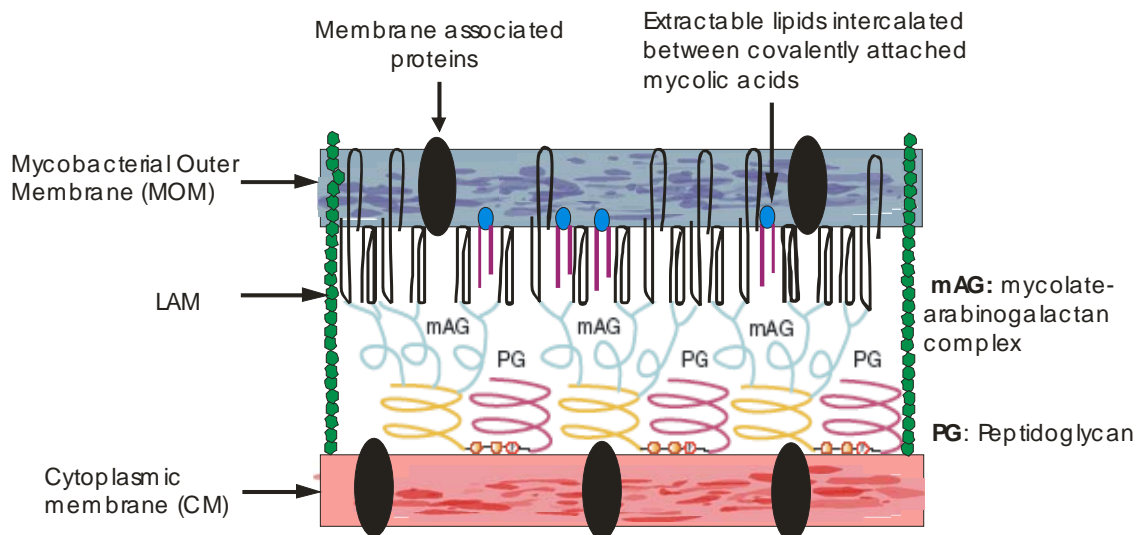


Figure 1.2: A new theoretical model for the cell wall of *M. tb*. Polar and non-polar MAs are attached perpendicular to the arabinogalactan-peptidoglycan complex. The extended MAs tether the outer mycobacterial membrane to the rest of the cell wall, while TDM and TMM intercalate between the folded MAs which form the thin, electron transparent layer, below the outer lipid bilayer (82, 86, 94).

1.4.1 Protein antigens of the *M. tb* cell wall

Most antigenic proteins to date identified from *M. tb* are excreted proteins in culture filtrates (95) or cytoplasmic (96) and plasma membrane proteins (97). The isolation of cell wall protein is more cumbersome than isolation from the above mentioned fractions, because mycobacterial peptidoglycan is not cleavable by lysozyme and release of cell wall proteins thus requires disruption with trifluoromethanesulfonic acid from SDS-extracted protein fractions (98). Protein antigens isolated from the *M. tb* cell wall include the 71 kDa, 60 kDa, 45 kDa, 28 kDa, 23 kDa proteins, and an iron-regulated protein (Irep28).

The 71 kDa cell wall protein isolated by Dhiman and Khuller (98) was found to be an immunodominant antigen when compared to the 60 kDa and 45 kDa antigens isolated from the *M. tb* cell wall. The less antigenic 60 kDa and 45 kDa proteins were not investigated further, but the 71 kDa protein was found to resemble other 70 kDa heat shock proteins from *M. leprae* (99) and had ATPase activity (98). Based on the T cell and antisera responses from mice immunised with whole cell lysates and individual proteins, the 71 kDa protein was found to be more effective than the currently used BCG vaccine strain. The 71 kDa protein thus has good potential as a candidate for a subunit vaccine and has also shown potential in a diagnosis for tuberculous meningitis (100).

In 1990, Hirschfield *et al.* (101) described the isolation of another cell wall protein, an extremely hydrophobic 23 kDa protein. The 23 kDa protein was also analysed for antigenicity and good responses were obtained from the antisera of rabbits immunised with the whole bacteria. However, no further immunochemical analysis on this protein has been performed and the use of this protein in vaccines and diagnosis remains to be shown.

Recently, an iron-regulated protein of 28 kDa was isolated from the mycobacterial cell wall (102). This protein was subsequently designated Irep28 and reacted with antibodies from tuberculosis patients. The Irep28 antigen is specific for the *M. tb* complex and is a promising candidate for diagnosis of tuberculosis.

1.4.2 Glycolipid and lipid antigens of the *M. tb* cell wall

1.4.2.1 Acyl trehaloses

The triacyl trehaloses (TAT) are trehalose esters of which the 2, 3, and 6-positions are esterified to stearic, palmitic and mycolipenic acyl substituents (103). An antigenic 2, 3, 6-triacyl trehalose was only discovered in 1997 and subsequently shown to have a possible function in the diagnosis of active tuberculosis (104). The tri-methyl-branched fatty acid substituents of the TAT are limited to the virulent strains of the *M. tb* complex, but the species specific acyl chains are not the epitopes recognised by antibodies, implying that a serodiagnostic test based on this antigen would not be able to distinguish between *M. tb* and NTM bacterial infections.

A diacyl trehalose (DAT) (105) identified as being antigenic and to be recognised by antibodies from tuberculosis patients was the 2, 3-diacyl trehalose sulfate (106). This antigen was later reinvestigated and was shown not to be a sulfolipid, but a 2, 3-diacyl trehalose (107). The DAT has been investigated for its use in the serodiagnosis of TB and found to give one of the highest specificities (88-100%), but the sensitivity in ELISA has never reached more than 52% (108,109). This antigen has the further complication that the antigenic epitope is not species specific and would not be able to distinguish between TB and NTM infections.

Of the acyl trehaloses which contain a sulfate group, the sulfolipids, only one has been shown to be antigenic (110). The diacyl sulfoglycolipid (figure 1.3) was shown to be presented on cluster of differentiation 1b (CD1b) molecules of antigen presenting cells (APC) and was capable of stimulating specific CD8⁺ T cells. The diacyl sulfoglycolipid is currently being investigated for its potential use as a vaccine, but has not been investigated for the diagnosis of TB.

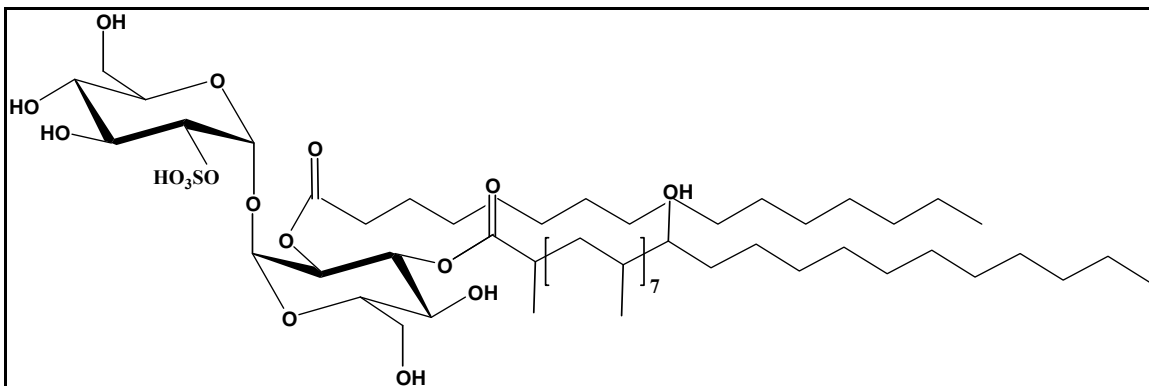


Figure 1.3: The structure of the diacyl sulphoglycolipid from *M. tb* containing palmitic acid and hydroxyphthioceranoic acid as acyl substituents and a sulphate moiety on the 2nd position of trehalose (110).

1.4.2.2 Trehalose dimycolate

The polar glycolipid, trehalose-6, 6'-dimycolate (TDM) is a deeply imbedded extractable cell wall lipid, initially known as cord factor (111). TDM consists of trehalose, to which any two MA subtypes are attached. It has a large repertoire of biological activity, some of which depend on the route of administration (112). One of the first major indications of the antigenicity of TDM was its ability to form tubercles in the lungs of mice indistinguishable from tubercles induced by BCG infection (113). Since then, it has been shown that TDM can stimulate the proliferation of specific T cell clones (114) and antibodies to TDM (115), or a glycolipid preparation containing TDM (62) is useful in the serodiagnosis of TB. The major epitope of TDM has subsequently been shown to be the attached MAs (116).

1.4.2.3 Mycolic acid

Mycolic acids represent 40-60% of the dry weight of the mycobacterial cell wall (117) and are present in all bacteria of the Mycolata family. The α -alkyl, β -hydroxy long chain lipids are attached as clusters of four onto the terminal penta-arabinofuranosyl residues of the arabinogalactan (76), and are the only components of the arabinogalactan-peptidoglycan-mycolate layer that have been proven to be antigenic (118). It was with MA that it was first shown that a subset of T cells could recognise lipid antigens when

presented on CD1 molecules (119,120). Antibodies to MA have subsequently been detected in the serum of tuberculosis patients (121), but with a sensitivity not yet accepted for a serodiagnostic assay (64,72). Mycolic acids remain good antigens for investigation because they are generally species specific, their profiles change between the different growth stages of *M. tb* (122) and they could thus possibly be used to distinguish between latent and active disease.

1.5. Mycolic acid structure and biological activity

1.5.1 Mycolic acid structure elucidation

It was Stodola *et al.* (123) who named the hydroxy acid present in all of the wax fractions of the tubercle bacillus and other acid fast bacteria, “Mycolic acid”. From that point forward, researchers have set out to determine the structure of this lipid (124). It was shown that MA had a basic structure of $R^2CH(OH)CH(R^1)COOH$ (figure 1.3) in which R^1 represents an alkane branch ($C_{22}-C_{24}$) and R^2 an alkyl chain ($C_{30}-C_{60}$) containing different functional groups (125).

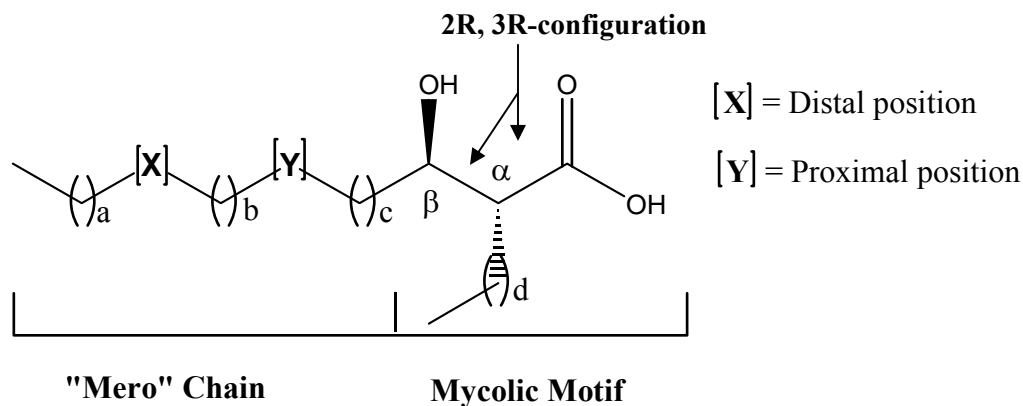


Figure 1.4: General structure of MA. The alkyl chain attached to the α -position is termed the alpha branch and is part of the mycolic motif, which is common to all MAs. The Meromycolate chain, from here on referred to as the “mero” chain, contains functional groups at positions X and Y. The inter-chain lengths are depicted by the letters a, b, c and d and vary within and between mycobacterial species. The stereochemistry of the α - and β -positions is common to all MAs and is in the 2R, 3R-configuration (124).

Mycolic acids are common to the genera *Mycobacteria*, *Nocardia*, *Corynebacteria*, *Dietzia*, *Rhodococcus*, *Gordonia*, *Williamsia*, *Skermania* and *Tsukamurella* (73). The major difference between the MA from the different genera is the difference in overall chain lengths, but MAs also differ with regards to the intra-chain lengths between the functional groups, as well as the identity of the functional groups present in the “mero” chain (126). Overall, the MAs form a family of approximately 500 intimately related chemical structures which was initially identified to be a single compound (123).

The MAs from the genus *Mycobacterium* are the longest MAs known and range between C₆₀-C₉₀ in chain length (73). In 2001 and 2002, the methyl esters of MA from 24 representatives of *M. tb*, *M. bovis*, *M. microti*, *M. Kansasii*, and *M. avium* were separated and it was determined that the “mero” chain usually contains two functionalities, and rarely three (127,128). Based on the different functionalities present in the “mero” chain, MAs are divided into subclasses. The MAs containing only desaturation or *cis*-/ *trans*-cyclopropane rings are referred to as alpha-MA (α -MA). The oxygenated MAs are characterised by having either a methyl ether (methoxy-MA), carbonyl (keto-MA), epoxide (epoxy-MA) or ester (wax ester MA) functionality in the distal position of the “mero” chain (X, figure 1.4) and either *cis*-/ *trans*-double bonds or *cis*-/*trans*-cyclopropane rings at the proximal position (Y, figure 1.4). A characteristic of the *trans*-double bonds, *trans*-cyclopropane rings and oxygenated functionalities, is that they all have an adjacent methyl branch (128).

1.5.2 Distribution of MA subclasses

The α -MA is present in all mycobacteria analysed to date, but the methoxy-MA (MeO-MA) appears to be limited to the pathogenic mycobacteria with the exception of 5 species (126). The keto-MA (Ket-MA) and epoxy-MA subclasses do not appear to be restricted by pathogenicity. The three MA subclasses present in *M. tb* are the α -, MeO-, and Ket-MA (129). Each subclass represents a homologous series of at least 7 related compounds of which the most dominant species are represented in figure 1.5 (127,128).

The exact quantity present of each subclass in the mycobacterial cell wall differs between species and growth conditions, but overall the alpha: oxygenated MA remains in an approximate 1: 1 ratio. The average percentage subclass composition of *M. tb* grown on agar plates is 57% of α -MA, 33% of MeO-MA and 11% of Ket-MA (130). It has however been shown that *M. tb* entering a state of dormancy accumulates α -MA and almost completely stops producing Ket-MA (131), while *M. tb* grown in vivo in macrophages, produces increased amounts of Ket-MA (25%) and α -MA, but approximately two fold less MeO-MA (132).

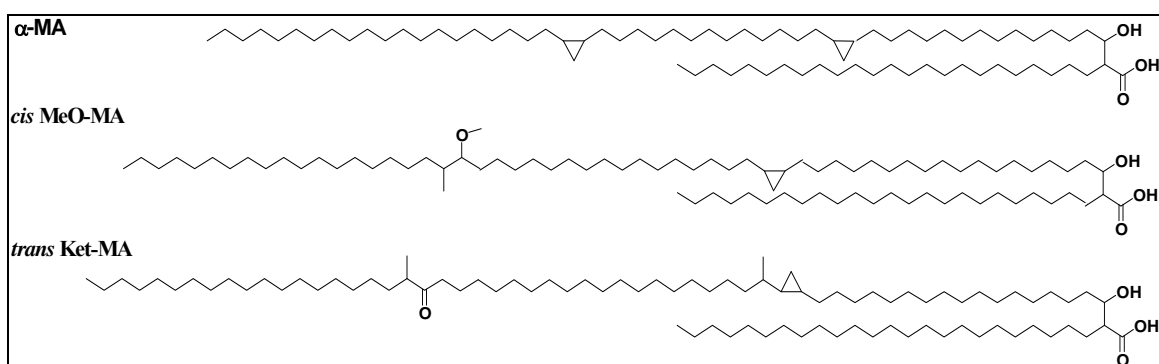


Figure 1.5: The most abundant α -, MeO- and Ket-MA subclasses found in *M. tb* (128).

1.5.3 Conformation of MA

Apart from the fine chemical structure, it has been shown that MA subclasses also assume different conformations in compressed monolayers (91,133), and these conformations have been postulated to exist within the mycobacterial cell wall (fig 1.6) (61). In the temperature dependent studies of monolayer packing of MA it was found that the Ket-MA subclass preferred a condensed conformation, termed the “W” shape, in which the “mero” chain together with the α -branch (figure 1.6) folded to form four alkyl stretches juxtaposed to one another (61,91).

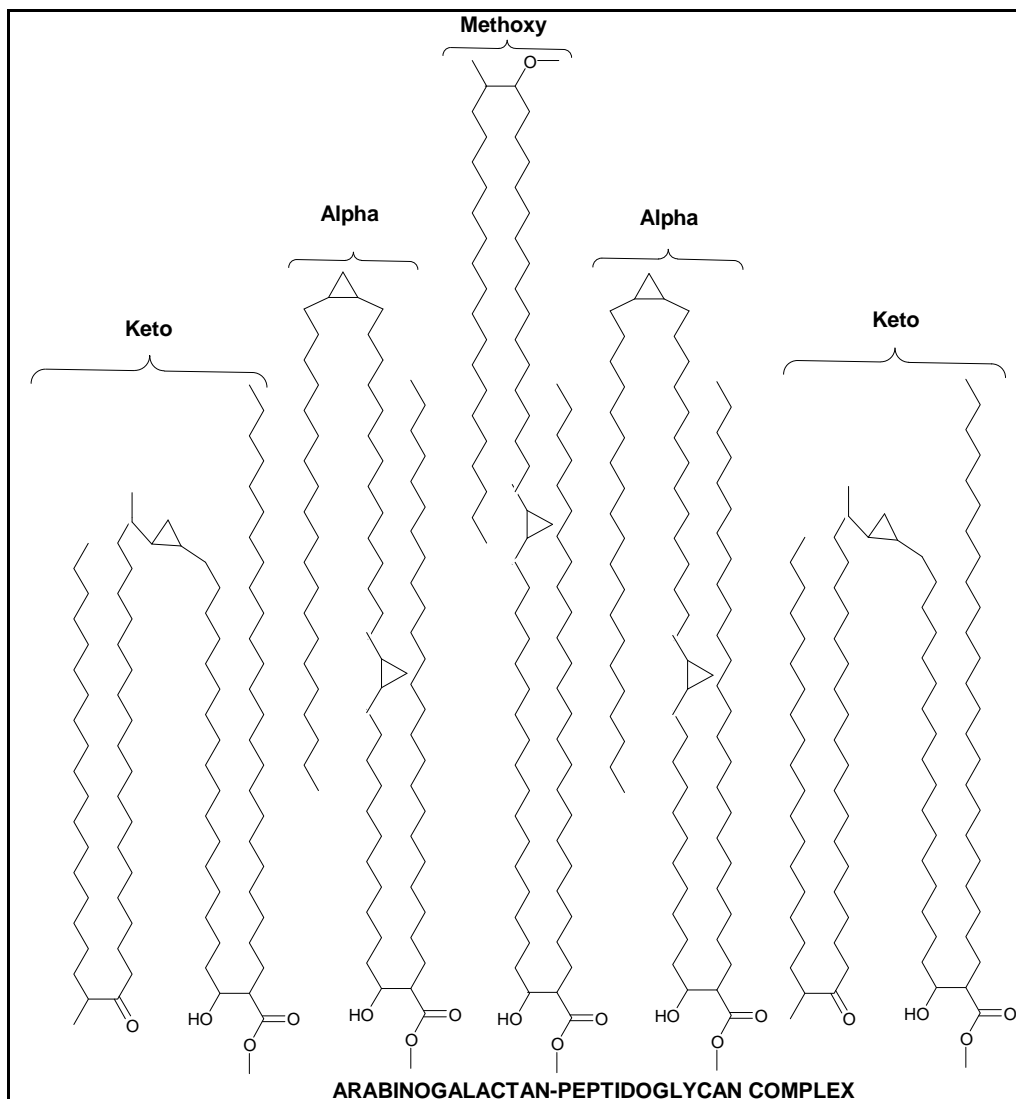


Figure 1.6: Possible arrangement of MA subclasses in the cell envelope of M. tuberculosis (61).

The MeO-MA appeared to favour a “W” conformation at low temperature and a more relaxed conformation at elevated temperatures. The α -MA subclass generally prefers the more relaxed conformations, which can either have the three arms form a curved hydrophobic surface, or in which the arms are extended (61,91,92).

1.5.4 Fine structure of MA defines its biological activity

The determining role of MA in the impermeability and integrity of the mycobacterial cell wall was illustrated in a mutant of *M. smegmatis*, which failed to produce the long chain

fatty acids (90). These mycobacteria, deficient in synthesising long chain MA, had an altered cell wall in which the electron transparent region, characteristic of the mycolate layer, was absent and the cell wall was thermally unstable and permeable to hydrophobic drugs. Each MA subclass appears to have a distinct role to play in cell wall function. A mutant *M. tb* strain producing only α -MA had a more rigid and impermeable cell wall (134), while a mutant producing increased amounts of Ket-MA with respect to MeO-MA, had a more fluid cell wall (130). From these studies it became apparent that the fluid state and integrity of the cell wall of each Mycobacterium is determined by the MA composition. Individual functionalities, such as the distal cyclopropanation, have been shown to increase resistance to killing by reactive oxygen species (135) and proximal cyclopropanation affects fluidity of the cell wall (136). In addition, the avirulent strain of *M. tb* produces substantially more MAs with three functional groups in the “mero” chain, overall shorter MA chains and no *trans*-double bonds. Of the *M. bovis* BCG strains, only the Tokyo strain appears to produce a substantial amount of MeO-MA (73), while the other attenuated strains only produce trace amounts of the MeO-MA subclass (127), which may imply an important role of MeO-MA in virulence.

The structure of MA has also been shown to influence the presentation of the antigen to host immune cells. Mycolic acid is presented by professional APC on CD1b molecules, a class of molecules dedicated to lipid and glycolipid presentation (119). The structure of the CD1 molecule is such that it contains a deep groove lined with hydrophobic amino acids in which the long acyl chains are accommodated (137), allowing the hydrophilic moiety of MA to interact with CD1 restricted T cells in an aqueous environment (138). The arrangement of the polar functionalities on MA in close approximation for recognition by the TCR is said to form a “combinatorial epitope” (139). A hypothetical model for MA binding to the CD1 molecules is depicted in figure 1.7.

The possibility that chain length or functional group composition plays a role in CD1 presentation came from the results of Beckman *et al.* (119), who showed that the long chain MAs from *M. kansasii* and *M. tb* could stimulate T cells, but not the shorter MA from *M. smegmatis* or *M. phlei*.

Combinatorial epitope

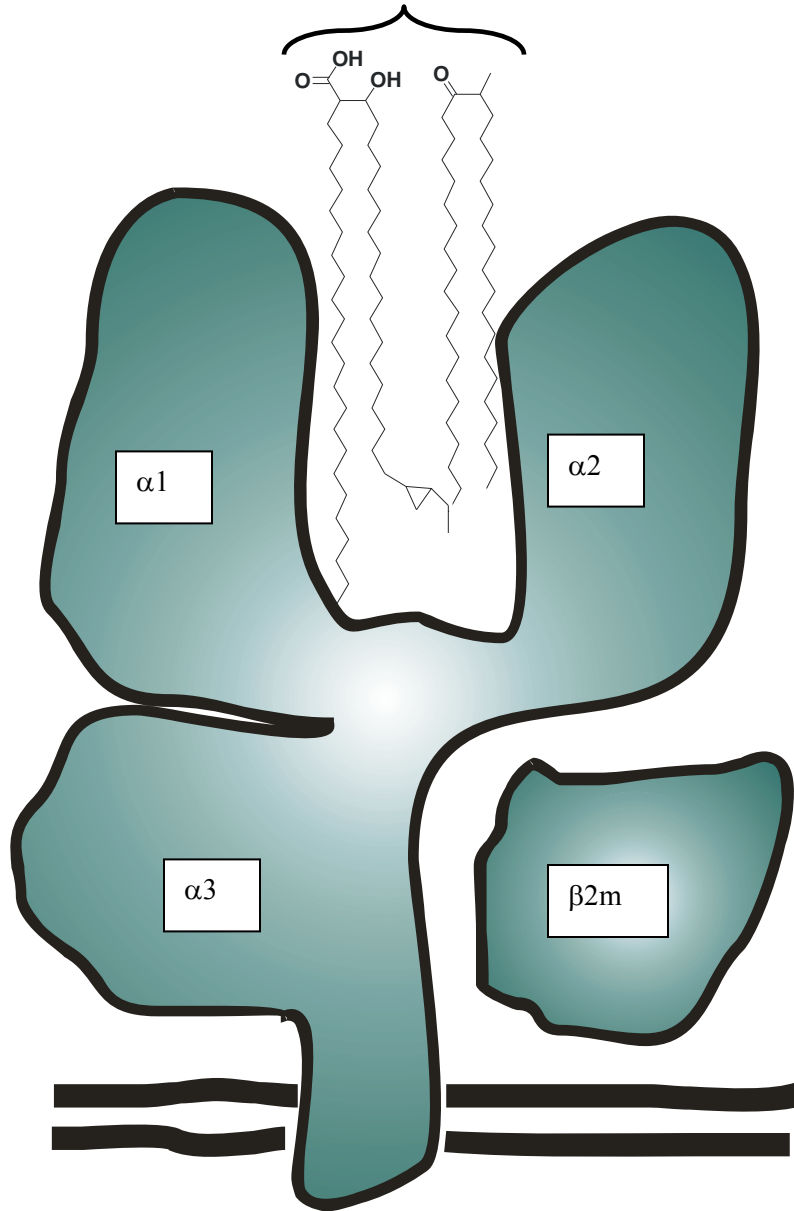


Figure 1.7: A hypothetical model of CD1 antigen presentation of mycolic acid. The two extra cellular domains $\alpha 1$ and $\alpha 2$, form a hydrophobic pocket hypothesised to accommodate the acyl chains of MA, while the polar groups of MA possibly form a combinatorial epitope, which is exposed to the aqueous environment to interact with CD1 restricted T cells

It has generally been accepted that the cellular immune system, rather than antibodies, plays the important role in host defence against *M. tb*. The CD1 restricted T cells recognising lipid and glycolipid antigens are the $CD4^+CD8^- \alpha\beta^+$ T cells (119), $CD4^+CD8^-$

$\gamma\delta^+$ T cells (120), $CD8^+ \alpha\beta^+$ T cells (140), and recently also $CD4^+$ T cells (141,142). It has also been shown that the CD1 restricted T cells kill infected macrophages and secrete cytokines characteristic of a Th1 response (143). However, antibodies to *M. tb* antigens have been identified, and there is a strong suspicion that the humoral immune system may also play a role in the host defence mechanism (144). Antibodies produced in rabbits after immunising the animals with TDM, recognised the methyl esters of MA as antigenic epitopes (116). It has further been reported that the IgG rabbit antibodies could even distinguish between the subclasses of MA from *M. tb*. The greatest response of the antibodies was to the MeO-MA subclass. It was subsequently reported that antibodies present in TB patients could also recognise the methyl ester of MA and again, the MeO-MA appeared to be the most antigenic subclass (121). The antibody response to MA from TB positive patients was subsequently shown by Schleicher *et al.* (64) not to be affected by the HIV sero-positive status of the patients. The mechanism of antibody production to lipid antigens is not yet understood, but the fact that anti-MA antibodies are maintained in immune compromised individuals, suggests that their titres are not affected by decreasing CD4 T cell counts (64). A serodiagnostic assay based on detecting antibodies to MA, and possibly a particular MA subclass, could hold potential especially in HIV-burdened populations.

1.6 The structural relatedness between MA and cholesterol

The low specificity obtained when analysing for antibodies to MA in ELISA (64) was described to be due to the high background responses of TB negative patients to MA. It was postulated that the hydrophobic MA surface captured cholesterol from the serum, which in turn would result in anti-cholesterol antibodies present in all human individuals, (145) binding to the ELISA plate to give false positive values. The possible accumulation of cholesterol onto the MA lipid coat could either be due to non-specific hydrophobic association or due to specific interactions emanating from the agreement in possible conformational features between the two molecules.

In an attempt to increase the sensitivity and specificity of an assay based on detecting antibodies to MA, a different technique to ELISA, was analysed. A resonant mirror biosensor was tested for its ability to detect antibodies to MA (71). Mycolic acids were immobilised on the surface of the biosensor cuvettes in liposomes containing phosphatidylcholine (PC), with cholesterol added for stabilisation. It was observed that TB patient sera bound equally well to liposomes containing MA and those without. Again, two possibilities existed, i) serum bound non-specifically to the PC/ cholesterol liposomes or ii) there was a cross-reactivity of serum between MA and cholesterol. The apparent cross-reactivity of serum was subsequently confirmed in ELISA. These results lead to the hypothesis that molecular mimicry existed between MA and cholesterol and a folded structure for the MeO-MA subclass was proposed, which could be envisaged to resemble cholesterol (Figure 1.8). The proposed MA structure was equivalent to the “W” shape recently predicted to exist within Langmuir monolayers for MeO-MA (91).

Based on the results of Siko (71), and the possibility of a molecular mimicry between MA and cholesterol, it was investigated whether cholesterol-binding molecules could aid in the cell wall penetration of the anti-TB drug, isoniazid (INH) (146). Because of the concept of a cholesterol nature of MA, it was thought that would compete with MA precursors in the process of cell wall renewal, and therefore retard the multiplication of *M. tb* in BACTEC culture. This was found not to be the case. Contrary to what was expected, cholesterol reduced the efficiency of the INH drug. From the knowledge that INH inhibits an enzyme synthesizing MA, it was hypothesized that the “molecular mimic”, cholesterol, bound to the enzyme before the drug could. Interestingly, the enzyme for INH is part of the steroid dehydrogenases family of enzymes (146). These results led to the hypothesis that the MA substrate for the enoyl-ACP reductase enzyme, mimicked cholesterol.

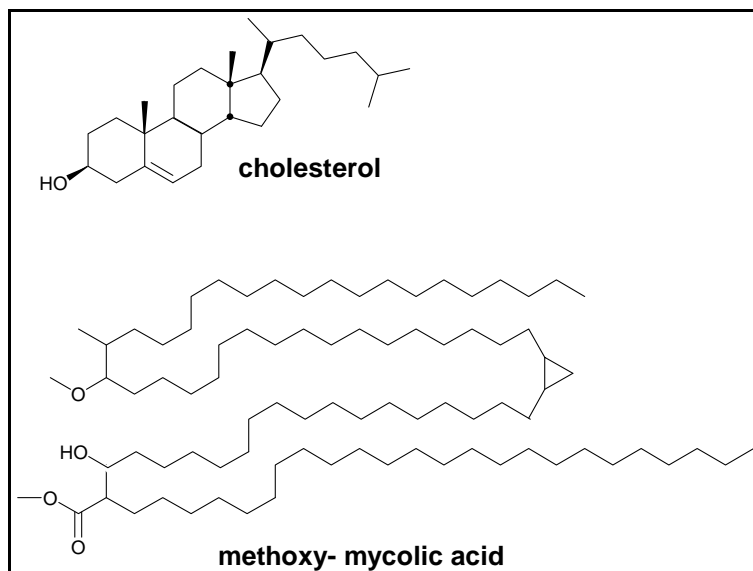


Figure 1.8: A predicted folded conformation for MeO-MA representing a possible molecular mimicry with cholesterol (71).

The first direct evidence of a structural relatedness between MA and cholesterol was provided by Deysel (147), who measured the direct interaction between MA and cholesterol liposomes on the resonant mirror biosensor. This was done before by Siko (71), but in order to confirm that the interaction between the lipid containing vesicles was not just due to hydrophobic Van der Waals interactions, appropriate negative controls were used in which functional entities, possibly involved in specific hydrogen bonding, were blocked. The results indicated that the MA-cholesterol liposome interactions were specific and depended on the ability of MA to assume a particular folded conformation. From the specific interaction between MA and cholesterol it was concluded that MA in liposomes has a cholesteroloid nature.

To further give direct support for the idea of a cholesteroloid nature of MA, Benadie (148) analysed the interaction of the anti-fungal macrolide, Amphotericin B (AmB), with both MA and cholesterol. Amphotericin B is known to bind to cholesterol and was subsequently also shown to interact specifically with MA. The interaction of AmB with both MA and cholesterol indicated that MA shared structural features with cholesterol.

The above results supported the hypothesis of a cholesterol nature of MA, but not that of molecular mimicry. In order to prove molecular mimicry between two compounds, it needs to be shown that both molecules are recognised by an established binding agent, which indicates resemblance in the three-dimensional structure. The congruence of antibody titres from whole sera to MA and cholesterol (71), could have been due to two or more unrelated antibodies binding to the respective antigens, and not one single entity that was cross-reacting. Furthermore, the results of Sebajane (146) gave no direct evidence of cholesterol binding to the enoyl-ACP reductase active site. The results provided by Deysel (147) indicated that the MA and cholesterol association was specific, but this does not imply that the three-dimensional structures are identical. In addition, sterol molecules are thought to interact with AmB by i) specific hydrogen bonding with the macrolide amino-sugar group and ii) through hydrophobic association of the planar sterol with the conjugated double bonds of AmB (149). The fact that the MA-AmB interaction resembles that of cholesterol-AmB binding implies that MA assumes a conformation which is similar in rigidity to that of cholesterol, and has the same specificity of hydrogen bonding. However, AmB is not necessarily a reporter of the three dimensional structure of either of the molecules and cannot be used to infer molecular mimicry.

Thus, this study set out here to determine whether MA mimics cholesterol using antibodies as reporters of three dimensional structure, and whether anti-cholesterol antibodies were responsible for the binding seen to MA from TB negative patient sera in ELISA. It was also investigated whether antibodies were the serum components binding to MA liposomes on the resonant mirror biosensor, giving greater sensitivity than that obtained with the ELISA assay. Last, but not least, it was investigated whether a particular subclass of MA would better be able to distinguish between TB positive and TB negative serum populations in ELISA, rather than the mixture of MA previously used.

Chapter 2: Investigation of the cholesterol nature of mycolic acid using serum antibodies

2.1 Introduction

Mycolic acids are the major cell wall constituents of *M. tb* (150), and antibodies to MA have recently been investigated as surrogate markers for tuberculosis (64,116). MAs are attractive antigens because they are generally species specific (126) and elicit antibodies that are maintained in HIV individuals (64). The detection of anti-MA antibodies in patient sera as indicator of active TB using the ELISA assay (64), could however not match the sensitivity obtained when detecting antibodies against TDM, a cell wall associated lipid containing MA (63). There was also a lack of specificity, which manifested as the recognition of MA by antibodies from TB negative patient sera. The serum component responsible for this possible cross-reactivity of TB negative serum was thought to be an anti-cholesterol antibody, as the response of sera to cholesterol and MA was indistinguishable (71). For anti-cholesterol antibodies to cross-react with MA, there would have to be some structural relatedness between MA and cholesterol.

One method to investigate a structural relatedness between two substances is by measuring the recognition of the two substances by an established binding agent. Recently members of our group have shown that there is a structural relatedness between MA and cholesterol by showing that an established cholesterol binding macrolide, AmB, also binds to MA (148). The binding between AmB and MA was further shown to be specific. The fact that MA bound more to AmB than cholesterol, could have been due to MA assuming a more planar arrangement than cholesterol (149), and exposing the hydrophilic moiety for hydrogen bonding with AmB.

The folding of MA into different conformations has been studied by Villeneuve *et al.* (91) and in one such conformation the “mero” chain folds to interact with the alpha-

branch to give four parallel, interacting hydrocarbon stretches with the polar functions on the mero-chain in close approximation to the β -hydroxy and carboxyl head (fig 2.1).

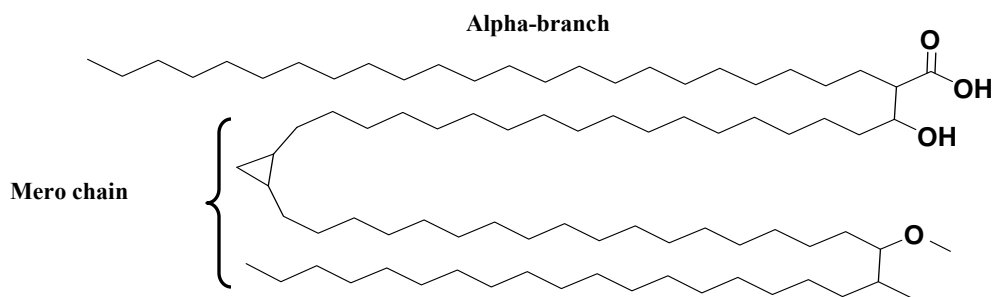


Figure 2.1: An example of a MA (MeO-MA) with the “mero” chain folded to interact with the alpha-branch resulting in four hydrocarbon stretches juxtaposed and the polar groups in close proximity.

The conformation in which the four hydrocarbon stretches are parallel has been termed the “W” shape (61) and was envisioned by Siko (71) to be the conformation which resembles cholesterol. Other conformations for MA also exist (91), but it is not yet known which of these conformations is responsible for the interaction of MA with the cholesterol binding agent, AmB, or whether the interaction is restricted to a specific MA subclass.

Another method for analysing the structural relatedness between cholesterol and MA is with the use of antibodies. Antibodies can recognise a single molecule or some arrangement of molecules either as shapes or surfaces (151). Antibodies may thus be good reporters of structure and structural arrangement.

Antibodies to cholesterol were first induced in mice in 1988 by the group of Swartz *et al.* (152) by immunizing with liposomes containing 71 mol % cholesterol. It was found that the anti-cholesterol antibodies recognised cholesterol in liposomes in a concentration dependent manner, as tested by the ability of antibodies to induce immune damage. The greatest immune damage was caused by anti-cholesterol antibodies elicited against liposomes containing a molar ratio of cholesterol above 56 mol %. Subsequently, anti-cholesterol antibodies have been identified to exist in the sera of all people (145). It would appear that the human anti-cholesterol antibodies (ACHA) (153) recognise a

similar epitope as the anti-cholesterol antibodies produced in mice, which is defined by the concentration of cholesterol in a lipid environment. Human anti-cholesterol antibodies have been shown to recognise some arrangement of cholesterol absorbed onto ELISA plates as well as high concentrations of cholesterol (>50 mol %) contained in very low and low density lipoprotein (VLDL and LDL) particles (153,154). The anti-cholesterol antibodies have also been shown to be able to recognise specific structural attributes such as the 3 β -hydroxy group and to cross-react with cholesterol analogues containing that functional group (153,155).

This study set out to determine whether liposomes containing different concentrations of cholesterol would be recognised by ACHA and whether these antibodies could also recognise MA contained in liposomes. Each analysis was performed using an inhibition assay on ELISA, normally referred to as the Competitive Enzyme Linked Inhibition Assay (CELIA). It was then assessed whether ACHA were the cross-reactive antibodies from TB negative serum recognising MA coated onto ELISA plates.

2.2 Hypothesis

The structural relatedness between cholesterol and MA is dependent on some structural arrangement of MA within lipid vesicles or on the surface of ELISA plates rather than direct molecular mimicry.

2.3 Materials

2.3.1 Source of sera

For the experiment determining the specificity of serum binding to MA and cholesterol in ELISA, TB positive human sera were selected from a pulmonary TB positive collection stored at -80°C that was made in 1994 by the MRC Clinical and Biomedical TB Research Unit at King George V Hospital, Durban, KwaZulu-Natal and donated by Dr PB Fourie and. The TB neg/ HIV negative sera were selected from a collection of sera made in the

year 2000, initially for another study by Schleicher *et al.* (64). These TB negative patients were hospitalised for various reasons other than TB or AIDS.

For the CELIA experiments determining whether AHCA recognises cholesterol and MA containing liposomes, the sera of six healthy individuals were pooled to constitute a TB negative control serum. The individuals were from the Biochemistry Department at the University of Pretoria, South Africa, working in research groups other than the TB research team. The individuals showed no clinical signs of tuberculosis and their HIV status was not known.

The CELIA experiment determining the nature of the antibodies from the TB negative control serum recognising MA coated onto ELISA plates, utilized the same pooled TB negative control serum as that described above.

For the CELIA experiments determining whether anti-MA antibodies from TB positive sera could recognise MA or cholesterol containing liposomes, six TB positive sera were selected from a group of patients (aged between 18 and 65) and pooled. These sera were collected in the year 2000, initially for another study by Schleicher *et al.* (64). The patients were admitted to the general medical wards of the Helen Joseph Hospital; Johannesburg, South Africa. Of the 6 TB positive sera chosen, 3 were co-infected with HIV.

2.3.2 List of reagents and buffers

The following reagents were obtained from Merck (Wadeville, Gauteng, South-Africa under license of Merck, Darmstadt, Germany), unless stated differently.

Chloroform (UnivAR), cholesterol (99%, Sigma), hydrogen peroxide urea adduct (H₂O₂, BDH chemicals, Laboratory reagent), L- α -Phosphatidylcholine Type XVI- ξ (99%, Sigma-Aldrich), 96 well plates (Sero-Well®, Bibby sterilin Ltd., Stone, Staffs, UK).

Mycolic acid: Mycolic acids from the *M. tb* 27294 *M. tb* H37rv strain were purchased from the American type Culture Collection (ATCC), Maryland, USA. The MAs were isolated by S. van Wyngaardt according to the method described by Goodrum *et al.* (156).

Synthetic protected α -MA ester (AMAME): This synthetic MA was kindly provided by Dr. J. Al Dulayymi according to the method stated in Al Dulayymi *et al.* (157).

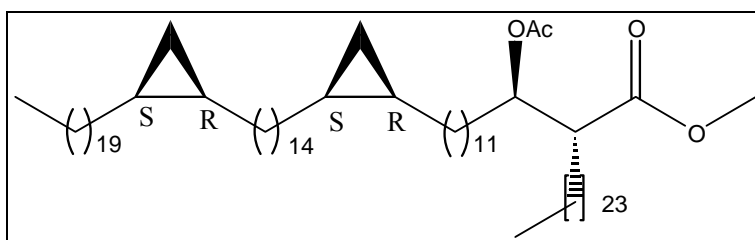


Figure 2.2: The acetylated and methylated α -MA ester.

Phosphate buffered saline (PBS): 20 x PBS stock was prepared by dissolving 160 g of sodium chloride (NaCl), 4 g potassium chloride (KCl), 4 g of di-hydrogen potassium phosphate (KH₂PO₄), and 23 g of di-sodium hydrogen phosphate (Na₂HPO₄) in a total of 900 ml of ultra-pure double distilled, de-ionized water (ddd H₂O), while stirring. The solution was brought to a final volume of 1L with ddd H₂O and filtered through a 0.22 μ m filter paper.

1 x PBS: This was prepared by dissolving 50 ml of the 20 x PBS buffer in 950 ml of ddd H₂O. The pH was checked to be 7.4.

0.5% Casein / PBS: PBS (50 ml, 20 x buffer) was added to a 1L flask and 700 ml of ddd H₂O was added. To this solution 5 g of casein (carbohydrate and fatty acid free, Calbiochem) was added and dissolved by stirring at 37 °C for 2 hours. The solution was then stored at 4 °C overnight and the next day the pH was adjusted to 7.4 with 1 M sodium hydroxide (NaOH) and volume finally made up to 1L using ddd H₂O.

Goat anti-human IgG peroxidase conjugate (whole molecule, Sigma, Steinheim, Germany): The conjugate was prepared by adding 10 μ l of peroxidase conjugate to 10 ml of 0.5% Casein/PBS. This was prepared 5 min prior to use.

0.1 M Citrate buffer: 0.1 M citric acid (450 ml) solution was added to a 0.1 M citrate tri-sodium solution (450 ml) until a pH of 4.5. The solution was then brought to a final volume of 1L with ddd H₂O.

O-phenylenediamine dihydrochloride (OPD) Substrate: The substrate was prepared just before use and kept in the dark. To 10 ml of 0.1 M citrate buffer, 10 mg of OPD (Sigma, Steinheim, Germany) and 8 mg of crushed urea hydrogen peroxide (35% H₂O₂) was added.

0.9% Saline: This was prepared by dissolving 9 g of sodium chloride in 100 ml of ddd H₂O.

2.4 Methods

2.4.1 Liposome preparation

Empty liposomes, containing only PC, were prepared as well as liposomes containing PC in different molar ratios to MA or cholesterol. The 2 mol % MA liposomes consisted of MA (0.25 mg) mixed with PC (9.75 mg), 4 mol % MA liposomes of MA (0.5 mg): PC (9.5 mg) and 8 mol % MA liposomes consisted of MA (1 mg) and PC (9 mg). For the preparation of different cholesterol liposomes, the 26 mol % cholesterol liposomes contained cholesterol (1.5 mg) and PC (8.5 mg), whereas the 51 mol % cholesterol liposomes consisted of cholesterol (3 mg) and PC (6 mg) and the 75 mol % cholesterol liposomes of cholesterol (6 mg) and PC (4 mg). The above mentioned lipid combinations were initially dissolved in chloroform in an amber glass vial and vortexed to ensure mixing. The samples were then dried at 85 °C under a stream of N₂ (g), and sonicated in saline (2 ml) for 8 minutes at room temperature. Sonication was done using the Virsonic sonifier (Model: 600) supplied by United Scientific at setting no. 12. Subsequently the

liposomes were divided into aliquots (200 μ l), freeze-dried and stored at -70 °C until required for use. Before use, the liposomes were reconstituted in PBS (1 ml, pH 7.4), to afford a final liposomes concentration of 1 mg/ ml. The solutions were heated at 80 °C for 20 minutes and sonified as described above. The liposome solutions were allowed to cool to room temperature before use.

2.4.2 Specificity of serum binding to MA and cholesterol

ELISA plates were coated containing MA, protected α -MA (AMAME, Fig 2.2), cholesterol and PBS respectively. Each lipid sample (250 μ g) was dissolved in 1 x PBS (4 ml, pH = 7.4) and placed on the heat block at 85 °C for 20 minutes. One vial of 1 x PBS (4 ml) served as control. The solutions were vortexed for 30s before sonifying for 2 minutes using the Virsonic sonifier at setting no. 2. The warm solutions were subsequently loaded onto the ELISA plates (50 μ l per well) and the presence of oily drops viewed under a light microscope. The plates were kept at 4 °C overnight in plastic bags. The following day, plates were aspirated and blocked with 0.5% Casein/PBS (400 μ l/ well) for 2 hours. After 2 hours the blocking buffer was aspirated and serum (1:20 dilution in 0.5% Casein/PBS, pH= 7.4) was added to the plate (50 μ l/ well). After 1 hour of serum incubation, the wells were washed 3 times with Well Wash4 ELISA washer (Labsystems) and flicked out before adding the goat anti-human IgG peroxidase conjugate solution (50 μ l/ well) for 30 minutes at room temperature. Subsequently, plates were washed three times and flicked out before adding the OPD substrate solution (50 μ l/ well). Absorbancies were measured with a SLT 340 ATC photometer at 450 nm with a reference filter at 690 nm at time intervals of 10, 40, 50 and 60 minutes respectively. Only the readings after 50 minutes were used for further analysis.

Background binding of the serum to the plate was corrected for by subtracting the average binding signal of serum to PBS coated wells. Final values were expressed relative to the MA signal of a TB positive serum sample (reference serum no. 318).

Statistical analysis

The TB positive and TB negative serum responses were analysed to MA, cholesterol or the protected α -MA using the student T-test in Microsoft Excel. The two populations were considered to have unequal variances and to follow a normal distribution. Using an $\alpha = 0.05$ a P-value was obtained which was compared to the calculated test statistic. If the P-value was larger than the test statistic, the two populations were considered to be significantly different.

2.4.3 Measuring ACHA binding to cholesterol and MA containing liposomes

2.4.3.1 CELIA using cholesterol liposomes

ELISA plates were coated with cholesterol and PBS as described in section 2.4.2 and blocked with the 0.5% Casein/PBS solution (400 μ l) for 2 hours. After aspirating the blocking buffer, the serum samples were added (50 μ l/ well) and ELISA performed as described in 2.4.2. The serum samples were prepared during the blocking step. Serum was incubated with 26 mol %, 51 mol % and 75 mol % cholesterol liposomes (as prepared in section 2.4.1) at room temperature for 2 hours. Each of the cholesterol containing liposomes (26 mol %, 51 mol % and 75 mol %) was tested at 20, 40 and 80 times dilution of serum. For all serum dilution experiments, the liposome concentration was maintained at 0.5 mg/ml.

Background binding was corrected for by subtracting the binding signal of serum samples to PBS from the binding signal of serum samples to MA.

2.4.3.2 CELIA using MA liposomes

The experimental procedure was followed as described in 2.4.3.1 using the same dilutions of TB negative control serum. In this experiment however, different MA liposomes were used (2 mol %, 4 mol % and 8 mol %), as prepared in section 2.4.1. The serum incubated with PC liposomes only served as control (2.4.3.1).

2.4.4 Using the CELIA assay to assess the nature of the cross-reactive antibody to MA from a TB negative control serum

ELISA plates were prepared containing MA (3 µg/ well) and PBS. Mycolic acid (250 µg) was dissolved in 1 x PBS (4 ml, pH= 7.4) and placed on the heat block at 85 °C for 20 minutes. One vial of 1 x PBS (4 ml) served as control. The solutions were vortexed for 30s before sonifying for 2 minutes using the Virsonic sonifier at setting no. 2. The warm solutions were subsequently loaded onto the ELISA plates (50 µl per well) and the presence of oily drops viewed under a light microscope. The plates were kept in plastic bags at 4 °C overnight. The next day the plates were flicked out and 0.5% Casein/PBS blocking buffer (400 µl) was added to each well and the plates incubated at room temperature for 2 hours. The blocking buffer was aspirated and the serum samples were added (50 µl/ well) and ELISA performed as described in 2.4.2.

The serum samples were prepared during the blocking step. TB negative control serum was incubated with 2 mol %, 4 mol % and 8 mol % MA liposomes as well as 26 mol %, 51 mol % and 75 mol % cholesterol liposomes (as prepared in section 2.4.1) at room temperature for 2 hours. Each of the antigen containing liposomes was tested at a 1 in 20 dilution of serum at a concentration of 0.5 mg/ml. As control, serum was incubated with PC liposomes for 2 hours.

Background binding was corrected for by subtracting the binding of serum samples to PBS from the binding of serum samples to MA.

2.4.5 Measuring antibody binding from a pooled TB positive patient serum to cholesterol and MA containing liposomes in a CELIA assay

ELISA plates were coated with MA as described above in section 2.4.4 and the pooled TB positive serum incubated with 2 mol %, 4 mol % and 8 mol % MA liposomes as well as 26 mol %, 51 mol % and 75 mol % cholesterol liposomes (as prepared in section 2.4.1) at room temperature for 2 hours. Each of the antigen containing liposomes was tested at a

1 in 20 dilution of serum at a concentration of 0.5 mg/ml. As control, serum was incubated with PC liposomes for 2 hours.

Background binding was corrected for by subtracting the binding of serum samples to PBS from the binding of serum samples to MA.

2.5 Results

2.5.1 Apparent molecular mimicry between MA and cholesterol

In order to determine the specificity of interaction of antibodies from TB negative sera with MA, an α -MA was synthesized (AMAME) of which the hydroxyl functionality was protected with an acetyl group while the carboxyl head was protected with a methyl group (fig 2.2). The selective protection was done to prevent the polar functionalities from interacting, allowing only hydrophobic interactions with antibodies. The AMAME subsequently turned out to be an ideal negative control antigen with little or no antibody binding in either of the TB positive patient or TB negative sera tested (figure 2.3).

The results presented in figure 2.3 confirmed the observation of Siko (71) in which no statistical significant difference between serum recognition of MA and cholesterol was seen in either of the TB positive or the TB negative serum populations. It was noted from figure 2.3 that there was a significant difference between the average corrected MA signal of TB positive and TB negative sera populations ($P < 0.03$). These results supported the finding that TB positive and TB negative patient sera could be distinguished using a mixture of natural MA coated onto ELISA plates (64,71).

The absence of binding of both TB positive and TB negative sera populations to AMAME (figure 2.3) confirmed that binding of antibodies to MA was specific and could be abolished by protecting the carboxyl and hydroxyl groups of MA. These results thus identified the polar head group of MA as being essential for antibody recognition.

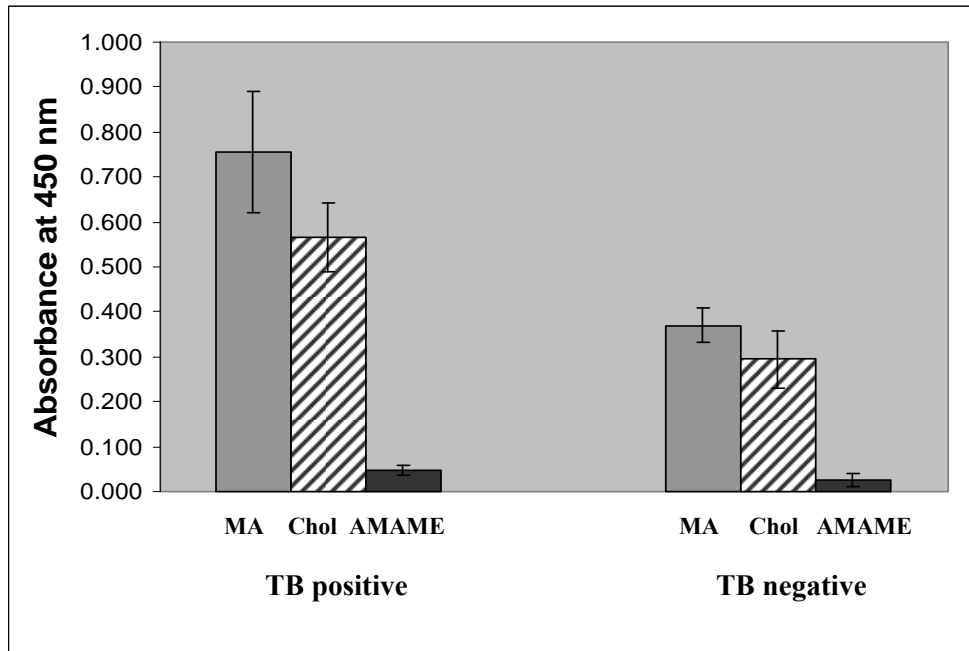


Figure 2.3: Specificity of MA recognition by serum antibodies in ELISA. The response of 10 TB positive and 5 TB negative sera at a 1:20 dilution was measured twice in quadruplicate to MA, cholesterol and the synthetic protected AMAME. The average responses of the TB positive patients (10 patient sera, each done in triplicate) measured to each lipid sample were combined and the combined average and standard error of the mean (error bars) presented above. The same was applied to the TB negative patient sera.

2.5.2 Specificity of anti-cholesterol antibodies in TB negative control serum

2.5.2.1 Inhibition of ACHA with cholesterol containing liposomes

It has been demonstrated that naturally occurring anti-cholesterol antibodies occur in all individuals and that these antibodies can be inhibited with VLDL and LDL preparations in ELISA (153,154). We set out to determine whether anti-cholesterol antibodies present in a TB negative control serum could be inhibited using prepared lipid vesicles containing different concentrations of cholesterol. We termed the inhibition assay the CELIA assay following a similar method to that previously described by Horvath *et al.* (153). The only differences were that i) here whole serum was used instead of an IgG preparation, ii) cholesterol was coated at a concentration of 3 $\mu\text{g}/\text{well}$ instead of 5 $\mu\text{g}/\text{well}$, and iii) inhibition was effected with experimentally defined cholesterol containing liposomes, instead of naturally isolated VLDL/ LDL preparations. Inhibition of ACHA

was measured at different serum dilutions to determine the optimal serum concentration at which to perform the subsequent experiments.

In the CELIA assay, the response of serum was measured to cholesterol after incubating the TB negative control serum with 26, 51 or 75 mol % cholesterol containing liposomes. The range of results generated at each dilution of serum was then compared using the Duncan's t-test provided in the Statistical Analysis System (SAS). This is a multiple range test comparing the means of many samples simultaneously, which are then described by letters of the alphabet as can be seen in figure 2.4. Samples given the same letter do not significantly differ from each other.

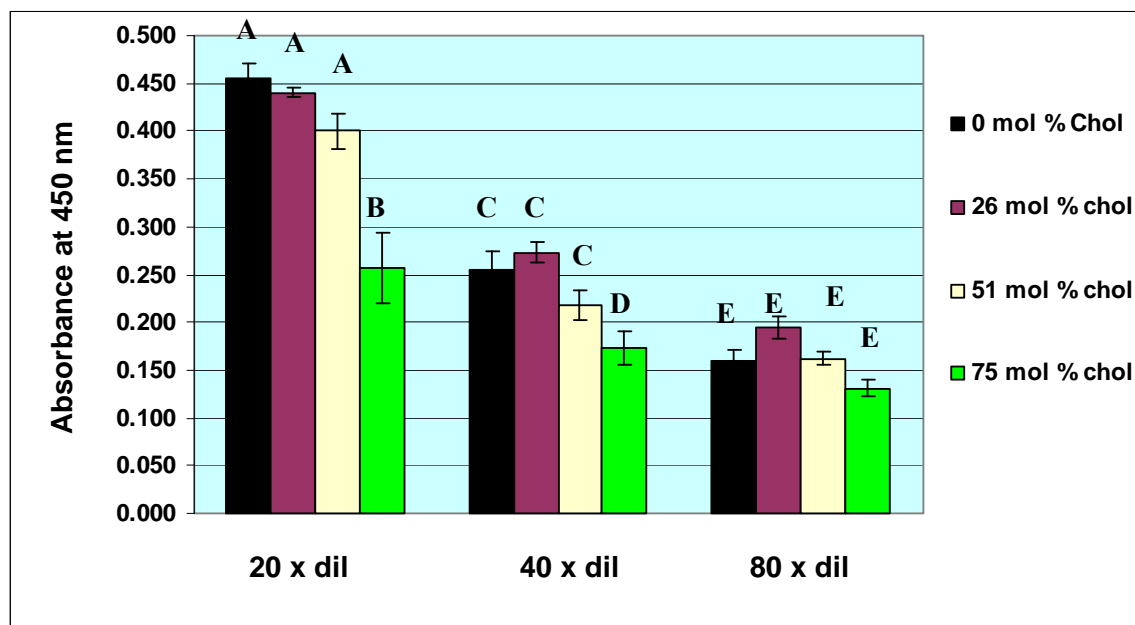


Figure 2.4: Cholesterol liposomes inhibit the ELISA signal of a TB negative control serum using a CELIA assay. The response of the TB negative control serum to cholesterol coated wells was measured after pre-incubation with liposomes containing different concentrations of cholesterol. Serum dilutions of 1 in 20, 40 and 80 were pre-incubated with 0, 26, 51 and 75 mol % cholesterol liposomes. Sample means were compared using the Duncan multiple range. Samples given the same letter do not differ significantly. Error bars indicate the standard error of the mean with $n \geq 4$.

As seen from figure 2.4, the liposomes containing the highest concentration of cholesterol (75 mol %), were capable of inhibiting the ELISA signal to cholesterol in serum

concentrations down to 1:40 dilution, but not at lower concentrations of serum. A sharp decrease in the ELISA signal was observed in general when moving from the 1 in 20 to the 1 in 40 dilution of serum (fig 2.4), suggesting that the binding of ACHA to cholesterol was not of a very high affinity. The greatest amount of inhibition of the cholesterol signal was seen at the 1 in 20 dilution of serum. Inhibition of the cholesterol signal was not significant using liposomes containing 51 or 26 mol % cholesterol.

The results presented in figure 2.4 thus indicated that the ELISA signal generated by ACHA from a TB negative control serum to immobilized cholesterol that was coated from hot PBS, cross-reacted with liposomes containing 75 mol % cholesterol. It was concluded that the ACHA in TB negative sera that produce an ELISA signal to immobilized cholesterol, recognised some arrangement of cholesterol in the solid phase that approximates the structure of a high concentration of cholesterol in liposomes.

2.5.2.2 Inhibition of ACHA with MA containing liposomes

In order to further investigate the structural relationship between cholesterol and MA, it was determined whether antibodies to cholesterol (ACHA) could recognise MA contained in liposomes. The CELIA assay performed here measured the binding of ACHA to cholesterol coated ELISA plates after incubating TB negative control serum with liposomes containing different concentrations of MA. The liposomes used consisted of 0, 2, 4 and 8 mol % MA. The reason for the use of liposomes containing lower concentrations of MA than that used for cholesterol liposomes, was due to the limitations set by the solubility of MA and the capacity of liposomes to carry MA (158). The sample means were analysed in SAS using the Duncan's multiple range t-test to determine if there were significant differences.

As can be seen from Figure 2.5, ACHA present in TB negative control serum could be inhibited by MA contained in liposomes. At the 1 in 20 dilution of serum both the 4 and 8 mol % MA liposomes were able to inhibit the anti-cholesterol signal, while at a 1: 40

dilution only the 8 mol % MA liposome preparation was still able to inhibit the cholesterol signal.

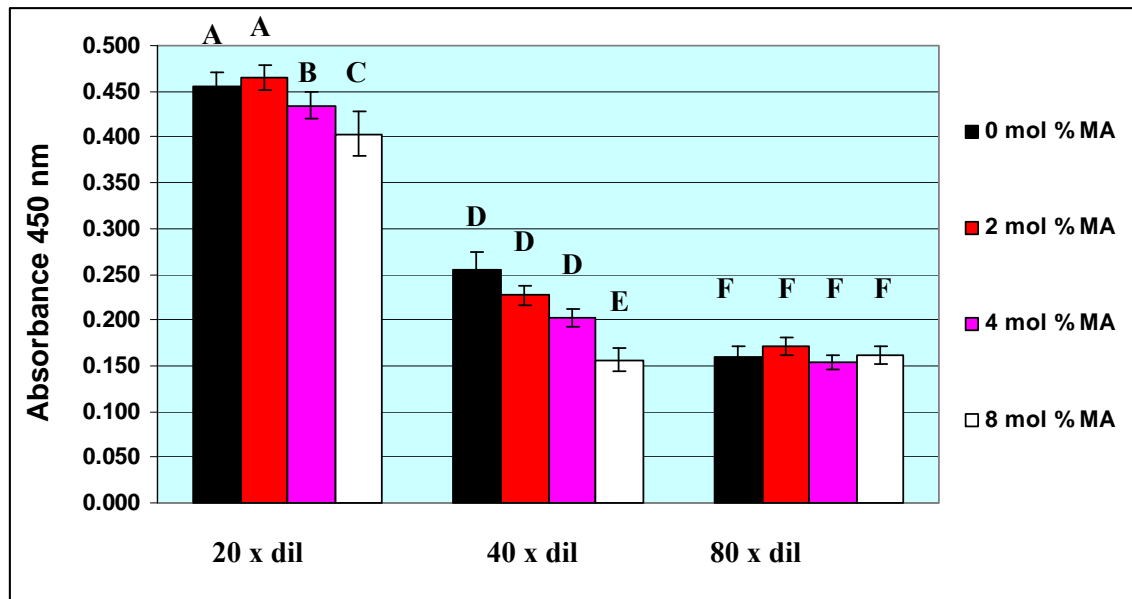


Figure 2.5: Determining whether ACHA in TB negative serum cross-react with MA containing liposomes in the CELIA assay. The response of a TB negative control serum at 1:20, 1:40 and 1:80 dilutions was measured to cholesterol coated wells after pre-incubation with liposomes containing 0, 2, 4 or 8 mol % MA. Samples given the same letter do not significantly differ as determined with the Duncan multiple range *t*-test. Error bars indicate the standard error of the mean with $n \geq 4$.

From these results it was deduced that anti-cholesterol antibodies do cross-react with MA contained in liposomes. Based on our results and that from literature (153,154), it was concluded that ACHA does not recognise an epitope defined by an individual cholesterol molecule, but rather some organisation of cholesterol at high concentrations in liposomes. Thus, the cross-reactivity of ACHA with MA contained in liposomes is not due to direct molecular mimicry between MA and cholesterol, but rather due to the formation of a similar epitope between MA and cholesterol defined by the concentration in the liposomes.

2.5.3 Nature of the cross-reactive antibody to MA from a TB negative control serum

It has previously been postulated that anti-cholesterol antibodies are the serum components in TB negative sera responsible for cross-reacting with MA in ELISA (71). It

has subsequently been shown here that ACHA from a TB negative control serum cross-reacts with MA contained in liposomes, but it still remained to be shown that ACHA cross-reacts with MA coated on ELISA plates. To investigate whether ACHA are the cross-reactive antibodies from TB negative patient serum recognising MA in ELISA, plates were coated with MA and the response of a TB negative control serum to MA measured after incubation with both MA (2, 4 and 8 mol % MA) and cholesterol (26, 51 and 75 mol % cholesterol) containing liposomes in a CELIA assay.

The results obtained from figure 2.6 showed that the antibody binding from a TB negative control serum to MA was inhibited with the 4 and 8 mol % MA containing liposomes in a concentration dependent manner. The antibody recognising MA coated onto ELISA plates from the TB negative control serum did not recognise liposomes containing high concentrations of cholesterol (50 and 75 mol % cholesterol). There was however an apparent inhibition of the MA signal with the 26 mol % cholesterol liposomes.

The inability of the cholesterol loaded liposomes to inhibit the MA binding signal from the TB negative control serum could be due to the anti-cholesterol antibodies having a greater affinity for MA or that the antibody binding to MA from TB negative serum is not an anti-cholesterol antibody. These results suggested that the antibody from the TB negative control serum recognising MA on ELISA plates, could be an anti-MA antibody, which could recognise solid phase MA as well as MA contained in liposomes, as previously seen for TB positive sera in ELISA and biosensor assays (64,72). The presence of anti-MA antibodies in TB negative control serum could be due to previous BCG vaccination, latent infection with *M. tb* or infection with non-pathogenic mycobacteria in an HIV burdened population.

The apparent inhibition seen using the 26 mol % cholesterol liposomes, could be due to the anti-MA antibodies cross-reacting with the cholesterol liposomes, or the cholesterol liposomes accumulating onto the hydrophobic MA surface (71), preventing anti-MA antibody binding.

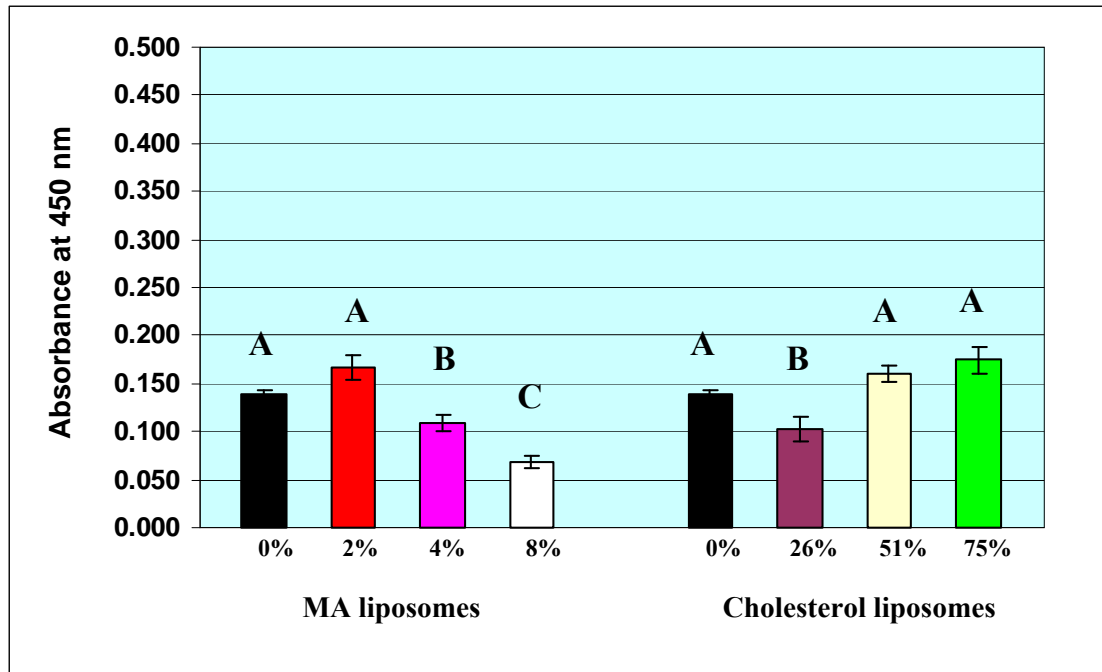


Figure 2.6: The nature of the antibodies found in TB negative control serum recognizing MA. Analysis was performed using the CELIA assay with MA immobilized on the plates and various concentrations of MA and cholesterol in liposomes as inhibitors. The response of a TB negative control serum at 1:20 dilution was measured to ELISA plates coated with MA, after pre-incubation with MA and cholesterol containing liposomes. The serum was pre-incubated with 0, 2, 4 and 8 mol % MA liposomes or with 0, 26, 51, and 75 mol % cholesterol containing liposomes. Samples given the same letter do not significantly differ as determined with the Duncan multiple range t-test. Error bars indicate the standard error of the mean with $n \geq 4$.

Thus, these results suggest that anti-MA antibodies could also present in TB negative control sera, but that the cross-reactivity of these antibodies with cholesterol cannot be demonstrated in this configuration of the CELIA assay, as cholesterol itself possibly participates in the MA binding activity.

2.5.4 Specificity of antibodies recognising MA in TB positive patient sera

It is known that TB positive serum contains antibodies to MA (64). In order to gain a deeper understanding of the nature of the antibodies recognising MA from TB negative serum, the reactivity of anti-MA antibodies from TB positive patient serum to MA coated plates was compared to that of TB negative serum. The TB positive patient serum was

incubed with MA (2, 4 and 8 mol % MA) and cholesterol containing liposomes (26, 51 and 75 mol % cholesterol) at a 1 in 20 dilution of serum, as performed for the TB negative control serum.

The results in figure 2.7 indicated that TB positive serum was inhibited with both the 4 and 8 mol % MA containing liposomes, in the same way as seen for TB negative control serum (figure 2.6). It was also seen that the 26 mol % cholesterol containing liposomes could apparently inhibit the MA signal, but not the 51 nor the 75 mol % cholesterol liposomes, as was also the case for the TB negative control serum.

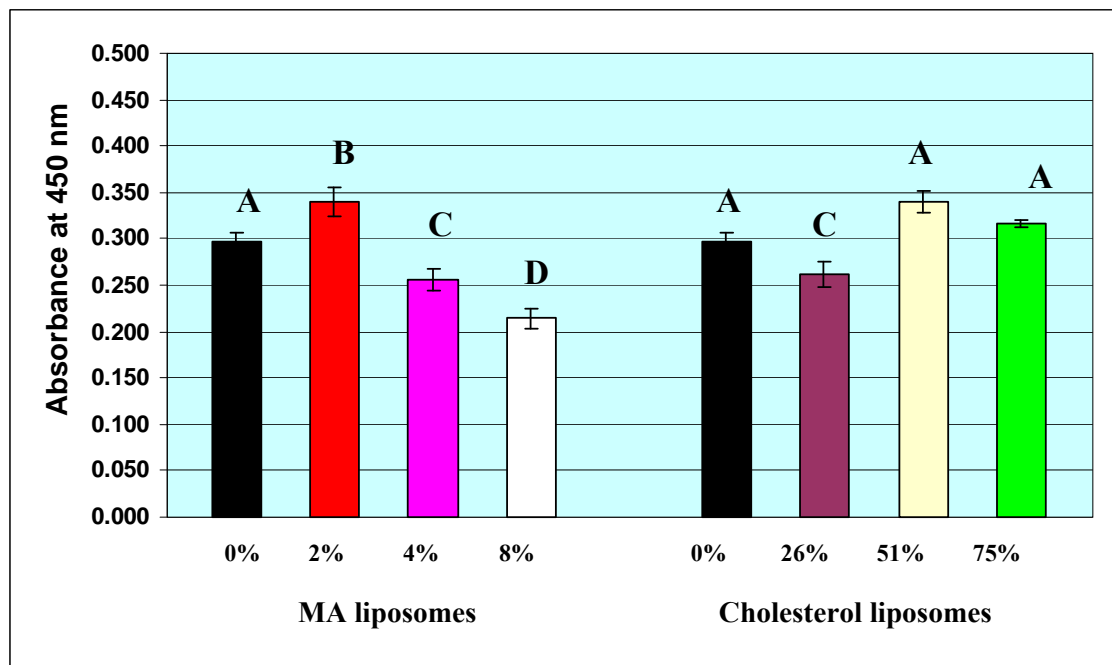


Figure 2.7: Anti-MA antibodies from TB positive sera do not cross-react with cholesterol containing liposomes in the CELIA assay. ELISA plates were coated with MA from hot PBS and the response of a pooled TB positive serum at a 1:20 dilution was measured after pre-incubation with either MA or cholesterol containing liposomes. Pre-incubation of serum was done with 0, 2, 4, or 8 mol % MA containing liposomes or with 0, 26, 51 and 75 mol % cholesterol containing liposomes. Samples given the same letter do not significantly differ as determined with the Duncan Multiple range t-test. The error bars indicate the standard error of the mean with $n \geq 4$.

The correlation in binding profiles between the antibodies recognising MA from the TB negative control serum (figure 2.6) and the TB positive patient serum (figure 2.7), support the hypothesis that TB negative serum also contains anti-MA antibodies. These results do however not eliminate the possibility that cross-reactive anti-cholesterol antibodies in both TB positive patient and TB negative serum do not bind to MA on ELISA plates. Furthermore, due to the possible accumulation of 26 mol % cholesterol liposomes onto MA coated plates, the cross-reactivity of anti-MA antibodies with cholesterol could not be unequivocally determined by pre-incubation of sera with cholesterol containing liposomes when MA was the immobilized antigen.

2.6 Discussion

The low sensitivity and specificity previously obtained in ELISA when using MA as antigen (64) has been proposed to be due to the cross-reactivity of anti-cholesterol antibodies (71). It was further suggested that the congruence of MA and cholesterol titres was due to molecular mimicry between MA and cholesterol (71) and molecular mimicry between MA and cholesterol has also been assumed to be the reason behind AmB (cholesterol binding macromolecule) binding to MA (148). The apparent molecular mimicry between MA and cholesterol was investigated here by first establishing the specificity of the antibody interaction with MA and secondly, whether anti-cholesterol antibodies could recognise MA contained in liposomes as well as coated onto ELISA plates.

It was confirmed here that a congruence of MA and cholesterol titres existed in the sera of both TB positive and TB negative sera. The antibody binding to MA was subsequently shown to be specific (as published in Benadie *et al.* [161]) and to depend on the presence of the polar functionalities on the mycolic motif. The synthetic α -MA (AMAME), which turned out to be an ideal negative control, contained protecting groups on both the hydroxyl and carboxyl groups. The lack of antibody binding to AMAME by TB positive and TB negative sera could have been due to the protection of both, or either of the polar functionalities of the mycolic motif. However, there remains some controversy with

regards to the importance of the carboxyl group in antibody recognition. The results presented by Pan *et al.* (121) showed the methyl esters of MA being recognised by anti-TDM antibodies, while another member of our group failed to detect any antibody binding to the methyl esters of MA (147). It was thus concluded that the polar head of the mycolic motif is essential for antibody recognition of MA, but at this point, interaction could not be limited to a particular polar group of the mycolic motif.

The fact that there was a congruence of the MA and cholesterol antibody titres and that binding was specific, supported the hypothesis that anti-cholesterol antibodies from TB negative sera were the antibodies cross-reacting with MA in ELISA (71). The first step towards analyzing whether anti-cholesterol antibodies cross-reacted with MA was to determine whether anti-cholesterol antibodies could recognise MA contained in liposomes. In order to do so, it first had to be shown that anti-cholesterol antibodies recognised cholesterol contained in liposomes. Liposomes were used as carriers of the antigens, as these model membranes create a micro-environment similar to the natural system (159).

Previously, Horvath *et al.* (153) performed inhibition assays on ELISA showing the reduction of the anti-cholesterol antibody binding signal after incubation of the antibody preparations with VLDL and LDL lipoprotein particles. It was subsequently shown here that the cholesterol signal of TB negative control serum was inhibited with liposomes containing a high concentration of cholesterol (75 mol % cholesterol). These results provided here gave further proof that ACHA recognises cholesterol in a concentration dependent manner within lipid vesicles. It has previously been shown that antibodies generated to cholesterol in mice also recognise cholesterol in a concentration dependent manner, with the greatest response being to the liposomes containing more than 56 mol % cholesterol (152). From these results it was concluded that the cholesterol epitope recognized by ACHA is defined by a particular lipid phase transition induced by high molar ratios of cholesterol in PC double layers. Almeida *et al.* (160) showed that cholesterol is in a liquid ordered state in PC liposomes containing >50 mol % cholesterol.

Thus, we concluded that ACHA recognises the liquid ordered state of cholesterol in liposomes.

It was also shown here that ACHA cross-reacted with MA containing liposomes in a concentration dependent manner. These results provided additional proof for the cholesterol nature of MA (161), but showed here that antibody recognition of MA in liposomes was not due to a direct molecular mimicry, but rather due to the MA in liposomes resembling the liquid ordered state of chol in liposomes.

After showing that ACHA cross-reacted with MA contained in liposomes, it was attempted to demonstrate that ACHA are the cross-reactive antibodies recognising MA coated onto ELISA plates. The apparent cross-reactivity of antibodies from TB positive patient and TB negative serum with 26 mol % cholesterol liposomes in the CELIA assay could not be unequivocally demonstrated on plates coated with MA, due to the possible interference of cholesterol liposomes with the MA coat. It has previously been shown that cholesterol liposomes have an affinity for MA contained in liposomes coated on the resonant mirror biosensor (71). The reduction in the MA signal observed here due to the 26 mol % cholesterol liposomes, could thus possibly also have been due to cholesterol liposomes accumulating on the MA coat, and preventing anti-MA antibodies from binding.

Contrary to what was expected however, the binding signal to MA from TB negative control serum could not be inhibited by liposomes containing high molar ratios of cholesterol, as would be expected for ACHA. Antibody binding to the MA coated plate from the TB negative control serum was however inhibited with MA containing liposomes. The apparent correlation in binding profile between the antibodies from TB negative control serum and TB positive patient sera in the CELIA assay, led to the hypothesis that the antibodies from TB negative serum binding to MA were anti-MA antibodies. Another possibility also considered, was that ACHA may have had a greater affinity for MA on ELISA plates than for cholesterol contained in liposomes, and hence the inability of cholesterol liposomes to inhibit the binding signal to MA from TB

negative control serum.

The presence of anti-MA antibodies in TB negative serum was previously not considered to be an option (64,71,72,162), but recently antibodies to another cell wall antigen presented on CD1 molecules, lipoarabinomannan (LAM), have been detected in TB negative individuals (163). Antibodies to LAM have been shown to be induced and maintained upon BCG vaccination and are only elevated during active disease (65,164), as would seem to be the case here for antibodies to MA. Generation of anti-MA antibodies in TB negative patients could also be the result of latent TB infection (165) or due to constant immune stimulation from non-pathogenic mycobacteria.

The possible existence of anti-MA antibodies in TB negative serum is further supported by the results obtained by members of our group (71,72) using the resonant mirror biosensor assay. In the biosensor assay both TB positive patient and TB negative serum have been shown to be inhibited by MA liposomes, but to significantly different degrees, as is the case with antibody binding to MA in ELISA. The ability of the biosensor assay to reach a higher sensitivity (86%) compared with the ELISA assay (51%) using MA as antigen, is probably due to the fact that in the biosensor assay, the binding step is not followed by a washing step as in ELISA or CELIA. This would allow all possible antibody binding to be observed, including those of the low affinity antibodies. It has however not been established whether antibodies are the serum components binding to the MA liposomes on the resonant mirror biosensor and this is investigated in the next chapter.

Chapter 3: Analysis of antibody binding to MA liposomes immobilized on a resonant mirror biosensor surface

3.1 Introduction

Accurate diagnosis is one of the first steps towards the management of TB, especially in HIV burdened populations where TB is the major cause of death in HIV/AIDS co-infected individuals. Serodiagnostic techniques have the possibility to be rapid, non-invasive and inexpensive, but the serological tests currently available have limited sensitivity in children and HIV populations (166). In an attempt to reach the required sensitivity ($> 80\%$) and specificity ($> 95\%$) set out by the World Health Organisation (57), members of our group have developed a new serodiagnostic assay based on the mycobacterial lipid antigen, MA, using resonant mirror biosensor technology (162). The advantage of using the biosensor is that the samples do not need to be chemically modified for detection, but the disadvantage of not labelling the substrate or analyte, is that the identity of the interacting molecules is often unknown. The serum components binding to MA contained in liposomes on the resonant mirror biosensor was thought to be due to serum antibodies, but required confirmation.

The biosensor assay can detect molecular interaction between analyte and immobilized antigen in real time within the picomolar range. Various immobilization methods exist for lipid analysis on the resonant mirror biosensor, of which the most preferred is incorporation of the substrate into model membranes. Model membranes have the advantage of providing a physiological environment in which molecules can move and are flexible for interaction (167). Supported lipid bilayers (SLB) can be formed either by sequential deposition using the Langmuir-Blodgett technique or with the aid of liposome fusion (168). It has previously been shown that when phospholipid vesicles are added to an already coated lipid support, a monolayer of phospholipid is formed on top of the supported surface to yield a fluid lipid bilayer (169). A similar method was employed by Siko in 2002 (71) for the immobilization of MA onto the resonant mirror biosensor

cuvette surface (71). The MA/ PC liposomes were immobilized onto a supported lipid layer of cetyl pyridinium chloride (CPC) intended to form a bilayer as depicted in figure 3.1.

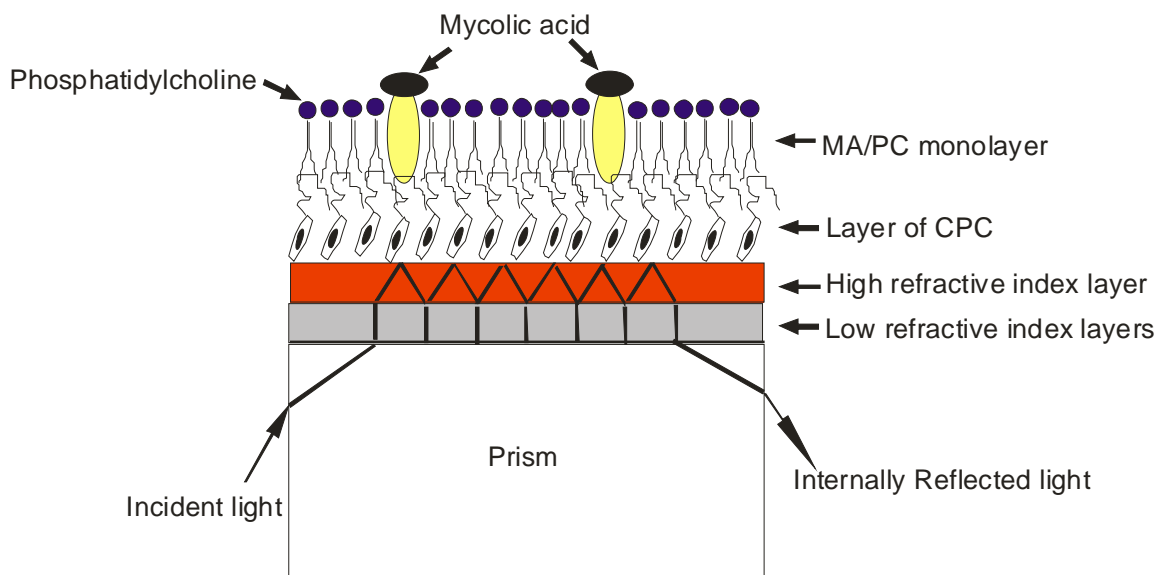


Figure 3.1: The possible arrangement of MA/ phosphatidylcholine (MA/ PC) liposomes on the modified surface of the IAsys Affinity resonant mirror biosensor. Cetyl pyridinium chloride (CPC) is added to the hafnium oxide cuvette surface to create a hydrophobic environment for the adsorption of liposomes. Accumulation of serum components onto the MA/ PC supported bilayer occurs within a few 100 nm from the cuvette surface. The region of interaction is called the evanescent field and is an electromagnetic field generated when incident light is internally reflected between the high refractive index layer (hafnium oxide) and the low refractive index layer (silica). Molecular interaction within the evanescent field results in a change of refractive index and subsequently also changes the angle of incident light required to maintain internal reflection. The change in resonant angle is measured in arcs x second and is proportional to the mass of the accumulated substances.

The serum components binding to the supported MA/ PC lipid bilayer on the resonant mirror biosensor were thought to be antibodies (72). Apart from antibodies, other serum proteins which are also capable of recognising phospholipid membranes are albumin and lipoproteins (64,170,171).

Human albumin is the most abundant serum protein and consists of a single polypeptide of 66.5 kDa in size that functions to maintain the oncotic pressure of serum, and to

transport a wide range of molecules, including long chain fatty acids (172). Bovine serum albumin (BSA), the bovine equivalent of human serum albumin (HSA), has been shown to adsorb onto PC liposomes (170). Furthermore, plasma lipoproteins such as Apolipoprotein A and B (ApoA and ApoB) have also shown to be able to adsorb onto monolayers containing egg PC and dimiristoylphosphatidylcholine (DMPC) as well as other phospholipid containing vesicles (171,173). It is thus expected that some of the accumulation seen on the resonant mirror biosensor to MA containing liposomes could be due to albumin and lipoproteins interacting with the PC containing lipid coat (72). However, because all patients contain serum albumin and lipoproteins, it is unlikely that the distinction made between a range of TB positive patient and TB negative sera on the biosensor would be due to these proteins. It is more likely that the serum component which is possibly related to disease status and capable of distinguishing between TB positive and TB negative patients on the resonant mirror biosensor is an anti-MA antibody. In order to confirm that antibodies of the immunoglobulin subclass G (IgG) are the serum components accumulating onto the MA/ PC liposomes of the IAsys Affinity biosensor, this study set out to isolate IgG from TB positive and TB negative sera, and assess the binding of the isolated IgG fractions to the immobilized MA containing liposomes. Protein A conjugated to Sepharose was used to isolate IgG from serum, as it has been shown to be specific for IgG but not the other immunoglobulin subclasses (174). It was also assessed whether the isolated IgG could be inhibited with MA/ PC containing liposomes to a similar extent as whole serum fractions previously analyzed (162).

3.2 Hypothesis

The ability of the resonant mirror biosensor technology to distinguish between TB positive and TB negative patient sera is due to the binding of antibodies of the IgG isotype to MA/ PC immobilized liposomes.

3.3 Materials

3.3.1 Source of sera

Immunoglobulin G was isolated from a TB positive patient serum (no. 260) which was selected from a collection of sera supplied by the Medical Research Council (MRC) (Clinical and Biomedical Research Unit: King George V Hospital, Durban, 1994). The only criterion for selecting the TB positive serum was that it had previously given good responses to MA on ELISA (unpublished results). The TB negative sample selected for IgG isolation consisted of pooled sera from 6 healthy individuals working in the Biochemistry Department at the University of Pretoria in research groups other than the TB research group and with no clinical signs of tuberculosis.

3.3.2 List of reagents

3.3.2.1 Chemicals obtained from Saarchem, a division of Merck, South Africa (unless stated otherwise)

Acetone (analytical grade), ammonium peroxydisulfate (APS, 98% pure), ammonium sulphate, analytical thin layer chromatography plates (aluminium sheets, 20 x 20 cm, silica gel 60, Merck, Germany), casein (fatty acid and amino acid free, Calbiochem, Merck, Germany), chloroform (analytical grade, stabilized with 25 ppm amylene/ethanol 0.4-1%), di-sodium hydrogen phosphate (Na_2HPO_4), di-hydrogen potassium phosphate (KH_2PO_4), ethylene diamine tetra-acetic acid (EDTA), hexane (distilled 24 hours before use), potassium chloride (KCl), potassium hydroxide (KOH), sodium chloride (NaCl), N,N,N,N-tetramethylethylenediamine (TEMED), tris (hydroxymethyl)aminomethane (GR buffer substance).

3.3.2.2 Chemicals obtained from Sigma, a division of Aldrich, Germany

Bis-acrylamide (99%), cetyl-pyridinium chloride (99%), cholesterol (99% pure), deuterated chloroform (anhydrous, 99.8% pure), glycine (ACS reagent, $\geq 98.5\%$), glycerol (99%), goat anti-human IgG peroxidase conjugate (whole molecule), L- α -

phosphatidylcholine Type XVI- ϵ (99%, sodium dodecyl sulfate (SDS), saponin (from quillaja Bark), sodium azide ($\geq 99\%$)).

3.3.2.3 Chemicals obtained from other sources

Benzyl alcohol (Associated Chemical Enterprises, SA), bromophenol blue (Protea Laboratory Services, SA), calcium chloride anhydrous (BDH chemicals, UK), coomassie brilliant blue G-250 (Bio-Rad Laboratories, SA), spectrapor membrane (for dialysis, MW cut off of 3 kDa, Spectrum Medical Industries Inc., USA), dichloromethane (HPLC grade, BDH chemicals, UK), diethyl ether (LAB-Scan, Analytical Sciences), 96 well ELISA plates (Sero-Well®, Bibby sterilin Ltd.), Ministart Plus Filter (0.2 μm , Sartorius, Wicklow, Ireland), hydrogen peroxide urea adduct (BDH chemicals, General reagent), Low Molecular Weight Marker: phosphorylase (97 kDa); BSA (66 kDa); ovalbumin (45 kDa); carbonic anhydrase (30 kDa); soybean trypsin inhibitor (20.1 kDa); lactalbumin (14.4 kDa (Bio-Rad Co., South Africa), Protein A, immobilized on Sepharose (Fluka, BioChemika, Switzerland), VetaSpin Micro columns (400 μl , 100 kDa cut-off, Whatman Industrial Ltd., England)

Mycolic acid (MA): MA from the M.tb 27294 H37rv strain was purchased from the American type Culture Collection (ATCC), Maryland, United States of America. The MAs were isolated by S. van Wyngaardt according to the method described by Goodrum *et al.* (156).

3.3.3 List of buffers

0.5% Casein/ PBS: In a 1L flask, 20 x PBS (50 ml) was added to ddd H₂O (700 ml). To the diluted PBS solution, casein (5 g) was added and dissolved by stirring at 37 °C for 2 hours. The casein solution was then stored at 4 °C overnight and the next day the pH was adjusted to 7.4 with 1 M sodium hydroxide (NaOH) and the volume finally made to 1L using ddd H₂O.

Cetyl-pyridinium chloride (0.02 mg/ml): This solution was prepared freshly every week by dissolving 1 mg of CPC in PBS/AE (50 ml) at room temperature. The solution was allowed one day for dissolution and gently shaken every time before use.

0.1 M Citrate buffer: 0.1 M Citric acid (450 ml) solution was added to a 0.1 M tri sodium citrate solution (450 ml) until a pH of 4.5. The solution was then brought to a final volume of 1L with ddd H₂O.

Colloidal Coomassie Blue Stock: The stock solution was prepared by dissolving 100% phosphoric acid (8 ml) together with ammonium sulphate (40 g) and Coomassie blue (8 ml) in ddd H₂O to make a final volume of 400 ml and mixed thoroughly. This stock solution had to be prepared at least 24 hours before use.

Colloidal Coomassie blue stain: The staining solution was prepared by adding methanol (10 ml) to the colloidal Coomassie stock (40 ml) in a 50 ml tube. The solution was mixed well before use.

Colloidal destain buffer (part 1): This solution consisted of 25% methanol and 10% acetic acid in ddd H₂O.

Colloidal destain buffer (part 2): This solution consisted of 25% methanol in ddd H₂O.

0.1 M glycine (pH = 2.7): Glycine (1.5 g) was dissolved in ddd H₂O (100 ml) and the pH adjusted to 2.7 by the addition of concentrated HCl (32 mol %).

Non-reducing sample buffer for sodium dodecyl sulfate polyacrylamide gel electrophoresis (SDS-PAGE): The following reagents were added together in a 10 ml tube and gently mixed before use; ddd H₂O (4.4 ml), 0.5 M Tris HCl (1.0 ml), 99% glycerol (0.8 ml), 10% SDS solution in water (1.6 ml), 0.05% bromophenol blue dissolved in ddd H₂O (w/v, 0.2 ml).

Peroxidase conjugate solution (1:1000 dilution): The goat anti-human IgG peroxidase conjugate (10 μ l) was added to a solution of 0.5% Casein/PBS (10 ml). This was prepared 5 minutes prior to use.

20 x PBS (phosphate buffered saline) buffer: The PBS stock was prepared by dissolving sodium chloride (NaCl, 160 g), potassium chloride (KCl, 4 g), of dihydrogen potassium phosphate (KH_2PO_4 , 4 g) and di-sodium hydrogen phosphate (Na_2HPO_4 , 23 g) in ultra-pure double distilled, de-ionized water (ddd H_2O , 900 ml), while stirring. The solution was brought to a final volume of 1L with ddd H_2O and filtered through a 0.22 μ m membrane filter.

1x PBS Buffer: This was prepared by dissolving 20 x PBS (50 ml) in ddd H_2O (950 ml). The pH was checked to be 7.4.

Phosphate buffered saline (PBS) Azide, EDTA buffer (PBS/AE): To a 1 x PBS solution, EDTA (0.186 g) and sodium azide (0.125 g) was added and completely dissolved before adjusting the pH to 7.4. The solution was then filtered through a 0.22 μ m membrane filter.

Running buffer for SDS-PAGE: This buffer was prepared by diluting a 5 x stock solution containing the following reagents; Tris (30.3 g), glycine (144 g) and SDS (10 g) dissolved in a total of 2L of ddd H_2O .

Saponin (0.3 mg/ml): This solution was prepared on a weekly basis by dissolving 15 mg of saponin in PBS/AE (50 ml) at 37 $^\circ\text{C}$.

Separating gel (10%) for SDS-PAGE: In a conical flask, acrylamide stock (10 ml) was added to 1.5 M Tris HCl (pH= 8.8, 7.5 ml), 10% SDS solution (0.3 ml) and ddd H_2O (12.1 ml), and subsequently degassed for 30 minutes. After the degassing procedure the 10% APS (150 μ l) and TEMED (10 μ l) were added.

Stacking gel (4%) for SDS-PAGE: In a conical flask acrylamide stock (0.67 ml) was added to 0.5 M Tris HCl (pH= 6.8, 1.25 ml), 10% SDS solution (0.05 ml) and ddd H₂O (3 ml) and subsequently degassed for 30 minutes. After the degassing procedure the 10% APS (25 µl) and TEMED (2.5 µl) were added.

1M Tris HCl (pH= 8.08): The solution was prepared by dissolving Tris (60.5 g) in ddd H₂O (900 ml) and adjusting the pH with concentrated HCl (32 mol %) to a pH= 8.08. The solution was then made up to a final volume of 1L and the pH checked before and after autoclaving.

10 mM Tris HCl buffer (pH = 8.08): A 100 times dilution was made by dissolving 1 M Tris HCl (10 ml) in ddd H₂O (990 ml) and confirming the pH to be 8.08, after which the buffer was autoclaved.

100 mM Tris HCl (pH= 8.08): A 10 times dilution was made by dissolving 1 M Tris HCl (50 ml) in ddd H₂O (450 ml) and checking the pH to be 8.08, after which the buffer was autoclaved.

3.4 Methods

3.4.1 Isolation of IgG from a TB positive and TB negative serum using Protein A Sepharose

A TB positive patient serum and pooled TB negative serum were chosen for the isolation of antibodies using Protein A Sepharose. A modified method was used for the isolation of IgG (175,176), in which serum was incubated with a slurry of Sepharose beads and constantly rotated to allow IgG binding. The amount of Sepharose required was calculated based on the binding capacity, which was given to be 10 mg IgG/ ml of conjugated Sepharose. Thus, for 3 ml of Sepharose a total of 30 mg of IgG could be bound. To prevent overloading of the Protein A beads, only 1 ml of serum (8-17 mg IgG/ml serum) was added to 3 ml of Sepharose. The Protein A, immobilized on Sepharose (3 ml) was subsequently transferred to a 50 ml tube and centrifuged at 3000 rpm for 5

minutes at room temperature. The supernatant was discarded and replaced with 10 mM Tris HCl buffer (pH = 8.08) until the final volume in the tube was 20 ml. The washing procedure repeated another three times. After the last washing step, the supernatant was removed, leaving the Sepharose just covered in buffer. Serum aliquots (500 μ l each) were thawed at 37 °C for 30 minutes. Two aliquots (0.5 ml each) were added to the Sepharose and the volume was adjusted to 20 ml with 10 mM Tris HCl to effect a final serum dilution of 1: 20. The serum was incubated at room temperature with rotation for 2 hours after which the Sepharose was left to settle out. The IgG depleted serum fraction was removed and transferred to a labelled 50 ml tube.

The remaining unbound IgG was removed from the protein-A beads by washing with 100 mM Tris HCl, keeping the final volume in each tube 20ml and then removing the supernatant after gentle mixing. This was repeated twice, after which the buffer was changed to 10 mM Tris HCl for another three washes. The supernatant of the last washing step was measured at 280 nm against a suitable blank for the efficiency of washing. The Sepharose in the tube was finally washed once more with 10 mM Tris.

The bound IgG was removed by incubating the Sepharose with 0.1 M glycine (3 ml, pH = 2.7) for 2 minutes and transferring the supernatant into tubes containing 1M Tris HCl (200 μ l, pH= 8.08) to neutralize the acid. This process was repeated 7 times using 0.1 M glycine (2 ml) and incubation time of 2 minutes. The efficiency of protein elution from the Sepharose was monitored at 280 nm against a suitable blank. The IgG fractions were pooled and dialyzed against 1.5L of 1 x PBS with two exchanges after 12 hours and 6 hours. The IgG depleted serum fraction isolated earlier was also dialyzed in the same manner. After dialysis, the solutions were transferred to 50 ml tubes, of which 100 μ l was removed for protein concentration determination. To the dialyzed IgG from the TB positive serum (11.8 ml) and depleted serum fractions from the TB positive serum (11.8 ml), glycerol (8 ml, 40% final concentration) and 1% benzyl alcohol solution (200 μ l) was added and the mixture filtered through a 0.2 μ m Ministart filter into sterile 50 ml tubes and the IgG solution (20 ml) aliquoted into 0.5 ml cryotubes that were subsequently

stored at -20 °C. The same isolation process was performed for the TB negative serum sample.

3.4.2 Removal of glycerol from IgG samples for biosensor and ELISA analysis

To prepare the IgG and depleted serum fractions for IA sys biosensor analysis, the glycerol had to be removed by ultrafiltration. VetaSpin Micro columns were pre-washed with PBS (400 µl) by centrifuging at 10 000 x g for 15 minutes using a Hermle Z 160 M centrifuge (Hersteller Spintron Inc., Germany). The glycerol containing samples (400 µl) were then transferred to the spin columns and centrifuged at 10,000 x g for 40 minutes. The filtrate was removed and 200 µl of 1 x PBS added to the retentate and again centrifuged. This process was repeated another 5 times for each glycerol-containing sample. The final volume was reconstituted to the original sample volume (400 µl) with 1 x PBS. The concentration of IgG in the purified samples was determined by absorbance measurement at 280 nm using a SHIMADZU Spectrophotometer and an extinction coefficient of $1.4 \text{ M}^{-1}\text{cm}^{-1}$.

3.4.3 SDS-polyacrylamide gel electrophoresis (PAGE) of isolated IgG and depleted serum fractions

The purified IgG fractions and depleted sera were analyzed by SDS-PAGE according to the method of Ey *et al.* (177) in a MINIVE complete vertical electrophoresis system apparatus (Amersham Pharmacia Biotech AB, USA). The protein concentration of the IgG fractions as well as depleted serum fractions was determined using the absorbance at 280 nm and extinction coefficient of $1.4 \text{ M}^{-1}\text{cm}^{-1}$. The corresponding amount of 10 µg of protein was aliquoted into Eppendorf tubes and four times the volume of acetone added to each sample. The samples were then left to precipitate overnight at -70 °C. The next day the samples were centrifuged at 14,000 x g for 1 hour at 4 °C with the Hermle Z 160 M centrifuge. The supernatant was gently removed and the samples dried under vacuum for 20 minutes. To the dried precipitates, ddd H₂O (8 µl) was added to re-suspend the protein pellet as well as non-reducing sample buffer (8 µl). After boiling the samples (16 µl) at 100 °C for 5 minutes, sample (10 µl) was loaded on to a gel consisting of a 10%

separating and 4% stacking gel. The Low Molecular Weight Markers (14.5- 97 kDa) were loaded to indicate the mass distribution on the gel. The gel was subsequently run at 60V for one hour and then at 120V for three hours until the bromophenol blue line was 0.5 cm from the end of the gel. The gel was stained with a colloidal Coomassie blue stain for 24 hours and then destained with colloidal destain buffer (part 1) for one hour and subsequently with the colloidal destained buffer (part 2) for a further 24 hours.

3.4.4 Preparation of MA containing liposomes for biosensor analysis

Stock solution of PC (100 mg/ml) was prepared by dissolving the weighed amounts in chloroform. MA containing liposomes were prepared by adding PC stock (90 μ l) to dried MA (1 mg) in an amber glass vial at 4 °C. Empty liposomes, i.e. with no MA, were prepared by using only the PC stock (90 μ l). The liposome ingredients were dried with nitrogen gas in a heat block at 85 °C for 10 minutes. Liposome formation was induced by adding saline (0.9% NaCl, 2 ml) to the dried liposome ingredients and heating on a heat block at 85 °C for 20 minutes, with vortexing every 5 minutes. The liposomes were subsequently sonicated for 2 minutes at 30% duty cycle at an output of 3% with a Model B-30 Branson sonifier (Sonifier Power Company, USA). The sonicator tip was washed with chloroform and rinsed with distilled water before and after use. The liposomes were aliquoted (200 μ l) into 10 tubes and kept at -20 °C overnight before freeze-drying. After freeze-drying, PBS/AE buffer (2 ml) was added to each tube containing liposomes. The tubes were placed in a heat block for 20 minutes and sonicated as before.

3.4.5 Detection of anti-MA antibody (IgG) with IAsys affinity biosensor

The IAsys resonant mirror biosensor system and twin-cell non-derivatized cuvettes were from Affinity Sensors (Cambridge, United Kingdom). The sensor was set for a data-sampling interval of 0.4s, temperature of 25 °C and stirring rate of 75% for all experiments. The cells were rinsed three times prior to use with 96% ethanol followed by extensive washing with PBS/AE. Initially PBS/AE (60 μ l) was added into each cell of the cuvette to obtain a stable baseline for 1 minute. The PBS/AE was subsequently aspirated and the surface activated with CPC (50 μ l) for 10 minutes. This was followed by 5 times

washing with PBS/AE (60 μ l) and then substituted with PBS/AE (25 μ l) for a new baseline before immobilization of MA containing liposomes (25 μ l) to the surface for 20 minutes. The immobilized liposomes were then finally washed 5 times with PBS/AE (60 μ l) and substituted with saponin (50 μ l) incubated for 10 minutes. The cells were then washed 5 times with PBS/AE and each cell content substituted with PBS/AE (25 μ l) and left for about 5 -10 minutes to achieve a stable baseline. For first exposure of antigen to IgG an IgG solution (0.04 mg/ ml, 10 μ l) in PBS/AE was added to immobilized MA/ PC liposomes and binding measured for 10 minutes. After first exposure, a second exposure of antigen to IgG was performed. An IgG solution (0.08 mg/ ml, 10 μ l) pre-incubated with MA/ PC or PC (empty) liposomes, was added to the first exposure mixture, containing IgG and MA/ PC liposomes, and binding measured for a further 10 minutes. Finally, dissociation of antibodies was effected with 3 times PBS/AE washing and measurement of the response for 5 minutes.

3.4.6 Regeneration of non-derivatized cuvettes

Regeneration was effected by initial 3 times washing with 96% ethanol for one minute, followed by 7 times washing with 70 μ l PBS/AE for 1 minute. The surface was then finally treated with 50 μ l potassium hydroxide (12.5 M) for 2 minutes and followed by 7 times washing with 70 μ l PBS/AE for 1 minute.

3.5 Results

3.5.1 Isolation of IgG from a TB positive and TB negative serum using Protein A Sepharose

In order to determine whether antibodies are the serum components binding to MA liposomes immobilized on the surface of an IAsys affinity biosensor, antibodies had to be separated from the rest of the serum components and analyzed separately. The sera chosen for this purpose was a TB positive serum (no. 260) and a pooled TBnegativeserum, which gave good responses to MA in ELISA. The isolation of IgG

using Protein A Sepharose was monitored using a non-reducing SDS-PAGE gel (figure 3.2).

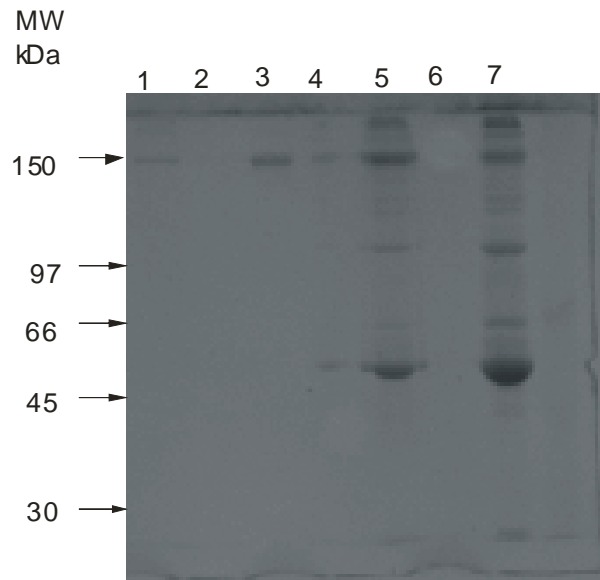


Figure 3.2: Non-reduced SDS-PAGE gel indicating the purity of the protein A purified human IgG fraction compared with a standard mouse IgG sample. Each lane was loaded with 10 μg of protein in non-reducing buffer. The samples represented are (1) mouse IgG (2) blank, (3) isolated IgG fraction from the TB positive patient, (4) blank, (5) TB positive serum before IgG isolation (6) blank, (7) TB positive serum depleted of IgG.

The results shown in figure 3.2 indicated that pure IgG was isolated from the TB positive serum (lane 3). The molecular weight of the isolated TB positive IgG correlated well with that of the pure mouse IgG (lane 1, 150 kDa band). The presence of IgG in the serum sample before antibody isolation can be seen in lane 5 of figure figure 3.2. There appeared to be some sample overflow from lane 5 to lane 4, which was not loaded with any sample. It was further noted that a band at 150 kDa still remained in the serum depleted of IgG (lane 7, fig 3.2). The same protocol for antibody isolation was used to deplete the TBnegativecontrol serum of IgG. From these results it could be concluded that IgG isolation using Protein A Sepharose yielded pure samples of IgG.

3.5.2 Biological activity of isolated and purified IgG in ELISA

The antibody activity of isolated IgG fractions from TB positive and TB negative control sera to MA and cholesterol was determined and compared to that of the whole sera using ELISA. Prior to ELISA analysis, the IgG samples were purified by ultrafiltration to remove the glycerol and benzyl alcohol preservatives which would interfere in the ELISA assay. Purified IgG samples were reconstituted in PBS buffer to represent a 1: 20 dilution of serum, previously optimized for ELISA (64).

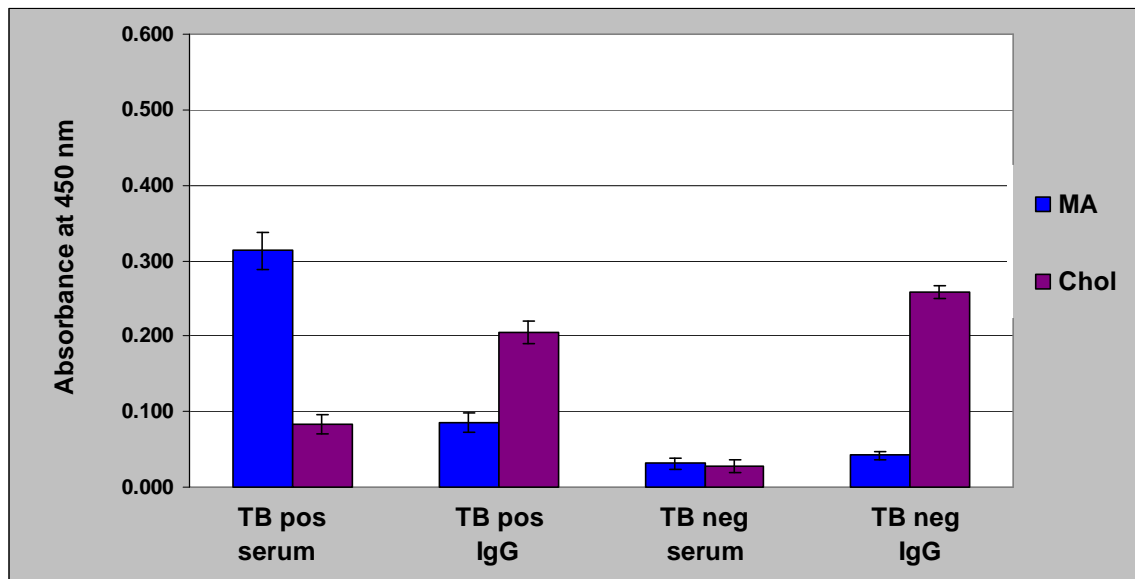


Figure 3.3: Response of serum and isolated IgG fractions to MA and cholesterol in ELISA. Absorbance was measured at 450 nm in ELISA, after incubation with whole serum and isolated IgG from TB positive and pooled TBnegative serum samples. The unfractionated serum samples were diluted 20 times and the IgG fractions were made up to represent a serum dilution of 1: 20. The error bars indicate the standard error of the mean with $n=3$ or >3 .

The results obtained in figure 3.3 indicated that the isolated and purified IgG from both the TB positive and TBnegative sera were still capable of recognizing both MA and cholesterol coated onto ELISA plates. It was also seen that there was a reduction in activity to MA in the TB positive IgG fraction compared with the whole serum, but activity to MA was retained in the TBnegative IgG sample. It was also noted that the

response to cholesterol of both the TB positive and TBnegativeIgG fractions was significantly more than that of the corresponding whole sera.

The ability to distinguish between the TB positive and TBnegativesera using MA in ELISA was retained in the isolated IgG fractions. The TB positive IgG sample responded significantly more to MA than the TBnegativeIgG fraction ($P < 0.003$). Thus, the isolated IgG fractions from both the TB positive and TB negative sera retained antibody activity even after the isolation and purification processes.

3.5.3 Biological activity of the isolated IgG fractions to MA/PC liposomes measured on a resonant mirror biosensor

It has been hypothesized that IgG present in patient serum was responsible for the binding seen to MA liposomes in the biosensor assay developed by Siko (71) and Thanyani (162), but this needed to be verified.

In order to confirm that IgG is the substance from serum responsible for the mass accumulation onto MA containing liposomes on the IAsys affinity biosensor, binding of the isolated IgG fractions (TB positive and TB neg) to immobilized MA/ PC liposomes was measured. The IgG fractions were purified by ultrafiltration to remove the glycerol and benzyl alcohol, which was shown to interfere with the biosensor analysis (data not shown). The concentration of the IgG samples was determined using the absorbance at 280 nm and the extinction coefficient of $1.4 \text{ M}^{-1}\text{cm}^{-1}$. The IgG samples were then made up to the required concentrations in PBS/AE buffer.

The results presented in figure 3.4 confirm that IgG present in serum is capable of recognizing MA/PC immobilized liposomes on the resonant mirror biosensor. It was also noted that although the two cuvette cells differed in responsiveness, they showed the same tendency. In both channel 1 and 2 (fig 3.4), the TB positive IgG fraction bound significantly more to the MA/ PC liposome layer than the TB negative IgG sample.

The results shown in figure 3.4 confirmed that IgG from human serum was one of the components which accumulated on immobilized MA/PC liposomes on the resonant mirror biosensor.

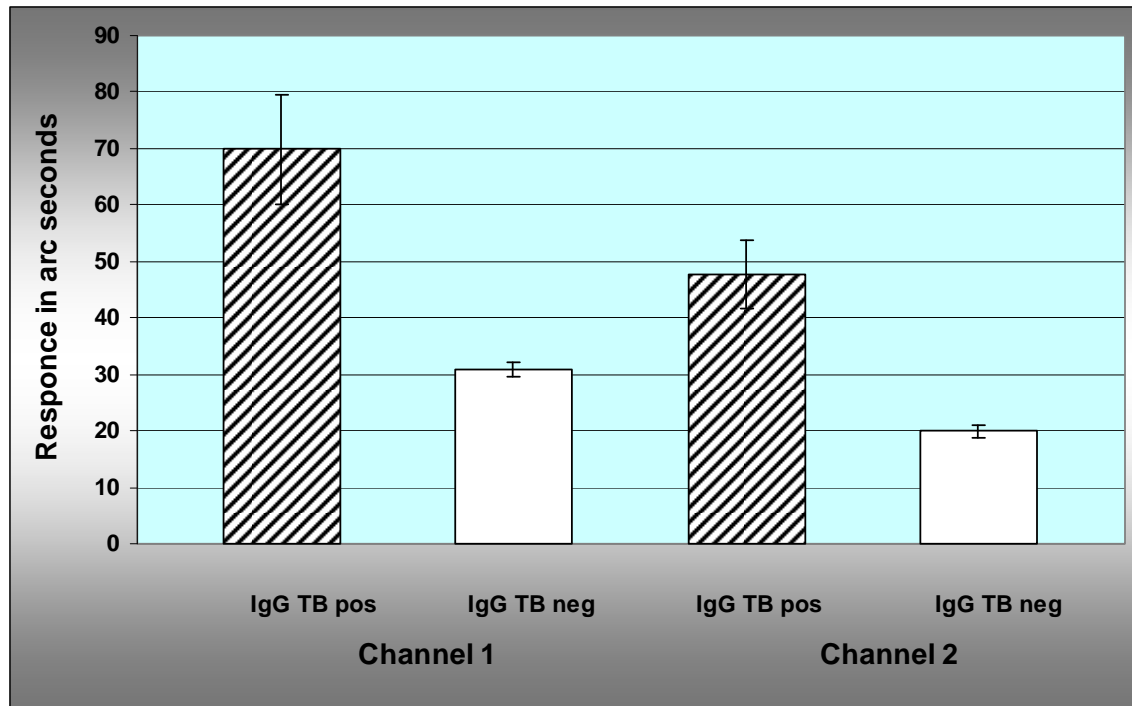


Figure 3.4: Response of isolated IgG from a TB positive patient and a pooled TB negative serum to MA / PC liposomes on a resonant mirror biosensor. The first exposure of MA/ PC liposomes to isolated and purified IgG from a TB positive and TB negative serum was at a protein concentration of 0.04 mg/ml. The binding was measured as a response in arc seconds in both cuvette cells of the biosensor (channel 1 and channel 2). The error bars indicate the standard error of the mean ($n = 5$).

3.5.4 Analysing the inhibition of IgG accumulation onto immobilized MA after pre-incubation with MA/ PC or PC liposomes

It was previously shown that TB positive patient sera could be inhibited with MA containing liposomes significantly more than TB negative sera (162). It was determined whether the inhibition previously seen on the resonant mirror biosensor using whole sera was due to the inhibition of serum antibodies. In order to accomplish this, the isolated IgG from the TB positive and TB negative sera was pre-incubated with liposomes

either devoid of MA or containing MA and the percentage inhibition determined on a resonant mirror biosensor.

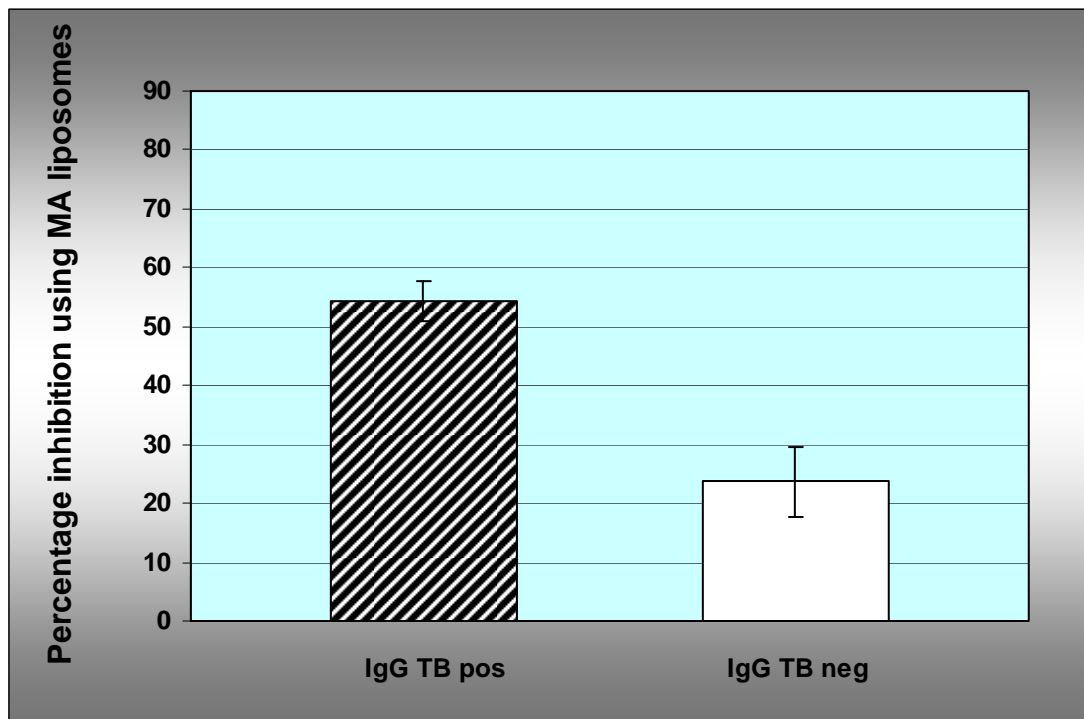


Figure 3.5: Percentage inhibition of IgG binding to immobilized MA/ PC liposomes after a pre-incubation of IgG samples with MA/ PC or PC only (empty) liposomes on a resonant mirror biosensor. The binding of isolated IgG from a TB positive patient (IgG TB pos) and TB negative serum (IgG TB neg) was measured to immobilized MA/ PC liposomes after pre-incubating the IgG samples (0.04 mg/ml) with a 0.5 mg/ml concentration of MA liposomes. The percentage inhibition represents the reduction in signal seen when comparing IgG pre-incubated with liposomes not containing MA and liposomes containing MA. Error bars indicate the standard error of the mean with $n \geq 4$.

Inhibition was calculated as the percentage reduction in signal seen between incubation with PC liposomes only, and after incubation with MA/ PC liposomes. From figure 3.5 it could be seen that the IgG isolated from TB positive serum (IgG TB pos) and TB negative serum (IgG TB neg) were both inhibited by MA containing liposomes, but to different degrees. The IgG from the TB positive patient was inhibited significantly more than the IgG from the TB negative patient serum ($P < 0.007$).

As could be seen from table 3.1, both the ELISA and the biosensor techniques were capable of making the distinction between the TB positive and TB negative sera and IgG fractions.

Table 3.1: Summary of ELISA and biosensor results for the TB positive and TB negative sera and IgG fractions

Technique	TB positive serum	TB negative serum	TB positive IgG	TB negative IgG
Corrected absorbance on ELISA	0.313 ± 0.024	0.032 ± 0.007	0.086 ± 0.013	0.043 ± 0.005
Percentage inhibition on resonant mirror biosensor	16 ± 0.7%	-50 ± 11%	54 ± 3%	24 ± 6%

The serum component analyzed in ELISA is known to be antibodies and from the results presented above and summarized in table 3.1, it has now been confirmed that antibodies are the serum components binding to MA liposomes on the resonant mirror biosensor and making the distinction between TB positive and TB negative patient sera.

3.6 Discussion

Mycolic acid has been recognized as an antigen and was analyzed for its potential use in a serodiagnostic assay in an HIV burdened population by Schleicher *et al.* (64). The low sensitivity obtained with ELISA was improved upon by using the resonant mirror biosensor (162). Furthermore, the newly developed Mycolic acid Antibody Real-Time Inhibition test (MARTI-test) (72) has shown to be able to distinguish between a range of TB positive and TB negative sera with 84% accuracy using MA immobilized onto the biosensor sensor surface. The improved sensitivity was ascribed to the ability of the resonant mirror biosensor to detect both the low and high affinity molecular interactions whereas ELISA only detects high affinity binding that can withstand extensive washing procedures after the binding event (178). The serum components binding to the

immobilized antigens and detected in real-time by the biosensor assay were thought to be antibodies.

It was set out to determine whether antibodies are one of the serum components capable of binding to immobilized MA/PC liposomes and which could distinguish between TB positive and TB negative sera on the biosensor surface. To achieve this objective, antibodies of the IgG isotype were isolated from a TB positive and TB negative serum using Protein A Sepharose. By performing SDS-PAGE it was confirmed that IgG isolation was successful and no contaminating proteins were present at the resolution capacity of the gel. Protein A is known to bind only IgG, excluding the IgG₃ subtype (179). The remaining protein band at 150 kDa in the serum depleted of IgG could thus have been unbound IgG₃ or IgA monomers present in serum (180).

The activity of the isolated IgG fractions from the TB positive and TB negative sera to both MA and cholesterol were subsequently analyzed using ELISA. From the ELISA assay it was noticed that some of the IgG activity to MA from the TB positive sample was lost during the isolation and purification process, but remained unchanged for the TB negative IgG sample. The antibody activity to MA from the TB positive IgG sample was still retained to such a degree that the distinction between the TB positive and TB negative samples could be made.

The loss in antibody activity to MA from the TB positive sample could have been due to denaturation of protein during elution from Protein A Sepharose. Elution of IgG was achieved by using a low pH glycine solution, which is known to result in protein aggregation and which may have caused some loss in antibody function (181). One method recently developed to overcome protein denaturation during antibody elution from Protein A columns is the use of an arginine solution (182). This could be investigated in future experiments.

In contrast, the antibody activity to cholesterol was increased in both the TB positive and the TB negative IgG samples compared with the serum response to cholesterol. It is

known that all people have antibodies of the IgG subclass to cholesterol (145). The increased response of the IgG samples to cholesterol was thought to be due to the release of lipoprotein-bound IgG from the serum during the IgG isolation process (155,183).

After showing that antibody activity was retained, the isolated IgG fractions were next evaluated on the resonant mirror biosensor to immobilized MA/ PC liposomes. It was previously found that TB positive serum bound more to a MA liposome coated surface than the TB negative control serum (71) and the results presented here using IgG fractions confirmed that the binding previously seen on the biosensor to MA/ PC liposomes was at least partly due to IgG antibodies. This data was used to support the principle of the MARTI-biosensor test for TB serodiagnosis (72). The IgG samples were also inhibited with MA containing liposomes in a similar manner as previously observed using whole sera (71,162). These results confirmed that anti-MA antibodies bind to MA/ PC liposomes immobilized onto a resonant mirror biosensor. In accordance with the ELISA results presented in chapter 2, it was again observed that TB positive patient serum contained significantly more anti-MA antibodies than TB negative serum, allowing for the distinction between TB and non-TB patients in the MARTI-biosensor assay (72).

In chapter 2 of this thesis it was also shown that cross-reactive anti-cholesterol antibodies do exist in TB negative serum capable of recognizing MA contained in liposomes. Previously, Thanyani (162) set out to determine whether anti-cholesterol antibodies would interfere in the biosensor inhibition assay. He tried to determine this by pre-incubating the sera with 50 mol % cholesterol liposomes in an attempt to inhibit the binding signal of a TB negative serum to MA/ PC liposomes on the biosensor. The results generated were however not conclusive, because it has been shown here and previously (145,152,153,154) that anti-cholesterol antibodies only recognize > 56 mol % cholesterol liposomes. It is thus not expected that 50 mol % cholesterol liposomes would inhibit anti-cholesterol antibody binding on the resonant mirror biosensor. To establish whether the binding of anti-cholesterol antibodies could be the reason behind the hampered

specificity of the resonant mirror biosensor assay using MA containing liposomes, further investigation would be required.

In conclusion, the results presented here confirmed that the biosensor based TB serodiagnostic assay (so-called MARTI-test) developed by Thanyani *et al.* (72) is based on the detection of IgG antibodies in the serum of tuberculosis patients. The newly developed biosensor assay has an accuracy of 84%, but the specificity and sensitivity still do not match that set out by the World Health Organization for a serodiagnostic assay. It is hypothesized that the use of a more specific antigen, such as a subclass of MA, could aid the biosensor to achieve the requirements set out by the WHO (57). For this reason, the antigenicity of the MA subclasses present in *M. tb* is investigated in the next chapter.

Chapter 4: Immunochemical analysis of MA subclasses from *Mycobacterium tuberculosis*

4.1 Introduction

The phenomenon that lipids can act as immunogenic substances has been known since 1941 (184), while the mechanism in which they are presented to the immune system has only recently been revealed (119). It has now been firmly established that lipids and carbohydrates can stimulate specific cellular responses and even generate IgG antibodies (185). Mycolic acids from *M. tb* were first identified as antigens in 1999 after it was shown that antibodies to the cell wall lipid, trehalose-6,6'-dimycolate (TDM), recognised the MA moiety as the major contributor to the epitope (116). Since then antibodies to a mixture of free MA have been investigated as surrogate markers for TB using techniques such as ELISA and affinity biosensors (64,72). The ELISA assay gave a sensitivity of 51% and specificity of 63% which did not comply with the requirements set out by the World Health Organisation for a serodiagnostic test (57). The biosensor inhibition assay (72) was subsequently developed and an improved sensitivity of 86.7% was obtained, but yielded a specificity which could not reach the specifications stipulated by the WHO of 95%. One way in which the accuracy of the ELISA and biosensor assays could possibly be increased, was to determine if a particular subclass of MA with distinct structural features, would prove to be a better antigen than the natural mixture of MA.

As discussed in the introduction of this document, mycolic acids (figure 1.4, p 15) are long chain α -alkyl β -hydroxy fatty acids from mycobacteria consisting of two hydrophobic chains and a polar head group (127,128,186). The “mero” chain contains polar and/or non-polar functional groups which define the MA subclass (187) and of which the exact locations have been revealed (128). The MA containing only *cis*-cyclopropanation or double bonds is referred to as the α -MA. The MeO- and Ket-mycolates contain an ether and carbonyl group at the distal position of the “mero” chain respectively and either *cis*-or *trans*-cyclopropanation at the proximal position (129). A

further characteristic of the oxygenated subclasses is that there is a methyl branch adjacent to the oxygenated as well as the *trans*-cyclopropane functional groups. The most abundant MA of each subclass present in *M. tb* is presented in the introduction (figure 1.5, p 17).

The MA subclasses not only differ with regards to their chemical structures, but they also assume different conformations in compressed monolayers (133). Initial studies on MA subclass conformation suggested that the “mero” chain folded at the proximal cyclopropane position to give a three chain conformation, which would then unfold to different degrees, depending on the MA subclass (133). More recent investigations have however shown the Ket-MA subclass to be more inclined to adopt a “W” shape, in which the “mero” chain together with the α -alkyl chain fold to form four alkyl stretches adjacent to one another (figure 1.6) (91). The other oxygenated subclass, MeO-MA, appears to favour a “W” conformation at low temperature, but above 37 °C tends to assume more relaxed conformations (figure 1.6) (91). The α -MA subclass exists as many different liquid condensed phases with change in temperature, of which the extended conformation is probably the most favoured (figure 4.1) (91). The different conformations assumed by the MA subclasses are also thought to exist within the mycobacterial cell wall (figure 1.6) (61).

The ability of MA to fold into a specific conformation seems to be dependent on the fine chemical structure, such as chain length (188) as well as the functional groups present in the “mero” chain (91). Apart from the intra-molecular bonding within the MA structure to yield various conformations, the possibility also exists that the MA subclasses associate inter-molecularly to form specific aggregated states.

The aggregated states of MA may differ depending on the composition of the sample. As determined in chapter 2 of this document, it would appear that a mixture of MA in liposomes consisting of all three subclasses present in *M. tb* resembles the liquid ordered state of cholesterol. The resemblance between MA and chol aggregated states could pose a complication in developing a serodiagnostic assay for TB. It was hypothesized that the

use of a single subclass of *M. tb* would form a different arrangement on ELISA plates and in liposomes, creating an epitope possibly more specific for recognition by anti-MA antibodies.

In this chapter, the naturally occurring MA subclasses from a virulent strain of *M. tb* were isolated and purified, and it was investigated whether any or all of the MA subclasses could make the distinction between a range of TB positive and TB negative sera in an ELISA assay. In literature, MA is analyzed in both the methyl-ester (121) and free acid form (64). In this study it was also determined which form of MA was optimal for antibody recognition, and if the solvent used for lipid coating would affect the response of patient serum antibodies to MA in ELISA.

4.2 Hypothesis

The strength of interaction and specificity of recognition of MAs by human antibodies is determined by: the nature of the MA coat, as a result of the solvent used for their introduction onto the ELISA plates, and the conformation of MA as determined by the functional groups within the “mero” chains of the representative MA subclasses.

4.3 Materials

4.3.1 Source of sera

The amount of sera available was limited and sera were selected and sometimes pooled to fulfil the requirements of each study.

For the first study, relating to the effect of coating solution on the recognition of MA by patient serum antibodies, a pooled TB positive and pooled TB negative serum were selected. The TB positive sample was created by pooling the sera of 6 patients, 3 TB positive /HIV positive and 3 TB positive /HIV negative, selected from the collection reported in Schleicher *et al.* (64). The TB negative sample consisted of pooled serum from 6 healthy individuals working in the Biochemistry department at the University of

Pretoria in research groups other than the TB research group and with no clinical signs of tuberculosis.

For the second study relating to the MA subclasses, 10 sera were selected from patients that were admitted to the general medical wards of the Helen Joseph Hospital; Johannesburg, South Africa as provided by Dr. G. Schleicher in 2000. The 5 TB positive (Patient no. 45, 129, 74, 42, 73) and 5 TB negative patient sera (Patient no. 22, 94, 90, 21, 7) were selected to be HIV negative and the TB positive patients were diagnosed according to standard clinical procedures as well as by biosensor technology previously performed for another study (72). The TB negative patients were hospitalized for medical conditions other than TB, but showing no evidence of active tuberculosis.

To assess for a prozone effect in the ELISA assay, a pooled TB positive serum was created by combining the same TB positive sera used for subclass analysis (Patient serum no. 45, 129, 74, 42 and 73 from the Schleicher collection, 2002). In the same manner a pooled TB negative serum was created using patient serum from the Schleicher collection, 2002 (Patient no. 22, 94, 90, 21, 7).

4.3.2 List of reagents and buffers

4.3.2.1 Chemicals obtained from Saarchem, a division of Merck, South Africa

Acetone (analytical grade), analytical thin layer chromatography plate, (aluminium sheets, 20 x 20 cm, silica gel 60), chloroform (analytical grade, stabilized with 25 ppm amylene/ethanol 0.4-1%), citric acid, tri-sodium citrate, ethyl acetate (analytical grade), hexane (distilled 24 hours before use), di-hydrogen potassium phosphate (KH_2PO_4), molybdato-phosphoric acid, potassium chloride (KCl), preparative thin layer chromatography plates (PTLC, 20 x 20, Silica gel 60), propan-2-ol (99% pure), silica gel 60 (0.04-0.063 mm), sodium chloride (NaCl), di-sodium hydrogen phosphate (Na_2HPO_4), toluene (analytical grade).

4.3.2.2 Chemicals obtained from Sigma, Aldrich, Germany

Cholesterol (99% pure), deuterated chloroform (anhydrous, 99.8% pure), L- α -phosphatidylcholine type XVI- ϵ (99%, lyophilized powder), trimethylsilyldiazomethane (TMDM, 2 M solution in diethyl ether).

4.3.2.3 Chemicals obtained from BDH chemicals, England

Calcium chloride (anhydrous), dichloromethane (HPLC grade, stabilized with 50 ppm 2-methyl-2-butene), hydrogen peroxide urea adduct (Laboratory reagent), methanol (HPLC grade).

4.3.2.4 Other

Diethyl ether (analytical reagent, LAB-Scan, Analytical Sciences, Ireland), ethanol (analytical grade, BDH chemicals, Halfway House, South Africa), 96 well plates (Serowell®, Bibby Sterilin, UK), potassium hydroxide (Chemical Suppliers, (Pty) LTD, South Africa).

Natural MAs (unesterified MA): The natural MA mixture was purchased from Sigma, South Africa, and was from the virulent human strain *M. tb* H37Rv, and of the batch M4537.

PBS (phosphate buffered saline) stock solution: 20x PBS stock was prepared by dissolving 160 g of sodium chloride (NaCl), 4 g potassium chloride (KCl), 4 g of di-hydrogen potassium phosphate (KH₂PO₄), and 23 g of di-sodium hydrogen phosphate (Na₂HPO₄) in a total of 900 ml of ultra-pure double distilled, de-ionized water (dddH₂O), while stirring. The solution was brought to a final volume of 1L with ddd H₂O and filtered through a 0.22 μ m membrane filter (Whatman Industrial Ltd., England).

1x PBS Buffer: This was prepared by dissolving 50 ml of the 20 X PBS buffer in 950 ml of ddd H₂O. The pH was checked to be 7.4.

0.5% Casein/ PBS: In a 1 litre flask, PBS (50 ml, 20 x PBS stock) was added to triple distilled deionised water (ddd H₂O, 700 ml). To this solution 5 g of casein (carbohydrate and fatty acid free, Calbiochem) was added and dissolved by stirring at 37 °C for 2 hours. The solution was then stored at 4 °C overnight and the next day the pH was adjusted to 7.4 with 1 M sodium hydroxide (NaOH) and volume finally made up to 1 litre using ddd H₂O.

Goat anti-human IgG peroxidase conjugate (IgG whole molecule, Sigma, Steinheim, Germany, lot 129 H4878): The conjugate was prepared by adding 10 µl of peroxidase conjugate to 10 ml of 0.5% Casein/PBS. This was prepared 5 minutes prior to use.

0.1 M Citrate buffer: 0.1 M citric acid (450 ml) solution was added to a 0.1 M tri-sodium citrate solution (450 ml) to a pH of 4.5. The solution was then made up to a final volume of 1L with ddd H₂O.

O-Phenylenediamine dihydrochloride (OPD) Substrate: The substrate was prepared just before use and kept in the dark. To 10 ml of 0.1 M citrate buffer, 10 mg of OPD (Sigma, a division of Aldrich, Germany) and 8 mg of hydrogen peroxide urea adduct (ground pellets of 32 mol %) were added.

0.9% Saline: This was prepared by dissolving 9 g of sodium chloride in 100 ml of ddd H₂O.

4.4 Methods

4.4.1 Quality considerations

The ¹H and ¹³C Nuclear Magnetic Resonance (NMR) spectra were recorded on a Bruker Advance DRX-500 spectrometer or Bruker AC-300 spectrometer with chemical shifts expressed in ppm and samples dissolved in deuterated chloroform. The outcome of chemical reactions and separations was first assessed by TLC, of which visualization was

done by staining with a 5% (w/v) solution of molybdato-phosphoric acid in methanol.

4.4.2 Methyl-esterification of MA

To form the methyl esters, unesterified MA (100 mg, ~ 0.1 mmol) was dissolved in a mixture of toluene: methanol (5:1, 18 ml). Thereafter trimethylsilyldiazomethane (TMDM, 2 M solution, 0.2 ml, 0.4 mmol) was added, followed by a further 3 additions of TMDM (0.1 ml, 0.2 mmol) every 45 minutes. The mixture was stirred for 72 hours and quenched by evaporation. The residue was dissolved in dichloromethane (15 ml) and water (10 ml) was added. The two layers were separated and the water layer extracted with dichloromethane (2 x 10 ml). The combined organic layers were dried and the solvent evaporated to give the desired compound (98 mg, ~ 97%). The NMR spectra of the compounds obtained, corresponded to those reported in the literature for methyl MAs (189).

4.4.2.1 NMR analysis of unesterified MA before methylation

δ_{H} (300): 3.7 (1H, m, CH_2OH), 3.33 (3H, s, CHOCH_3), 3.15 (m, unknown), 2.97 (1H, m, CHOCH_3), 2.52 (1H, m, $\text{CHC}=\text{O}$), 2.43 (1H, m, $\text{CH}(\text{CH}_2)_{23}\text{CH}_3$), 2.42 (2H, m, $\text{CH}_2\text{CHC}=\text{O}$), 1.72-1.0 (m, CH_2), 0.98-0.82 (m, CH_3), 0.65 (3H, m, CH *cis*-cyclopropane and CH adjacent to *trans*-cyclopropane), 0.56 (1H, td, J 4, 8.0 Hz, CH_2 *cis*-cyclopropane), 0.18-0.1 (3H, m, *trans*-cyclopropane), -0.33 (1H, m, CH_2 *cis*-cyclopropane), Appendix, figure 1.

δ_{C} (125.8 MHz): 200.03 (C=O), 178.9 (COOH), 85.9 (CHOCH_3), 72.71 (CHOH), 58.08 (OCH_3), 35.77 (CH_2CHOH), 32.13 (CH_2), 32.79 (CH_2), 30.6 (CH_2), 29.73 (CH_2), 29.1 (CH_2), 28.41 (CH_2), 27.94 (CH_2), 27.38 (CH_2), 26.1 (CH_2), 24.12 (CH_2), 23.00 (CH *cis*-cyclopropane), 16.15, 15.26 (CH cyclopropane), 14.46 (CH_3), 10.90 (CH_2 cyclopropane)

4.4.2.2 NMR analysis of the methyl ester of the natural MA mixture (ME-MA)

δ_{H} (300): 3.73 (3H, s, CO_2CH_3), 3.69 (1H, m, CH_2OH), 3.30 (3H, s, CHOCH_3), 2.97 (1H, m, CHOCH_3), 2.45 (1H, m, $\text{CH}(\text{CH}_2)_{23}\text{CH}_3$), 1.57-1.0 (CH_2), 0.90-0.81 (m, CH_3), 0.65 (3H, m, *cis*-cyclopropane and CH adjacent to *trans*-cyclopropane), 0.57 (1H, m, CH *cis*-

cyclopropane), 0.1 (1H, m, $\underline{\text{C}}\text{H}_2$ *trans*-cyclopropane), -0.35 (1H, m, $\underline{\text{C}}\text{H}_2$ *cis*-cyclopropane).

δ_{C} (125): 176.21 ($\underline{\text{C}}\text{O}_2\text{C}\underline{\text{H}}_3$), 85.43 ($\text{H}\underline{\text{C}}\text{O}\underline{\text{C}}\text{H}_3$), 72.29 ($\underline{\text{C}}\text{H}\text{O}\underline{\text{H}}$), 57.71 ($\text{C}\underline{\text{O}}\underline{\text{C}}\underline{\text{H}}_3$), 51.53 ($\text{C}\underline{\text{O}}_2\text{C}\underline{\text{H}}_3$), 50.90 ($\underline{\text{C}}\text{H}(\text{C}\underline{\text{H}}_2)_{23}\text{C}\underline{\text{H}}_3$), 35.70 ($\underline{\text{C}}\underline{\text{H}}_2$), 35.23 ($\underline{\text{C}}\underline{\text{H}}\text{C}\underline{\text{H}}_3$), 31.92 ($\underline{\text{C}}\underline{\text{H}}_2$), 30.45 ($\underline{\text{C}}\underline{\text{H}}_2$), 30.22 ($\underline{\text{C}}\underline{\text{H}}_2$), 29.7 ($\underline{\text{C}}\underline{\text{H}}_2$), 29.43 ($\underline{\text{C}}\underline{\text{H}}_2$), 29.36 ($\underline{\text{C}}\underline{\text{H}}_2$), 28.71 ($\underline{\text{C}}\underline{\text{H}}_2$), 27.41 ($\underline{\text{C}}\underline{\text{H}}_2$), 26.15 ($\underline{\text{C}}\underline{\text{H}}_2$), 25.72 ($\underline{\text{C}}\underline{\text{H}}_2$), 23.71 ($\underline{\text{C}}\underline{\text{H}}_2$), 22.69 ($\underline{\text{C}}\underline{\text{H}}$ *cis*-cyclopropane), 15.76 ($\underline{\text{C}}\underline{\text{H}}$ cyclopropane), 14.11 ($\underline{\text{C}}\underline{\text{H}}_3$), 10.90 ($\underline{\text{C}}\underline{\text{H}}_2$ cyclopropane).

4.4.2.3 Calculation to determine the percentage of each subclass present

The proton NMR of the unesterified MA sample (Appendix A, fig 1) was used to estimate the percentage of each subclass present in the original mixture. For this purpose, the integration of the peak at δ 3.73 (3 ppm) was taken to represent the β -proton (figure 1.4), 3 protons, one from each subclass.

$$\begin{aligned} \text{Equation 1: } I(\alpha) + I(\text{methoxy}) + I(\text{keto}) \\ = 1 \text{ unit area} \end{aligned}$$

Subsequently, the integration of the peaks in the region of δ 0.1-0.2 (0.42 unit area, 3 protons from *trans*-cyclopropane) and δ -0.33 (1.4 unit area, 1 proton from *cis*-cyclopropane) were taken to represent the total cyclopropane protons present.

$$\begin{aligned} \text{Equation 2: } 2(\alpha \text{ has two cyclopropane groups in the mero-chain}) + I(\text{methoxy}) + \\ I(\text{keto}) \\ = (0.42/3) + 1.4 \\ = 1.54 \text{ unit area} \end{aligned}$$

Lastly, the integration of the peak at δ 2.97 (0.9 unit area) was taken to represent the three methoxy protons of the MeO-MA subclass. Thus:

$$\begin{aligned} &= (0.9/3) \\ &= 0.3 \text{ unit area} \sim 30\% \end{aligned}$$

Thus, **30%** of the initial unesterified MA sample was represented by the **MeO-MA** subclass. The percentage α -MA

$$\begin{aligned} &= \text{equation 1} - \text{equation 2} \\ &= 1.54 - 1 \\ &= 0.54 \text{ unit area} \sim 54\% \end{aligned}$$

Thus, **54%** of the initial MA sample was represented by the α -MA subclass and the

remaining **16%** was the contribution from the **Ket-MA** subclass.

4.4.3 Separation of MA subclasses

A similar method was followed as described by Laval *et al.* (190), but differed in respect to the way in which MA was loaded onto the PTLC plates, the percentage of the molybdato-phosphoric acid solution used for visualization and the way in which MA subclasses were recovered from the silica gel plates. The methyl ester of MA (ME-MA, 10 mg) was dissolved in chloroform (0.5 ml) to give a solution a 20 µg/ µl concentration. The MA solution was then spotted on the extremities of the PTLC plates (each spot equivalent to 200 µg) for visualization and the remaining ME-MA was spotted as a band across the PTLC plate, 1.5 cm from the bottom and 2.5 cm from the side. The PTLC plates were run five times in a running solvent of hexane: diethyl ether (9:1) and dried with a heat gun on low heat in between runs. Visualization of the plate extremities was achieved using a 5% solution of molybdato-phosphoric acid in methanol (w/ v) with subsequent charring with a heat gun. The regions on the silica plates corresponding to each of the subclasses α -, MeO- and Ket-methyl MA were scratched off and the methyl esters of MA were extracted with dichloromethane (3 x 15 ml). After each extraction the extract was filtered (Whatman®, 110 mm diameter) and the solvent evaporated on a Buchi rotavapor.

4.4.4 Hydrolysis and purification of mycolic acid

The methyl ester of MA from each subclass (10 mg) was dissolved in a solution of potassium hydroxide and propan-2-ol (1 ml, 100 mg/ml). The mixture was stirred at 85 °C for 3 ½ hours. The reaction was then quenched by adding water (1 ml) and extracting 15 times with hexane (distilled). The combined organic layers were dried with calcium chloride pellets (anhydrous) and the solvent evaporated to yield the free MAs (9.2 mg, ~90%).

After ester hydrolysis, each MA subclass fraction was precipitated with acetone as described before by Goodrum *et al.* (156). The precipitate was then dissolved in a

solution of hexane: ethyl acetate (19:1) and further purified by column chromatography using silica gel 60. Initially the eluent was a hexane: ethyl acetate (19:1) solution, after which the ratio of ethyl acetate was gradually increased with respect to the hexane to a (16:1), (8:1), (6:1), (3:1) and finally (1:1) ratio of hexane: ethyl acetate. Elution of MA was monitored by analytical TLC stained with the 5% molybdatophosphoric acid solution. After solvent collection and evaporation each of the subclasses were submitted for NMR analysis and compared to spectra given in literature (127).

4.4.5 NMR analysis of the separated and purified MA subclasses

4.4.5.1 NMR analysis of purified α -MA

δ_{H} (500 MHz): 3.74 (1H, m, $\underline{\text{C}}\text{HOH}$), 2.48 (1H, m, $\underline{\text{C}}\text{H}(\text{CH}_2)_{23}\text{CH}_3$), 1.75-1.0 ($\underline{\text{C}}\text{H}_2$), 0.95-0.8 ($\underline{\text{C}}\text{H}_3$), 0.66 (2H, m, $\underline{\text{C}}\text{H}$ *cis*-cyclopropane no *trans*-cyclopropane), 0.57 (1H, td, J 4, 8.0 Hz, $\underline{\text{C}}\text{H}_2$ *cis*-cyclopropane), -0.33 (1H, m, $\underline{\text{C}}\text{H}_2$ *cis*-cyclopropane), Appendix, figure 2.

δ_{C} (125.8 MHz): 178.13 ($\underline{\text{C}}\text{OOH}$), 72.19 ($\underline{\text{C}}\text{HOH}$), 50.67 ($\underline{\text{C}}\text{H}(\text{CH}_2)_{23}\text{CH}_3$), 35.58 ($\underline{\text{C}}\text{H}_2$), 31.93 ($\underline{\text{C}}\text{H}_2$), 29.71 ($\underline{\text{C}}\text{H}_2$), 29.67 ($\underline{\text{C}}\text{H}_2$), 29.62 ($\underline{\text{C}}\text{H}_2$), 29.59 ($\underline{\text{C}}\text{H}_2$), 29.51 ($\underline{\text{C}}\text{H}_2$), 29.43 ($\underline{\text{C}}\text{H}_2$), 29.37 ($\underline{\text{C}}\text{H}_2$), 28.73 ($\underline{\text{C}}\text{H}_2$), 27.34 ($\underline{\text{C}}\text{H}_2$), 25.75 ($\underline{\text{C}}\text{H}_2$), 22.69 ($\underline{\text{C}}\text{H}$ *cis*-cyclopropane), 15.79 ($\underline{\text{C}}\text{H}$ *cis*-cyclopropane), 14.11 ($\underline{\text{C}}\text{H}_3$), 10.92 ($\underline{\text{C}}\text{H}_2$ *cis*-cyclopropane), Appendix, figure 3.

4.4.5.2 NMR analysis of purified MeO-MA

δ_{H} (500 MHz): 3.71 (1H, m, $\underline{\text{C}}\text{HOH}$), 3.36 (3H, s, $\text{CHO}\underline{\text{C}}\text{H}_3$), 2.97 (1H, m, $\underline{\text{C}}\text{HO}\underline{\text{C}}\text{H}_3$), 2.47 (1H, dt, $J_1=5.18$ Hz, $J_2=8.85$ Hz, $\underline{\text{C}}\text{H}(\text{CH}_2)_{23}\text{CH}_3$), 1.65-1.08 ($\underline{\text{C}}\text{H}_2$), 0.91-0.82 ($\underline{\text{C}}\text{H}_3$), 0.65 (3H, m, $\underline{\text{C}}\text{H}$ *cis*-cyclopropane and $\underline{\text{C}}\text{H}$ adjacent to *trans*-cyclopropane), 0.56 (1H, td, $J_1=4.2$ Hz, $J_2=8.3$ Hz, $\underline{\text{C}}\text{H}_2$ *cis*-cyclopropane), 0.45 (1H, m, $\underline{\text{C}}\text{H}$ -*trans*-cyclopropane, 10%), 0.21-0.1 (3H, m, *trans*-cyclopropane), -0.33 (1H, m, $\underline{\text{C}}\text{H}_2$ *cis*-cyclopropane), Appendix, figure 4

δ_{C} (125.8 MHz): 177.51 ($\underline{\text{C}}\text{OOH}$), 85.58 ($\underline{\text{C}}\text{O}\underline{\text{C}}\text{H}_3$), 72.16 ($\underline{\text{C}}\text{HOH}$), 57.69 ($\text{CO}\underline{\text{C}}\text{H}_3$),

51.56 ($\underline{\text{C}}\text{H}(\underline{\text{C}}\text{H}_2)_{23}\underline{\text{C}}\text{H}_3$), 35.58 ($\underline{\text{C}}\text{H}_2$), 35.37 ($\underline{\text{C}}\text{H}_2$), 32.39 ($\underline{\text{C}}\text{H}_2$), 31.93 ($\underline{\text{C}}\text{H}_2$), 30.50 ($\underline{\text{C}}\text{H}_2$), 29.98 ($\underline{\text{C}}\text{H}_2$), 29.94 ($\underline{\text{C}}\text{H}_2$), 29.70 ($\underline{\text{C}}\text{H}_2$), 29.61 ($\underline{\text{C}}\text{H}_2$), 29.58 ($\underline{\text{C}}\text{H}_2$), 29.51 ($\underline{\text{C}}\text{H}_2$), 29.42 ($\underline{\text{C}}\text{H}_2$), 29.36 ($\underline{\text{C}}\text{H}_2$), 28.72 ($\underline{\text{C}}\text{H}_2$), 27.57 ($\underline{\text{C}}\text{H}_2$), 27.33 ($\underline{\text{C}}\text{H}_2$), 26.16 ($\underline{\text{C}}\text{H}$ *trans*-cyclopropane), 25.74 ($\underline{\text{C}}\text{H}_2$), 22.69 ($\underline{\text{C}}\text{H}_2$), 15.80 ($\underline{\text{C}}\text{H}$ *cis*-cyclopropane), 14.90 ($\underline{\text{C}}\text{HCH}_3$ *trans*-cyclopropane), 14.10 ($\underline{\text{C}}\text{H}_3$), 10.92 ($\underline{\text{C}}\text{H}_2$ *cis*-cyclopropane), Appendix, figure 5

4.4.5.3 NMR analysis of purified Ket-MA

δ_{H} (500 MHz): 3.72 (1H, m, $\underline{\text{C}}\text{HOH}$), 3.35 (3H, m, $\text{CHO}\underline{\text{C}}\text{H}_3$, 1.68% contamination with MeO-MA), 2.53 (1H, m, $\text{CO}\underline{\text{C}}\text{HCH}_3$), 2.45 (1H, m, $\underline{\text{C}}\text{H}(\underline{\text{C}}\text{H}_2)_{23}\underline{\text{C}}\text{H}_3$), 2.42 (2H, t, $J=7.5$ Hz, $\underline{\text{C}}\text{H}_2\text{CO}$), 1.6-1.09 ($\underline{\text{C}}\text{H}_2$), 1.05 (3H, d, $J=6.9$ Hz, $\underline{\text{C}}\text{H}_3\text{CHCO}$), 0.91-0.8 (m, $\underline{\text{C}}\text{H}_3$), 0.66 (3H, m, CH *cis*-cyclopropane and $\underline{\text{C}}\text{H}$ adjacent to *trans*-cyclopropane), 0.56 (1H, ddd, $J_1=4.1$ Hz, $J_2=8.3$ Hz, $\underline{\text{C}}\text{H}_2$ *cis*-cyclopropane), 0.45 (1H, m, $\underline{\text{C}}\text{H}$ *trans*-cyclopropane, 53%), 0.2-0.1 (3H, m, *trans*-cyclopropane), -0.33 (1H, dd, $J_1=4.1$ Hz, $J_2=5.3$ Hz, $\underline{\text{C}}\text{H}_2$ *cis*-cyclopropane), Appendix, figure 6.

δ_{C} (125.8 MHz): 215.3 (C=O), 176.20 ($\underline{\text{C}}\text{OOH}$ not seen in the purified MA because only a very small amount was recovered), 72.14 ($\underline{\text{C}}\text{HOH}$), 51.00 ($\underline{\text{C}}\text{H}(\underline{\text{C}}\text{H}_2)_{23}\underline{\text{C}}\text{H}_3$), 50.54 ($\text{CO}\underline{\text{C}}\text{HCH}_2$), 46.34 ($\underline{\text{C}}\text{H}_2$), 41.16 ($\underline{\text{C}}\text{H}_2$), 38.14 ($\underline{\text{C}}\text{H}_2$), 37.43 ($\underline{\text{C}}\text{H}_2$ *trans* cyclopropane), 35.56 ($\underline{\text{C}}\text{H}_2$), 34.48 ($\text{CHCO}\underline{\text{C}}\text{H}_2$), 33.04 ($\underline{\text{C}}\text{H}_2$), 31.93 ($\underline{\text{C}}\text{H}_2$), 30.22 ($\underline{\text{C}}\text{H}_2$), 30.07($\underline{\text{C}}\text{H}_2$), 29.70 ($\underline{\text{C}}\text{H}_2$), 29.66 ($\underline{\text{C}}\text{H}_2$), 29.61 ($\underline{\text{C}}\text{H}_2$), 29.58 ($\underline{\text{C}}\text{H}_2$), 29.50 ($\underline{\text{C}}\text{H}_2$), 29.42 ($\underline{\text{C}}\text{H}_2$), 29.33 ($\underline{\text{C}}\text{H}_2$), 28.72 ($\underline{\text{C}}\text{H}_2$), 27.32 ($\underline{\text{C}}\text{H}_2$), 26.14 ($\underline{\text{C}}\text{H}$ *trans*-cyclopropane), 25.72 ($\underline{\text{C}}\text{H}_2$), 23.73 ($\underline{\text{C}}\text{H}_2$), 22.69 ($\underline{\text{C}}\text{H}_2$), 19.72 ($\underline{\text{C}}\text{H}_3$ adjacent to *trans*-cyclopropane), 18.63 (CH *trans*-cyclopropane), 16.36 (CH_3CHCO), 15.78 (CH *cis*-cyclopropane), 14.11 ($\underline{\text{C}}\text{H}_3$), 10.50 ($\underline{\text{C}}\text{H}_2$ *cis*-cyclopropane), Appendix, figure 7.

4.4.6 Immunological analysis of the natural mixture and separated subclasses of MA

4.4.6.1 Coating MAs onto ELISA plates

For coatings done in PBS, each lipid sample (250 μg) was dissolved in PBS (4 ml, pH=7.4) and placed on the heat block at 90 $^\circ\text{C}$ for 20 minutes. One vial of PBS (4 ml) served as control. The solutions were vortexed for 30s before sonifying for 2 minutes using the

Virsonic sonifier at setting no. 2. The warm solutions were subsequently loaded onto the ELISA plates (50 μ l per well) and the presence of oily drops viewed under a light microscope to confirm coating efficiency. The plates were kept at 4 °C overnight in plastic bags.

For the coatings done using hexane as coating solution, the lipid samples (250 μ g) were dissolved in hexane (4 ml, distilled) and vortexed for 30s. One vial of hexane (4 ml) served as control. Solutions were coated using a Hamilton syringe (50 μ l/ well) and the liquid was loaded in the centre of the wells. Lipid was visible as a circular waxy layer after 2 hours of evaporation of the hexane at room temperature. The plates were then stored in plastic bags at 4 °C overnight.

4.4.6.2 ELISA of sera to MA subclasses

The response of sera to each of unesterified MA, ME-MA, α -MA, MeO-MA, Ket-MA and cholesterol was tested using the ELISA assay. The lipid coated plates were transferred to 25 °C, after which the PBS coated plates were aspirated and then blocked with 0.5% Casein/PBS (400 μ l/ well) for 2 hours, while the hexane coated plates were directly blocked with the aforementioned buffer. After 2 hours, the blocking buffer was aspirated and serum (1:20 dilution in 0.5% Casein/PBS, pH= 7.4) was added to the plate (50 μ l/ well). After 1 hour of serum incubation, the wells were washed 3 times with the Well Wash4 ELISA washer (Labsystems) and flicked out before adding the goat anti-human Immunoglobulin G (IgG) peroxidase conjugate (whole molecule) for 30 minutes at room temperature. Subsequently, plates were washed three times and flicked out before adding the OPD substrate solution (50 μ l/ well). Absorbencies were measured with a SLT 340 ATC photometer at 450 nm with a reference filter at 690 nm at 30 minutes for hexane and 50 minutes for PBS coated plates respectively. Background binding of serum to PBS or hexane was corrected for by subtracting each serum response to PBS or hexane from the serum values obtained to the coated lipid antigens.

Statistical analysis

To determine whether sera responded significantly different to respective lipid samples, the data was analyzed using the student t-test in Microsoft Excel. A 95% confidence level was selected ($\alpha = 0.05$).

4.5 Results: Separation and purification of MA subclasses

This section describes the methyl-esterification, separation and purification of the MA subclasses from *M. tb*. For use in the immunoassays, the free acid form of the subclasses needed to be obtained; therefore the MA methyl ester subclasses were subsequently hydrolysed and purified.

4.5.1.1 Methyl-esterification of MA and separation into the three subclasses

Mycolic acid from *M. tb* was esterified as described previously by Watanabe *et al.* (191), in order to separate the three MA subclasses (α , MeO and Ket) by PTLC (147). Prior to the esterification of the MA, NMR analysis was done to verify sample composition.

The observed peak at δ 2.43 in the proton NMR of the unesterified MA (Appendix, figure 1) is characteristic of the α -proton in the mycolic motif and the peak at δ 3.7 represents the β -proton (figure 1.4). Using a method similar to that previously described by Watanabe *et al.* (127), the percentage of α -, MeO- and Ket-MA was estimated (4.4.2.3, table 4.1). The peak in the proton NMR of unesterified MA at δ 2.97 is characteristic of the methine proton adjacent to the methoxy group, while the peak at δ 2.52 represents the methine adjacent to the keto functionality. The peaks at δ 0.13-0.1 and δ -0.33 in the proton NMR indicated the presence of the *trans*- and *cis*-cyclopropanes respectively. As seen from table 4.1, the unesterified MA contains mostly α -MA (54%), with less MeO-MA (30%) and only 16% Ket-MA. The whole unesterified MA sample only contains 10.2% *trans*-cyclopropanation (table 4.1).

Table 4.1: NMR analysis of the whole MA sample before esterification and separation as well as the separated, hydrolysed and purified MA subclasses from M. tb (the 0% indicates that the signals were below the limit of detection in the proton NMR spectra)

	Before separation of the subclasses	After separation, demethylation and purification of the three subclasses present in M. tb	
	Composition (%)	Contamination (%)	trans-cyclopropane (%)
Whole MA	100	-	10.2
Alpha	54	0	0
Methoxy	30	0	10
Keto	16	Contaminated with approx. 1.68% of MeO-MA	53

After the purity and composition of the initial unesterified MA sample was determined the sample was esterified and the reaction gave an average yield of 95% (127). Esterification was confirmed by analytical TLC and NMR analysis indicated the appearance of the methylene protons at δ 3.69 in the proton NMR and CH₃ group at δ 51.00 in the carbon NMR. In order to confirm the subclass composition of the whole MA sample, the percentage of each subclass was also estimated from the methyl ester of MA using the Versadoc (Model 3000) imaging system. The Versadoc system measures the area and optical density of each spot on a TLC plate and determines the volume as a percentage of the total (figure 4.1).

As seen from figure 4.1, the percentage composition estimated using the volume analysis of the separated methyl ester MA subclasses on TLC corresponds well to the estimation obtained using NMR (table 4.1).

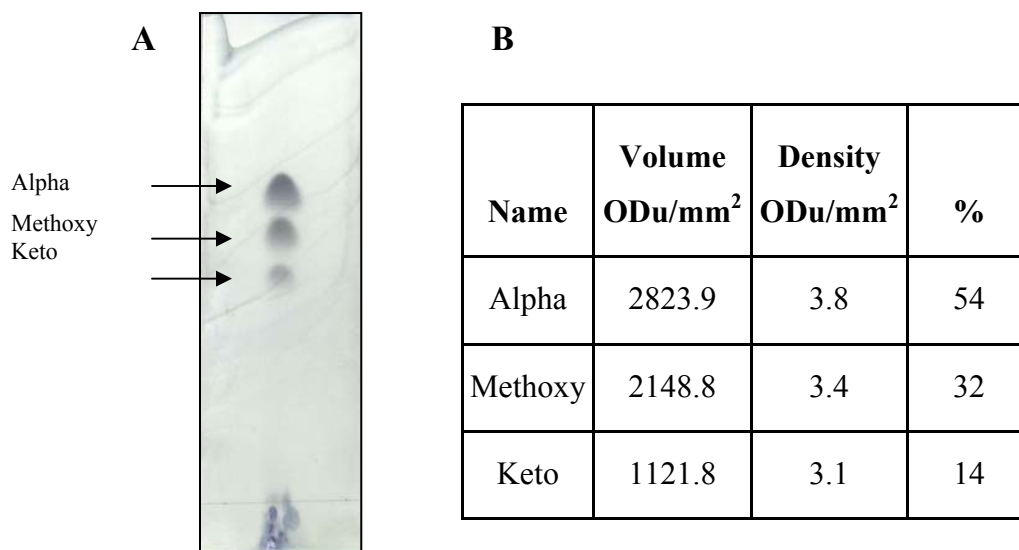


Figure 4.1: Quantitative analysis of TLC separation of the natural MA mixture A) TLC of the methyl ester of the MA mixture from *M. tb* B) Versadoc analysis of the spots from which the volume for each spot was given as a% of the total

Following the same procedure as previously described by Deysel (147), the methyl ester of the MA sample from *M. tb* was subsequently separated into the three subclasses with an overall yield of 53%. The low recovery was probably due to the selection of narrow silica bands corresponding with each subclass to prevent contamination, but could also be due to incomplete extraction of the MA from the silica gel. Even with caution, the α - and the MeO-methyl esters of MA were contaminated with the adjacent subclass and needed to be purified by column chromatography before continuing to the next step.

4.5.1.2 Hydrolysis and purification of each MA subclass

Once satisfied with the purity as analyzed by analytical TLC, the methyl esters of the MA subclasses were subsequently hydrolysed using a modified procedure described by Villeneuve *et al.* (91). The ME-MA subclasses were hydrolyzed within 3 hours instead of 2 hours and the free acids were purified not by TLC, but by subsequent precipitation from acetone and then column chromatography.

As seen in figure 4.3, the hydrolysis process resulted in the formation of epimer as well as the introduction of both non-polar (X) and polar (Y) impurities. Mycolic acids have always been found to be in the 2R, 3R-configuration at the α - and β -carbons (figure 1.4, p 15) and the epimer of natural MA is either in the 2S, 3R-configuration. The reason for the formation of epimer during the demethylation process has been ascribed to the use of the strong base for hydrolysis of the methyl group (129). The presence of the epimer was detected in the TLC after hydrolysis (figure 4.2, A) and was also detected in the NMR spectra as an additional CH₂ peak at δ 34.00, whereas the CH₂-group adjacent to the β -carbon of natural MA usually peaks at δ 35.70 in the ¹³C NMR. After purification, the epimer was reduced to below the NMR level of detection in all of the purified MA subclasses.

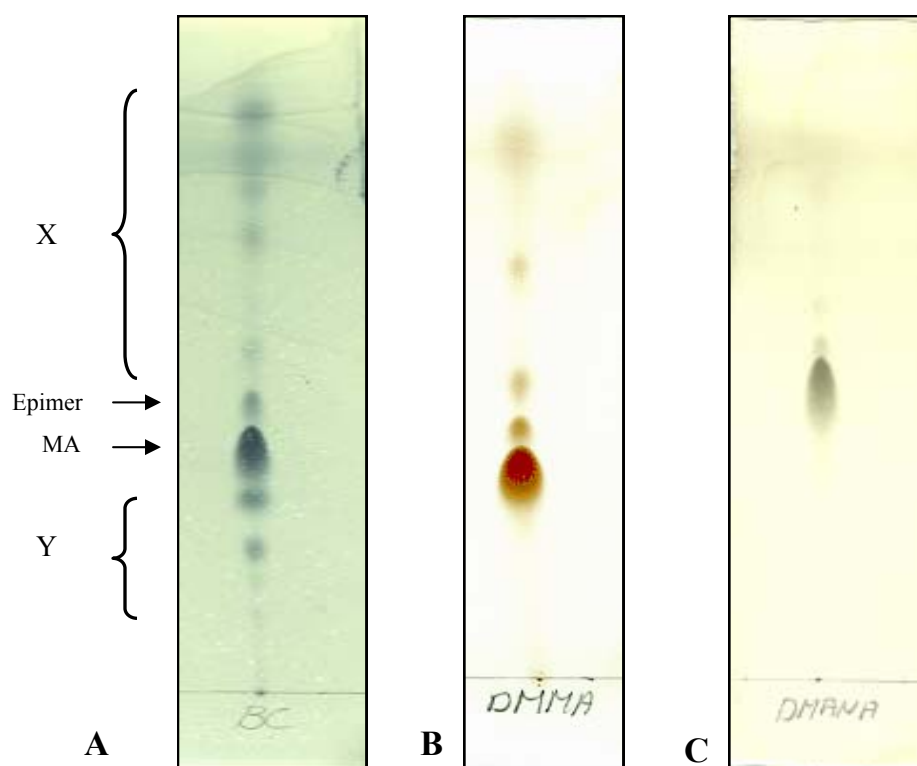


Figure 4.2: Purification of MA after the demethylation process. A) α -MA after demethylation, B) α -MA after acetone precipitation and C) α -MA after column chromatography. The designation of X represents the non-polar impurities while Y represents the polar impurities introduced during demethylation.

The polar impurities were removed by precipitation from acetone (figure 4.2, B) and the non-polar impurities were subsequently eliminated using column chromatography (fig 4.3, C). However, when analyzing the NMR spectra of all the MA subclasses, there remained an impurity seen as a triplet at δ 2.33 (figure 4.3). Another member of our group obtained the same triplet after performing demethylation on a very long unfunctionalised methyl MA in strong base. The triplet was identified to represent the CH_2 -group next to the carboxyl functionality of a long chain fatty acid.

It appeared that the hydrolysis process, if left for longer than 3 hours at 85 °C, was able to cleave the MA into its fatty acid (C_{26} -acid) and corresponding aldehyde (mero-aldehyde) as previously observed during pyrolysis (123,192). The long chain fatty acid impurity formed during hydrolysis was not visible in analytical TLC probably due to the co-migration with the very hydrophobic MA. The only method, by which this impurity was eliminated, was by precipitation from acetone for a 2nd or a 3rd time, indicated by the disappearance of the triplet seen at δ 2.33 in the proton NMR (figure 4.3).

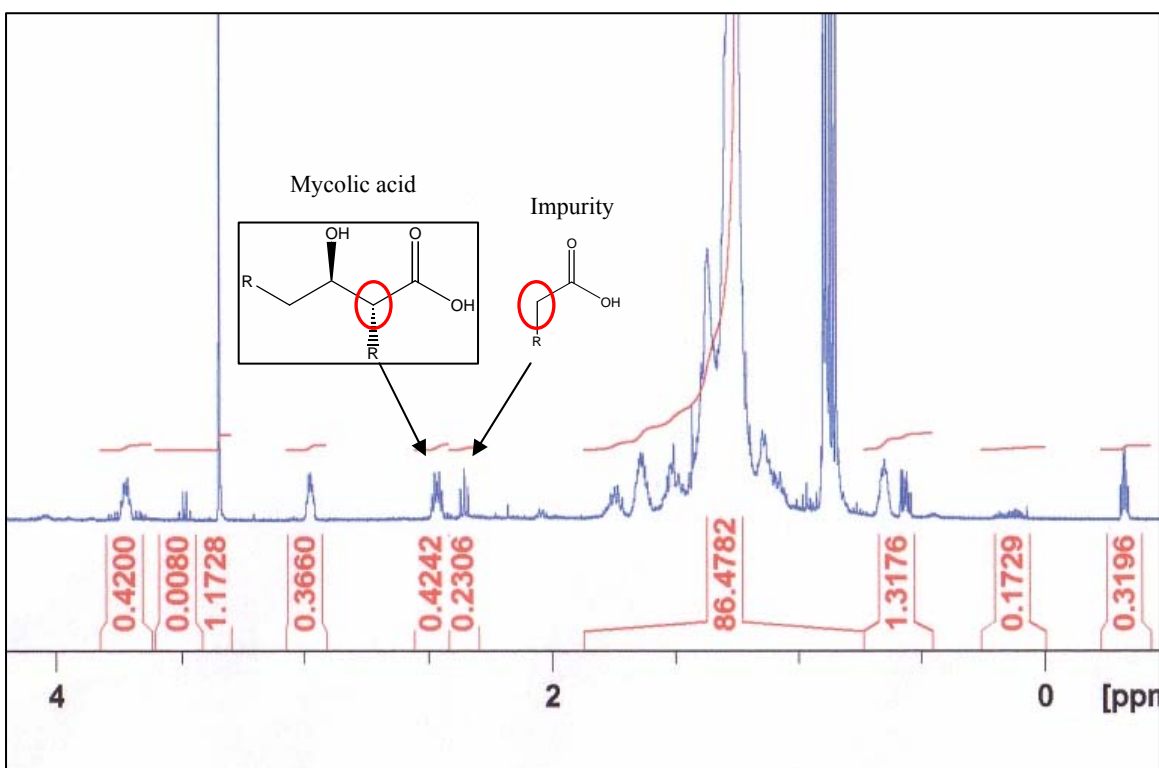


Figure 4.3: Proton NMR of MeO-MA indicating the proton on the β -carbon of MA seen at δ 2.45 and the peak at δ 2.33 characteristic of a CH_2 -group next to the carboxyl of a long chain fatty acid impurity.

The final purified MA subclasses were analyzed by proton and carbon NMR (Appendix) and the presence of *trans*-cyclopropanation as well as the percentage contamination with the neighbouring subclasses was determined and reported in table 4.1. As seen from table 4.1, the Ket-MA contains the largest amount of *trans*-cyclopropanation and the α -MA none, which agreed with that seen in literature (127). The percentage yield for the α -, MeO- and Ket-MA subclasses was 18%, 28% and 37.5% respectively.

4.5.2 Results: Immunochemical analysis of the purified MA subclasses

In this section, the antibody activity of a range of TB positive and TB negative sera were tested to the separated and purified MA subclass antigens from *M. tb*. Initially it was determined which form of MA, methylated or free acid, was required for antigenicity. Subsequently, the antigenicity of the MA subclasses was analyzed after coating the antigens from either PBS or hexane.

4.5.2.1 Investigation of the free and ME-MA in PBS and hexane

Prior to analyzing the separated MA subclasses it needed to be determined whether MA had to be in the free acid or methyl ester form, and whether the coating solvent affected the recognition of MA by antibodies. The sera used for this purpose was a 1: 20 dilution of pooled TB positive and pooled TB negative sera and the response was assessed to unesterified MA as well as ME-MA coated from either PBS or hexane.

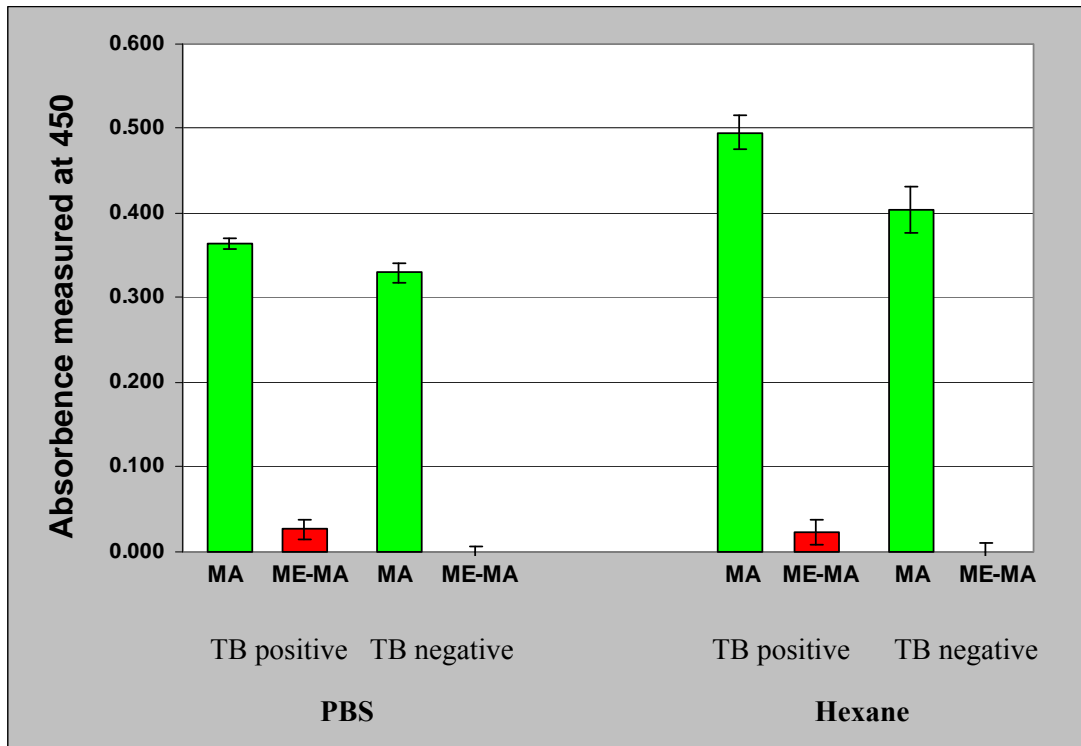


Figure 4.5: Comparison of different coating solutions on antibody recognition of MA and ME-MA in ELISA. The ELISA signals of pooled TB positive and pooled TB negative sera was measured at an absorbance of 450 nm to the whole fraction of MA and ME-MA antigens coated onto ELISA plates from either PBS or hexane. The error bars indicate the standard error of the mean (n=4).

From the results obtained in figure 4.5 it was determined that IgG antibodies from TB positive and TB negative sera were capable of recognising MA coated from either PBS or hexane. The sera did not respond to the ME-MA using either of the coating solvents. The MA signals in PBS and hexane were compared using a student t-test ($\alpha= 0.05$) and the response of sera to MA tended to be greater when coated from hexane than when coated from PBS. Both the coating solutions allowed for the distinction between the TB positive and TB negative sera with $P < 0.03$ for PBS and $P < 0.05$ for hexane.

Thus, MA needs to be in the free carboxylic acid form for antibody recognition using the ELISA protocol described in 4.4.6.2. Either of the PBS or hexane solvents can be used for coating the MAs onto ELISA plates.

4.5.2.2 Antigenicity of MA subclasses when coated from PBS

In the search for a more specific antigen than the natural mixture of MA from *M. tb*, the antigenicity of the individual MA subclasses was investigated after coating from PBS. The 10 sera selected for this purpose were from the Schleicher collection and consisted of 5 TB positive and 5 TB negative sera, all chosen to be HIV neg.

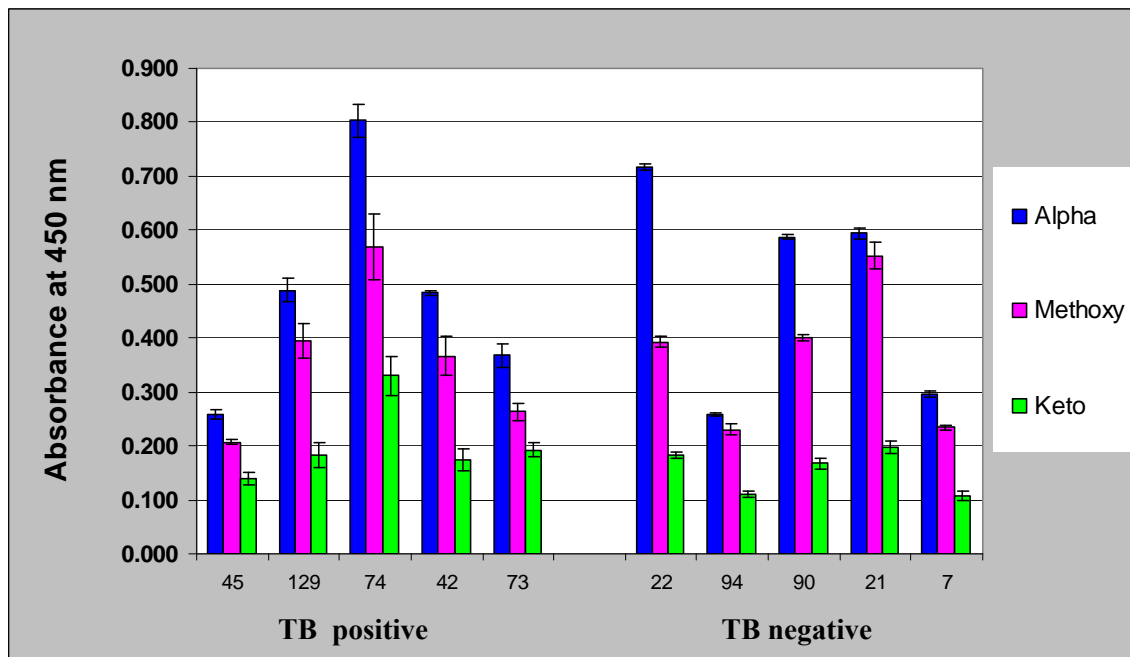


Figure 4.6: Antigenicity of MA subclasses when coated from PBS as determined by ELISA. The ELISA signal of 5 TB positive (Patient no. 45, 129, 74, 42 and 73) and 5 TB negative (Patient no. 22, 94, 90, 21 and 7) sera were measured at an absorbance of 450 nm to PBS coated α -, MeO- and Ket-MA. The number of data points collected for the TB positive sera to α -, MeO- and Ket-MA was 7, 6 and 9 respectively. For the TB negative sera to α -, MeO- and Ket-MA, $n=4$, 4 and 7 respectively. Error bars indicate the standard error of the mean.

As seen from figure 4.6, not one of the subclasses coated from PBS could make the distinction between TB positive and TB negative serum populations, even though the MA mixture had previously been shown to be able to make that distinction (64,161). The recognition of MA subclasses appeared to be affected by the nature of the functional group present in the distal position of the “mero” chain of the MA.

The first hypothesis was that the significantly reduced signal to the Ket-MA subclass was due to a prozone effect in which the IgG antibodies are highly concentrated and bind monovalently, instead of divalently. The monovalently bound antibodies would be removed during the wash steps of the ELISA assay. This hypothesis was tested by measuring the response of a pooled TB positive and pooled TB negative serum to all three the MA subclasses coated from PBS at dilutions of 1/ 20, 1/ 40 and 1/ 80 (figure 4.7).

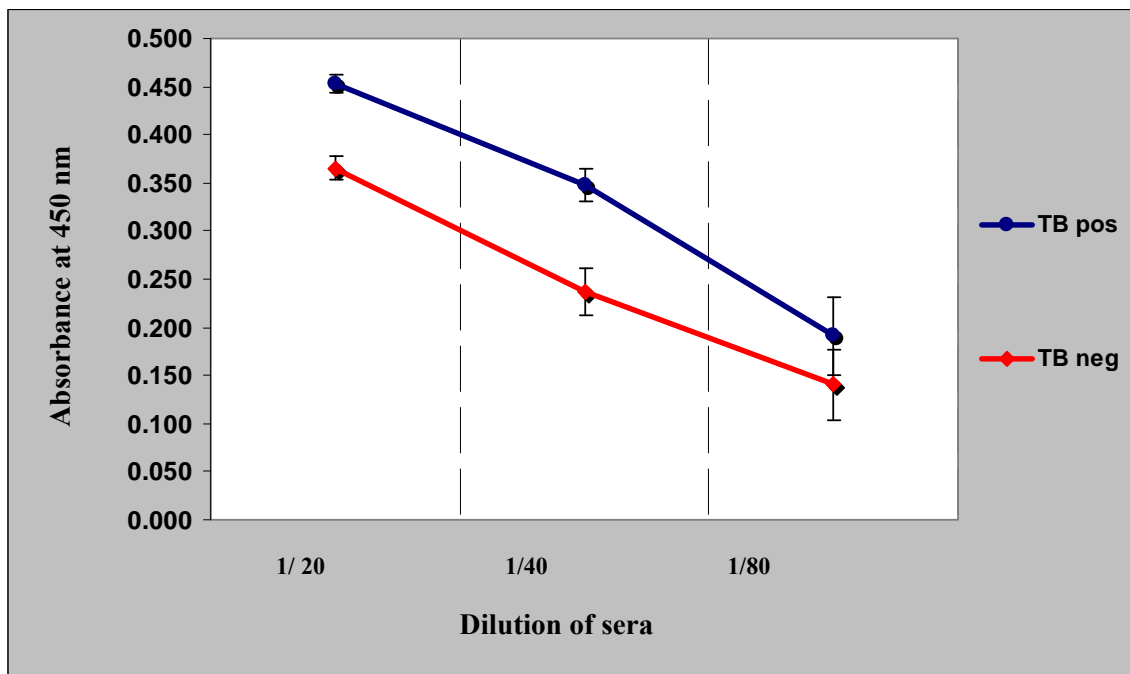


Figure 4.7: The effect of serum dilution in ELISA on antibody binding signals to MAs. The response of TB positive and TB negative sera to each of the three MA subclasses was measured at different dilutions of serum. The responses to the subclasses at each dilution were then combined and the average absorbance at 450 nm is presented above for the TB positive and TB negative sera separately. The error bars indicate the standard error of the mean with $n= 3$ for each data point.

The results obtained in figure 4.7 showed that the MA subclasses were recognized in a concentration dependent manner and that no prozone effects were observed. Thus, the hypothesis of a prozone effect was disproved.

A second hypothesis for the results seen in figure 4.6 was formulated, in which it was assumed that MA subclasses arrange differently on the ELISA plate, compared to the natural mixture of MA. It has previously been shown that MA subclasses assume different conformations within monolayers formed in Langmuir troughs (91), and it was postulated that this would also be the case for MA subclasses coated onto ELISA plates. From the results presented in figure 4.6, it was then concluded that the conformations assumed by the MA subclasses were not optimal for anti-MA antibody binding, resulting in the interference from non-specific antibody binding to the MA coat. This may be the reason why the MA subclasses coated from PBS can not distinguish between a range of TB positive and TB negative sera.

4.5.2.3 Antigenicity of MA subclasses when coated from hexane

The inability of the three subclasses from *M. tb* to distinguish between TB positive and TB negative sera populations when coated from PBS was thought to be due to the MA assuming a conformation not optimal for recognition by specific anti-MA antibodies. It was subsequently determined whether a particular MA subclass coated from hexane could assume a different arrangement, allowing the preferential binding of anti-MA antibodies from sera to better make the distinction between TB positive and TB negative populations. The sera used in this study were the same TB positive and TB negative sera used to analyze the MA subclasses coated from PBS (4.5.2.2).

From the results in figure 4.8 it was observed that the greatest response of sera was to the oxygenated MA subclasses (MeO- and Ket-MA). The α -MA subclass gave the lowest serum response when coated from hexane. However, when coating from hexane, both the α -MA ($P < 0.002$) and Ket-MA ($P < 0.01$) subclass was capable of distinguishing between the TB positive and TB negative serum populations.

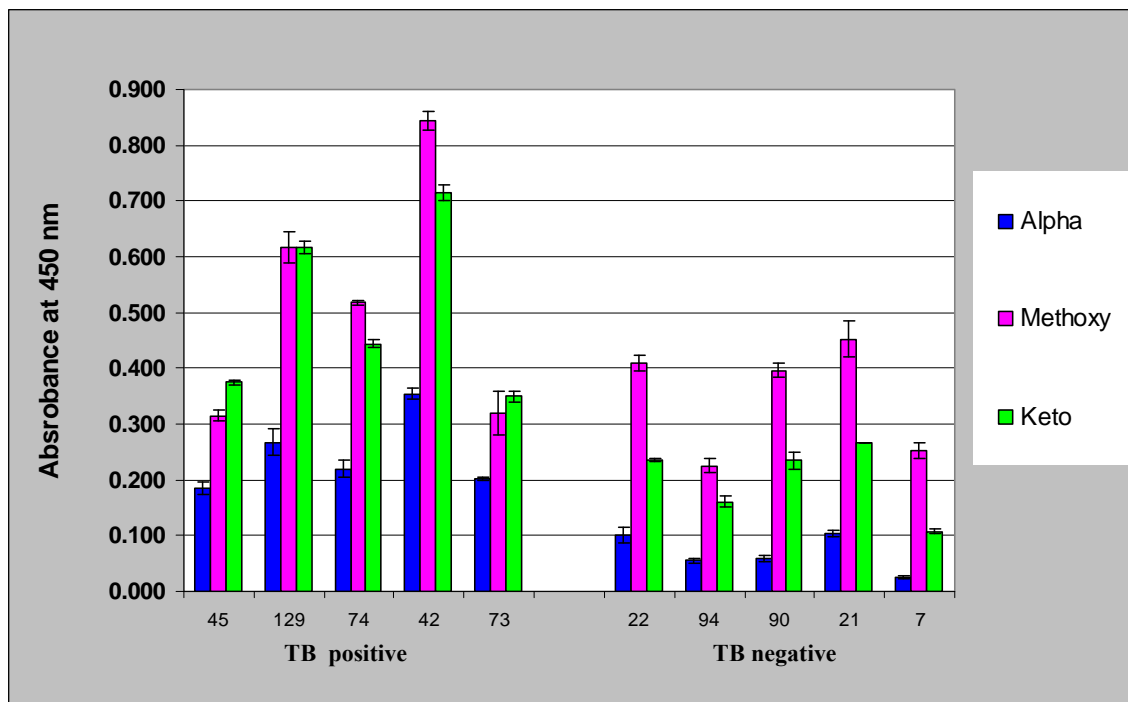


Figure 4.8: Antigenicity of MA subclasses when coated from hexane as determined in ELISA. The responses of 5 TB positive (nr 45, 129, 74, 42 and 73) and 5 TB negative (nr 22, 94, 90, 21 and 7) sera were measured at an absorbance of 450 nm to hexane coated α -, MeO- and Ket-MA in ELISA. The number of data points collected for the TB positive and TB negative sera to α -, MeO- and Ket-MA was 4 each. Error bars indicate the standard error of the mean.

The results presented in figure 4.8 supported the hypothesis that from hexane, MA subclasses arrange differently on the ELISA plates and are recognised preferentially by specific anti-MA antibodies, making it possible to distinguish between a range of TB positive and TB negative serum populations.

4.6 Discussion

In search of a better surrogate marker for TB, we investigated the specificity of antibody interaction with MA subclasses in an ELISA assay. For this purpose the three subclasses from *M. tb* (α -, MeO- and Ket-MA) were separated from the natural mixture of MA by first creating their methyl esters and then separating the ME-MA subclasses by PTLC. It needed to be determined whether the subclasses were antigenic as their methyl ester products or whether the MA subclasses had to be in their free acid form. In the literature,

Schleicher *et al.* (64) tested human serum responses to the natural unesterified mixture of MA coated from hot PBS, while the group of Pan *et al.* (121) made use of the ME-MA coated from hexane to assess antibody binding to the different MA subclasses. One aim of this study was to determine which form of MA would best suit the analysis to detect anti-MA antibodies from TB patients as surrogate markers of active TB, using the ELISA assay.

The results obtained after measuring the response of pooled TB positive and pooled TB negative sera to MA and ME-MA coated from PBS or hexane, indicated that MA had to be in the free acid form to be antigenic in either PBS or hexane coating solvents. Thus, the separated ME-MA subclasses had to be hydrolysed before use in ELISA.

It was next investigated whether a specific subclass of MA from *M. tb* would better distinguish between TB positive and TB negative sera in ELISA after coating the lipids from PBS. It was observed that both TB positive and TB negative serum populations responded to the MA subclasses in ELISA and that not one of the natural subclasses α -, MeO- or Ket-MA could improve on the distinction made between the two sera populations using the natural mixture of MA. The best signals were seen for the α - and MeO-MA with a significantly lower response to the Ket-MA. The significantly lower response of sera to the Ket-MA was shown not to be due to prozone effects. The apparent correlation between the antibody binding signals from sera, and the distal functional group on the “mero” chain of the MA subclasses, lead to the hypothesis that the MA subclasses assumed different conformations on the ELISA plates, as previously seen for monolayers of MA in Langmuir troughs (91). The inability of the MA subclasses to distinguish between TB positive and TB negative sera when coated from PBS was proposed to be due to the MA subclasses assuming conformations on ELISA plates, which were not optimal for recognition by anti-MA antibodies, and which would result in the simultaneous binding of non-specific antibodies. It was thus concluded that MA subclasses coated from PBS in ELISA would not be able to provide the resolution required to make the distinction between TB positive and TB negative patient sera populations for the purpose TB serodiagnosis.

It was subsequently determined whether the MA subclasses coated from hexane could assume a conformation which would be preferentially be recognised by specific anti-MA antibodies and make the distinction between TB positive and TB negative patient sera. Indeed, when coated from hexane both the α - and Ket-MA subclasses could make the distinction between the TB positive and TB negative patient serum populations. These results also supported the hypothesis that the MA subclasses assumed a conformation in hexane which was different from that in PBS and which was preferentially recognised by specific anti-MA antibodies. The inability of the MeO-MA to distinguish between TB positive and TB negative sera, even after coating from hexane, was probably due to this subclass assuming a conformation which was still recognised by non-specific antibodies.

These results also indicated that the individual subclasses (α - and Ket-MA) could distinguish between the two serum populations with a greater level of confidence (99%) than the mixture of MA (95%) (64), making the MA subclasses coated from hexane, preferred antigens for the use in the serodiagnosis of TB.

In conclusion, MA needs to be in the acid free form for the ELISA analysis following the protocol of Schleicher *et al.* (64). Furthermore, of the two solvents tested for coating MA, hexane allows the MA to assume an arrangement which is preferentially bound by anti-MA antibodies, making it possible to distinguish between TB positive and TB negative sera. Last, but not least, particular MA subclasses (Ket-or α -MA), when coated from hexane, could be used as antigens to provide the necessary resolution required for a serodiagnostic assay based on MA.

Chapter 5: General Discussion

Tuberculosis was declared a global emergency in 1993 by the World Health Organization (21) after a resurgence of the disease in the early to mid 1980s (193). Global TB strategies have since been put in place and the incidence of TB has stabilized in all areas of the world except for Africa, the Eastern Mediterranean and South-East Asia (18). Of the 15 countries with the highest incidence of TB, thirteen are in the sub-Saharan region (194). The continued increase of TB in low income regions has been attributed to factors such as poverty, ineffective treatment and patient monitoring, as well as MDR-TB and the HIV epidemic (193).

Tuberculosis is the major cause of death in HIV infected individuals (195), of which less than half of the cases are diagnosed before death (18). Among the reasons for the low diagnostic output of TB in HIV co-infected individuals, are inadequate mycobacterial content of sputum samples, impaired immunity, or premature death due to rapid TB development. The current gold standard for TB diagnosis remains mycobacterial culture from sputum, which can take up to 4-6 weeks to exclude the possibility of TB infection (17) and rapid and accurate diagnosis is urgently needed. HIV infected individuals are also more susceptible to opportunistic infections by NTB mycobacteria (196), of which the symptoms are often clinically indistinguishable from TB (197). In order to employ the correct treatment strategies, diagnostic assays need to be not only rapid but also to distinguish between Tuberculosis and NTB mycobacterial infections.

Members of our group (64,71,162) as well as research laboratories around the world (65,115) have focused on developing serological assays for the diagnosis of TB. Serology has the potential to be rapid, inexpensive, able to distinguish between latent and active disease, and to overcome the problems associated with extrapulmonary- TB (36).

Lipid antigens have gained much attention for serodiagnosis of TB because of species specificity, and also because of the altered immune presentation pathway compared to that for protein antigens (198). Protein antigens are presented on MHC class I and II molecules of APCs to CD4⁺ T cells (199,200), while lipid antigens are presented on CD1 (CD1a, -b, -c or -d) molecules to CD4⁻CD8⁻, CD8⁺ (120) or CD4⁺ T cells (141,142). The mechanism by which antibodies to lipids are produced is not fully understood yet. For some lipid antigens, the antibody titres appear not to be affected by the CD4⁺ T cell count of HIV infected individuals (64). Furthermore, the production of antibodies to the lipid antigen, TDM, has been shown to be unaffected by prior BCG vaccination (201), and also appears to coincide with disease status and chemotherapy progress (115). It thus follows that lipid antigens are preferable to protein antigens in serodiagnosis.

There is however controversy in the understanding of the duration of immune memory of anti-lipid antibodies. It has been found that the antibodies to the *M. tb* phenolic glycolipid were present in absence of disease, and that the antibody titre persisted for more than 18 months after TB patients had complete the chemotherapy course (202). Similarly, antibodies to LAM are affected by prior BCG vaccination (163), and also persist after the completion of chemotherapy (165).

The variation between the duration of the antibody responses to lipid antigens such as TDM and LAM could be due to differences in presentation to immune cells. Lipid antigens presented on different CD1 proteins follow different routes of association and trafficking within antigen presenting cells (198). It has been shown that LAM and free MA are presented by APCs on CD1b molecules to CD4⁻CD8⁻T cells (198), while TDM is presented in an as yet unknown manner to the immune system. It is thus possible that lipid antigens presented on different CD1 proteins stimulate different subsets of T cells resulting in variations in antibody production and activity.

Besides the advantages that anti-lipid antibodies may have in serodiagnosis in terms of the short immune memory, the major drawback in serodiagnostic assays remains the low sensitivity. Not a single serodiagnostic assay for TB has yet matched both the > 80% sensitivity and > 95% specificity set out by the World Health Organisation as criteria to

define the market need (21). The lack of sensitivity of the serological assays can in part be ascribed to the diversity of antibody responses between individual patient sera (115), cross-reactivity of antibodies produced to opportunistic NTB mycobacteria (32,203), impaired humoral responses due to HIV infection, as well as interference from previous BCG vaccination (204).

In the search for an effective serodiagnostic assay that will comply with the requirements set out by the World Health Organisation in terms of sensitivity and specificity, while simultaneously being able to assess the TB status of individuals who are infected with HIV, our group set out to investigate the potential use of the MA antigens from *M. tb*. Mycolic acid is the most abundant lipid in the cell wall of mycobacteria. It comprises a family of related structures of which the fine structure differs within and among mycobacterial species (205). Antibodies to MA were first described by members of our group in a patent dating back to 1994 and brought in the public domain in 2002 (64). Very promising was the fact that the antibody binding signal to MA was shown to be independent of the HIV status of TB/ HIV co-infected patients. The use of MA in serodiagnosis has been evaluated using both the ELISA technique (64), as well as a resonant mirror biosensor (72). The low sensitivity of 51% in the ELISA assay was improved to 86% using a competitive binding approach on the resonant mirror biosensor, but both assays still lacked specificity.

It is known that 15-20% of adult tuberculosis patients have negative sputum cultures, for which the percentage is increased in an HIV setting (23). It is thus possible that the false positive results obtained in the ELISA and biosensor tests using patient sera from a TB and HIV burdened region, were in fact true positive s, which were not detected by the sputum culture test. Furthermore, HIV positive individuals are often infected with opportunistic mycobacteria, such as *M. avium* (206), which contains some MA similar to that found in *M. tb*, and may be another reason for the large number of false positive s seen in the HIV positive populations (72) of the MA based tests. The MA preparation used in the ELISA and biosensor assays performed by our group contained all three of

the subclasses from *M. tb*, and it was hypothesized that a particular subclass of MA could make a better distinction between TB positive and TB negative sera.

One of the reasons for the low sensitivity previously obtained in ELISA (64), could have been due to the limitations of the technique to detect the low affinity antibodies (178). Another possible reason was postulated to be due to the presence of cross-reactive antibodies in TB negative patient sera. The cross-reactive activity was hypothesized to be due to anti-cholesterol antibodies due to a molecular mimicry between MA and cholesterol (71). It has since been demonstrated that MA does in fact assume a cholesteroid nature, by providing evidence that MA- and cholesterol liposomes attracted one another specifically in interaction measurements, and that MA was recognized similarly to cholesterol by the cholesterol binding macrolide, AmB, in biosensor analysis (161).

The aim of this study was to remove any doubt that antibodies in human sera cross-reacted in their binding to both cholesterol and MA. In order to analyse the possible cross-reactivity of antibodies in ELISA, it had to be shown with a competitive binding assay that soluble cholesterol liposomes could inhibit the anti-MA binding response comparable with that achieved using MA liposomes. In addition, it had to be ascertained that it was antibodies which bound to the MA coated cuvette surface of the biosensor and was inhibited with MA liposomes, as this device is mass sensitive, but without the ability to distinguish the character of the binding molecules. Finally, in an attempt to improve the diagnostic potential of the immunoassays for anti-MA antibodies, the individual subclasses of MA were tested as antigens to determine if they could better distinguish between the TB positive and TB negative serum populations in ELISA.

The response to MA from TB negative patient sera previously seen by Schleicher *et al.* (64) in ELISA and Siko (71) in biosensor analysis, could have been due to non-specific antibody binding to the lipid coat or specifically either by anti-MA antibodies or cross-reactive anti-cholesterol antibodies. We tested the specificity of antibody binding to MA in ELISA by measuring the serum binding response to an acetylated and methylated α -

MA ester (AMAME). The synthetic α -MA had all polar groups protected, to prevent hydrogen bonding with antibodies, but the hydrophobic acyl chains would still have been capable of non-specific “Van der Waals” interactions. No binding was observed to the synthetic protected α -MA from either the TB positive or TB negative patient sera, which indicated that antibody binding was specific and not merely due to non-specific, hydrophobic association. We have also shown, using the isolated natural mixture of MA, that protection of the carboxyl group alone diminishes the recognition by antibodies. These results were not as expected, because it was previously reported that human TB patient serum antibodies recognized MA of which the carboxyl group had been esterified with a methyl group (121). The group of Pan *et al.* (121) used hexane as coating solvent for the methyl MA, while our group coated the antigens from hot PBS. The response of sera to methyl MA coated either from PBS or hexane was subsequently tested here, but still no antibody binding was observed. It has thus been shown that the methyl ester of MA is not recognized in ELISA by any antibody isotype and that the carboxyl group of the mycolic motif is essential for antibody recognition. The requirement for the β -hydroxyl group in antibody recognition still needs to be determined.

After determining that the antibody response to MA from TB negative sera was specific for the polar functionalities on the mycolic motif (as published in Benadie *et al.* [161]) the nature of the antibody was determined. To investigate whether the antibody recognizing MA was a cross-reactive anti-cholesterol antibody, we used a competitive enzyme linked inhibition assay (CELIA) and measured the binding response of TB negative serum to cholesterol after incubation with liposomes containing MA. The anti-cholesterol human antibodies (ACHA) (145) recognized MA containing liposomes, but not liposomes containing PC only. These results, which indicated that ACHA recognized MA in PC lipid vesicles, provided further proof of the cholesterol nature of MA. Furthermore, our observations and that in literature (145,153,154) appear to indicate that ACHA recognizes an epitope defined by the concentration of cholesterol (> 50 mol % in lipid vesicles) and not individual cholesterol molecules. It was thus concluded that recognition of MA in liposomes by ACHA was not due to a molecular mimicry between MA and cholesterol (71,147), but rather due to the resemblance of surface packing in the

liposome. It has been shown that cholesterol exists in a liquid ordered state at concentrations above 50 mol % in PC containing liposomes (160) and thus, ACHA probably recognises an arrangement of MA in liposomes which resembles the liquid ordered state of cholesterol.

The arrangement of MA on ELISA plates probably differs from that within PC containing vesicles. It was also investigated whether ACHA would recognise a particular presentation of MA on ELISA plates, by measuring the decrease in the response of a TB negative control serum to MA after pre-incubation with MA and cholesterol containing liposomes. Different from what was expected, cholesterol liposome pre-incubation did not inhibit the antibody binding response in TB negative serum to immobilised MA. The inability of cholesterol to inhibit the binding signal to MA from TB negative serum could have been due to cross-reactive anti-cholesterol antibodies having a greater affinity for MA than for cholesterol. A second possibility is that anti-MA antibodies are also present in TB negative sera, as for the mycobacterial polysaccharide, LAM. Anti- MA antibodies in TB negative serum could be the result of prior BCG vaccination, latent infection or due to the constant stimulation from environmental, non-pathogenic mycobacteria.

A third, but not least possible reason for the congruence of MA and cholesterol titres seen here and previously by Siko (71), could be ascribed to factors related to disease pathology. In this regard, it has been suggested that cholesterol plays an essential role in the infection of macrophages by *M. tb* (207), for survival (208) as well as for the long term persistence within cholesterol rich foamy macrophages (209,210). During the different stages of mycobacterial pathogenesis, just like for HIV infection (211), cholesterol could be exposed in an antigenic manner, resulting in the increased production of anti-cholesterol antibodies in TB positive patients. This would explain why the TB positive patients tested previously (71) and those reported here have increased anti-cholesterol antibody titres when compared to TB negative patient sera.

The possible cross-reactivity of anti-cholesterol antibodies in TB negative serum with MA can thus not be confirmed or completely dismissed, because of the complexity of

working with polyclonal serum. Future experiments would require the use of monoclonal antibodies to gain a deeper understanding of the antibody-antigen interactions with regards to cholesterol and MA.

In an attempt to improve on the ELISA assay, an inhibition assay has been developed by members of our group on the resonant mirror biosensor using MA in liposomes (71,162). The serum components binding to the MA-containing liposomes to distinguish between TB positive and TB negative sera were thought to be antibodies. However, the biosensor only measures mass accumulation and cannot distinguish between the different binding entities present in serum. It was set out to confirm that antibodies are the serum components binding to MA liposomes in the biosensor assay by performing a binding assay with isolated IgG from TB positive and TB negative patient sera using Protein A Sepharose. During the isolation and purification of IgG, some activity was lost in the TB positive IgG fraction, but was still significantly elevated above that for the TB negative IgG fraction, as measured in ELISA. The antibody fractions were subsequently analyzed for their ability to bind to MA containing liposomes on the resonant mirror biosensor using the method previously developed by members of our group (71,162). As expected, both the IgG fractions from the TB positive and TB negative sera recognized MA liposomes coated onto the biosensor surface, with the TB positive IgG fraction binding significantly more to the liposomes, than the TB negative IgG fraction. These results agreed with what was previously observed for whole sera. It was also determined whether the TB positive and TB negative IgG fractions could be inhibited with MA liposomes. The results showed here that isolated IgG from the TB positive patient serum was inhibited significantly more by MA liposomes than the TB negative IgG fraction. These results also correlated with what was previously observed for whole sera (71,162). It was concluded and published, that antibodies are the serum components binding to MA liposomes in the resonant mirror biosensor inhibition assay that allow the distinction between TB positive and TB negative patient sera with 84% accuracy (72).

In our article on the biosensor assay for TB serodiagnosis based on antibodies to MA as surrogate markers for active TB, we reported low specificity for the HIV pos, TB

negative group of patients. This population was left out of the calculation of the accuracy of the assay, as it is known that standard TB assessment via culture based assays, underestimates TB prevalence by around 30% in the HIV positive group (23). A possible complicating factor in our biosensor assay, which was previously analysed by members of our group, is the cross-reactivity of ACHA with MA containing liposomes. The liposome preparation previously used to inhibit the MA response on the biosensor consisted of 50 mol % cholesterol liposomes (71,162). Although no inhibition of the MA signal was seen, the ELISA results generated here suggest that 50 mol % cholesterol liposomes are not adequate for the inhibition of ACHA binding, possibly because cholesterol at that concentration has not transformed into the liquid ordered state required for recognition. Anti-cholesterol antibody cross-reactivity with coated MA liposomes can thus not be excluded on the biosensor and the results previously presented would have to be repeated using liposomes containing concentrations of cholesterol greater than 50 mol %. This was however not the scope of this investigation.

The final aim of this work was to determine whether a particular subclass of MA could provide better distinction between TB positive and TB negative sera in ELISA, compared with the natural mixture of MA. The added advantage of possibly using a particular subclass is the knowledge that *M. tb* changes its MA subclass profile depending on its growth stage, which may allow the differentiation between latently infected individuals and those with active disease. The Ket-MA subclass for example, is severely reduced during persistence and dormancy of the Mycobacterium, but is increased during active replication within macrophages (130,131,122). In order to analyse the individual MA subclasses, α -, MeO-, and Ket-MA was separated and purified from a virulent strain of *M. tb*. This required that the MA carboxylic groups were methyl-esterified first, but after separation, the subclasses would have to be hydrolysed for recognition by anti-MA antibodies, because it was shown here that the carboxyl group is essential for antibody binding. The purified subclasses were then analysed for their ability to be recognised by anti-MA antibodies in ELISA.

Initially, the three MA subclasses were coated from PBS onto ELISA plates and the response of a range of TB positive and TB negative sera measured to the MA. In accordance with previous results (147), neither the natural α - nor the MeO-MA subclasses could make the distinction between TB positive and TB negative sera. The same tendency was observed here for the natural Ket-MA subclass. The inability of the MA subclasses coated from PBS to make a significant distinction between TB positive and TB negative sera, was thought to be due to the formation of MA conformations which were not optimal for specific antibody binding. The results led to the conclusion that the use of a particular natural MA subclass coated from PBS would not be of benefit for the use in a serodiagnostic assay of TB.

The experiment was repeated, but this time with the MA antigens in the ELISA wells coated from hexane. Contrary to what was expected, the sera responded to the MA subclasses significantly different from what was observed for the PBS coated antigens. The greatest response of TB positive and TB negative sera to MAs coated from hexane was to the Ket- and MeO-MA subclasses, with the lowest being to α -MA. Even more surprising was that both the Ket- and α -MA, but not MeO-MA, coated from hexane, could make the distinction between TB positive and TB negative sera. These results suggested that the coating solution used affected the way in which the MA subclasses were being presented to antibodies. The results confirmed the hypothesised that MAs assumed a more favourable conformation in hexane to which specific anti-MA antibodies could preferentially bind. This also explained the tendency seen here in which the MA signal was greater when coating the lipids from hexane than when coating from PBS.

The ELISA assay analysed here, following the procedure of Schleicher *et al.* (64) based on the natural mixture of MA subclasses, was capable of distinguishing between TB positive and TB negative patient sera at a 95% level of confidence in an HIV negative serum population. The ELISA assay based on MA has subsequently been improved upon by using hexane as coating solvent, and showing that the individual α - and Ket-MA subclasses could distinguish the two serum populations with more than 99% confidence as calculated using the Student t-test. These results showed that a particular subclass of

MA would probably constitute a better antigen for use in a serodiagnostic assay for tuberculosis based on the detection of anti-MA antibodies as surrogate markers of active TB.

Conclusion

Antibodies to MA are novel surrogate markers for the diagnosis of tuberculosis and have shown some potential in both ELISA and biosensor assays. The antibody binding activity to MA has been shown to be maintained in TB and HIV co-infected individuals, making it an attractive approach to diagnose TB in HIV burdened populations. The ELISA technique using MA as antigen however, previously gave a sensitivity that was too low for the purpose of TB diagnosis. The low sensitivity was ascribed to the presence of cross-reactive anti-cholesterol human antibodies in TB negative sera. In this work a deeper understanding on the cross-reactivity of antibody binding to MA and cholesterol has been achieved. It has been ascertained that recognition of MA by ACHA appears not to be due to direct molecular mimicry as previously proposed, but rather to MA/ PC liposomes resembling the liquid ordered state of cholesterol. The nature of the antibody from TB negative serum recognising MA coated onto ELISA plates, however, still requires further investigation. Several possibilities exist, of which ACHA cross-reactivity is still one of them. Another possibility which has now come to light is that TB negative serum, as for TB positive patient serum, may also contain anti-MA antibodies generated after BCG vaccination, latent TB infection, or exposure to saprophytic mycobacteria. The presence of anti-MA antibodies in TB negative sera creates the opportunity to distinguish between patients with active disease and those latently infected. Furthermore, in order to achieve greater distinction between TB positive patient and TB negative serum, more specific MA antigens, natural α - and Ket-MA, have been identified as possible substitutes for the natural MA mixture for use in TB serodiagnosis. Because Ket-MA varies greatly depending on the growth stage of *M. tb*, it might be that MA subclass which would enable resolution between latent infection and active TB disease. The use of Ket-MA in the resonant mirror biosensor inhibition assay could provide the specificity required for a fast and accurate serodiagnostic assay for TB.

To conclude, this study has defined the resemblance between MA and cholesterol contained in liposomes, has given support for the possible presence of anti-MA antibodies in TB negative serum, and has provided the foundation for a patent based on using a particular MA subclass in the serodiagnosis of TB.



Appendix

Figure 1: Proton NMR of unesterified sigma MA

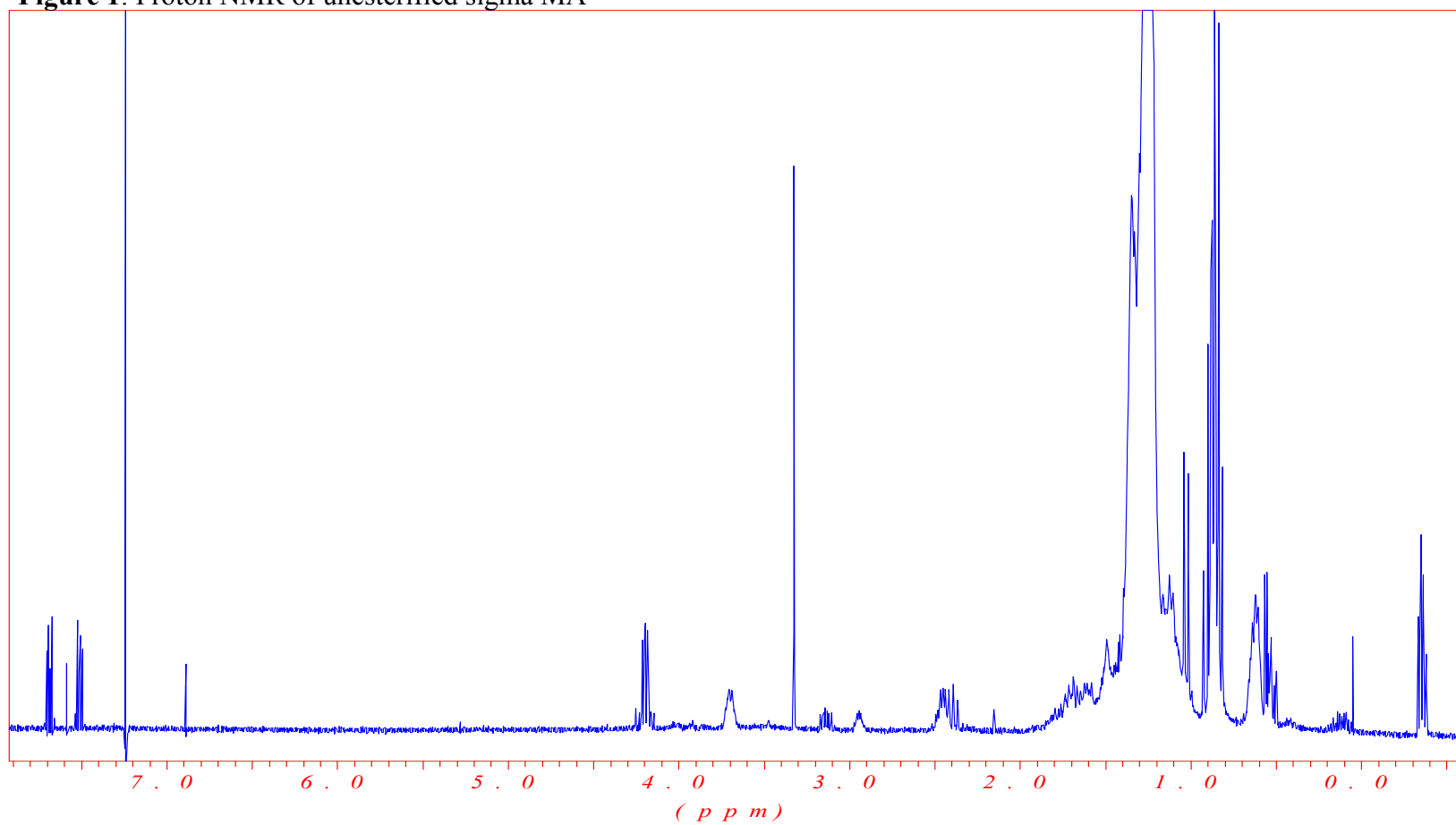




Figure 2: Proton NMR of purified α -MA

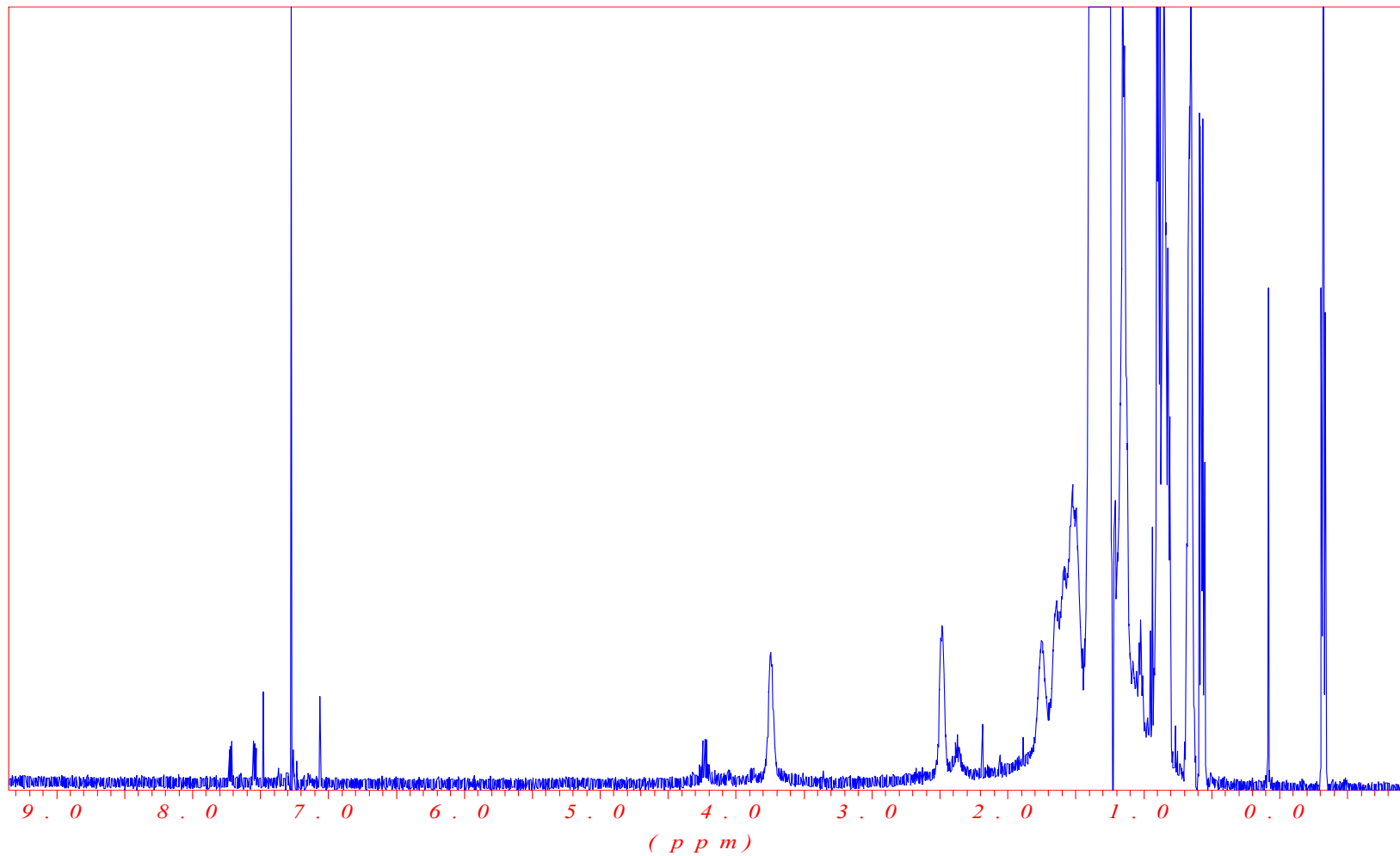




Figure 3: Carbon NMR of purified α -MA

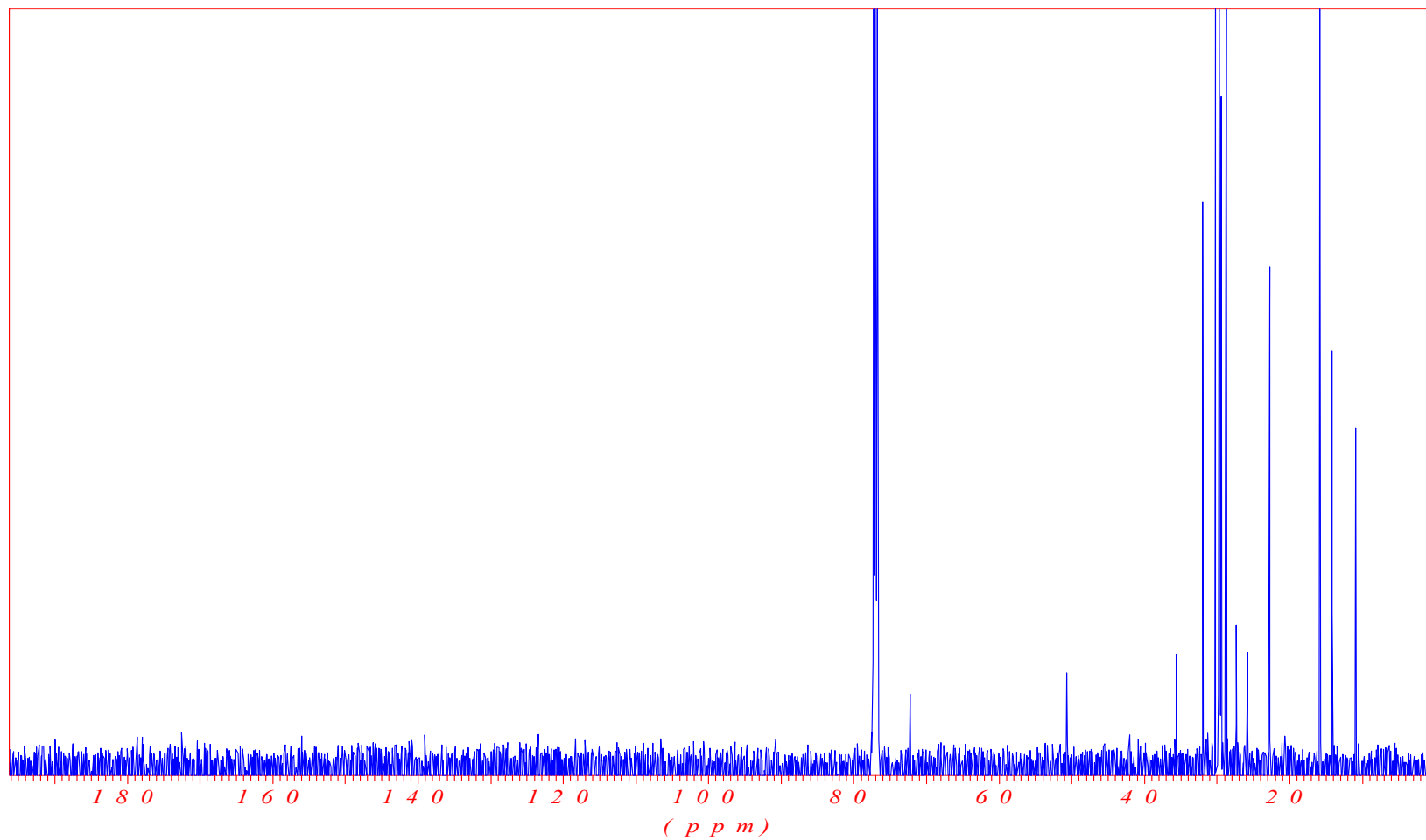




Figure 4: Proton NMR of purified MeO-MA

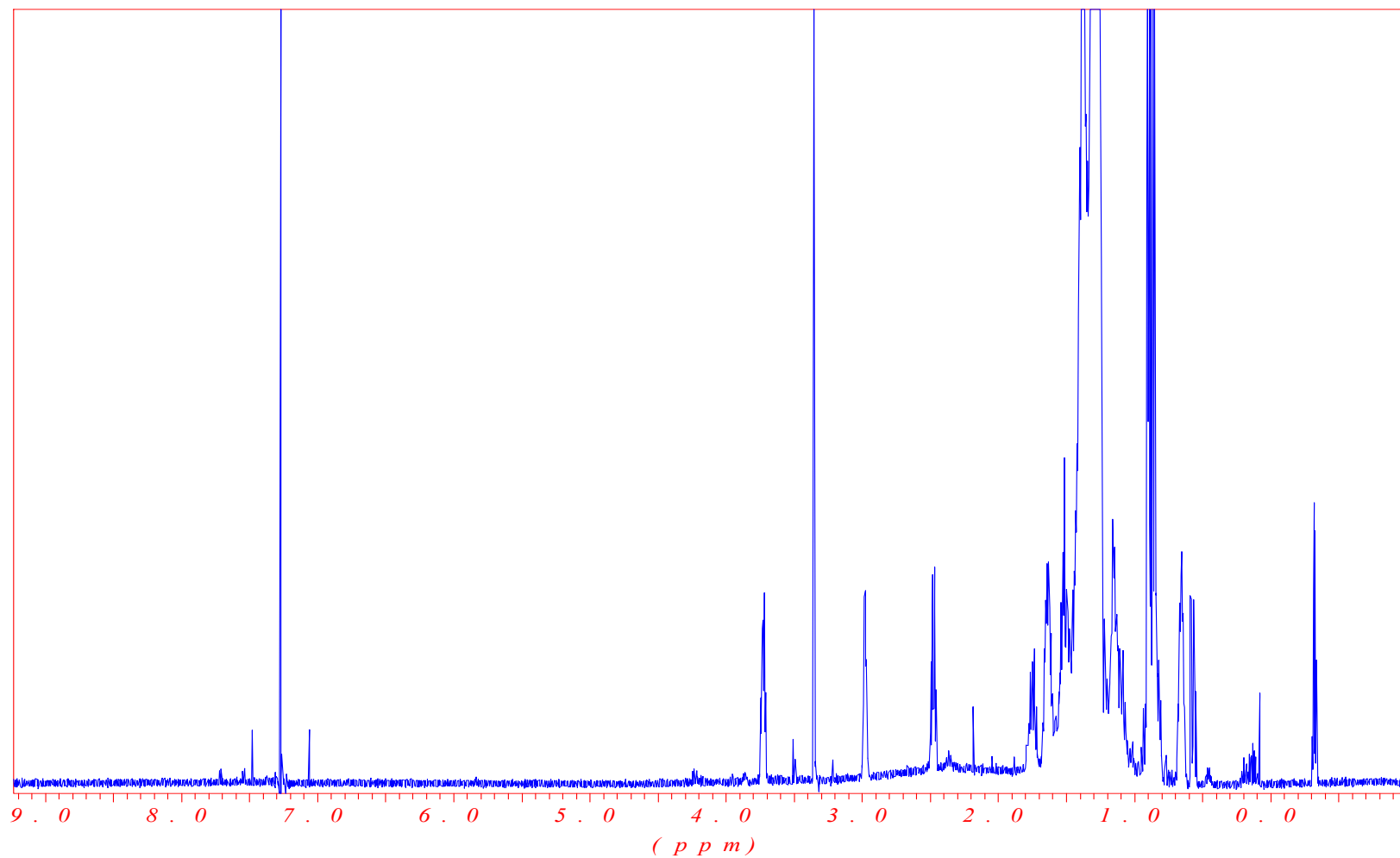




Figure 5: Carbon NMR of purified MeO-MA

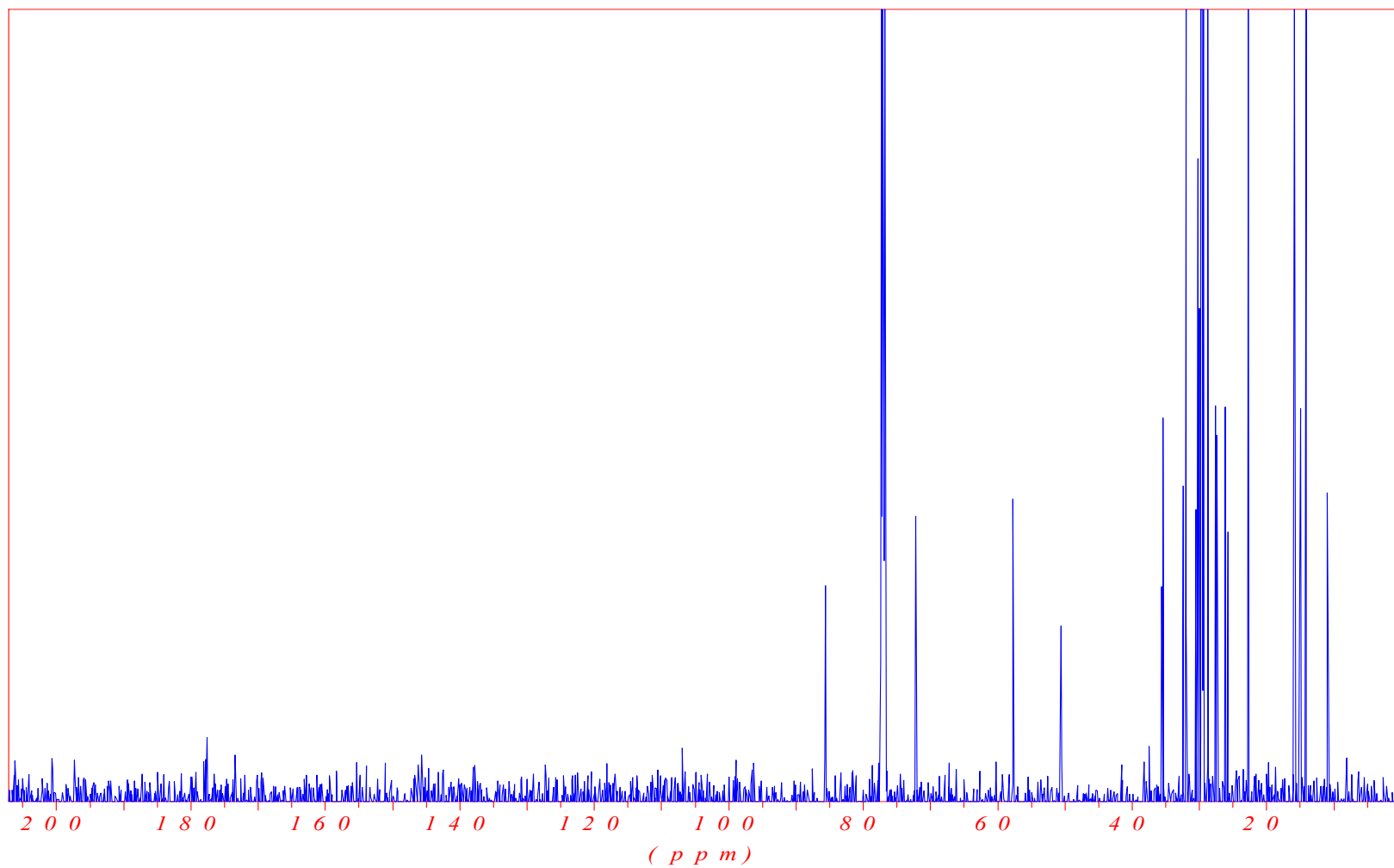




Figure 6: Proton NMR of purified Ket-MA

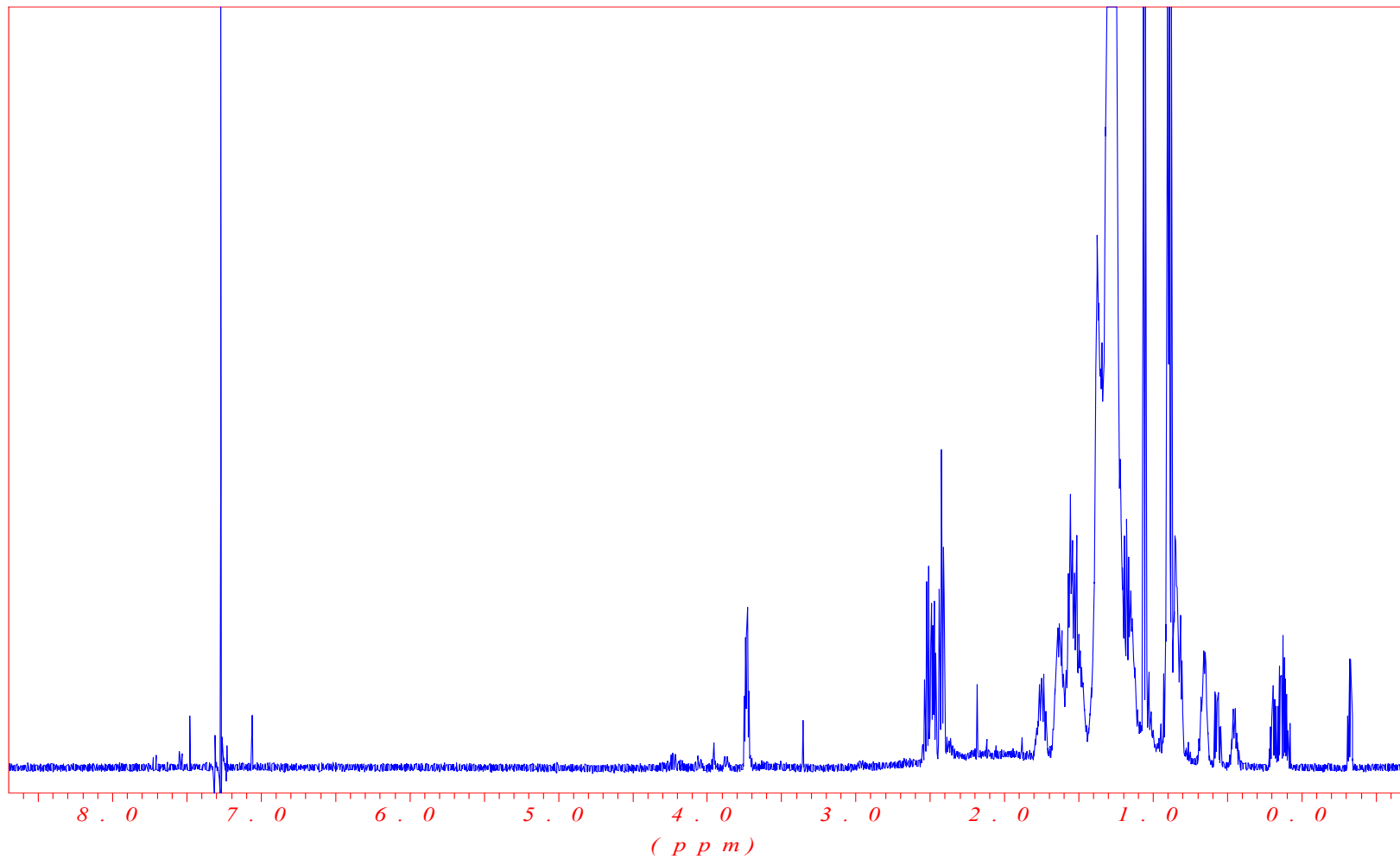
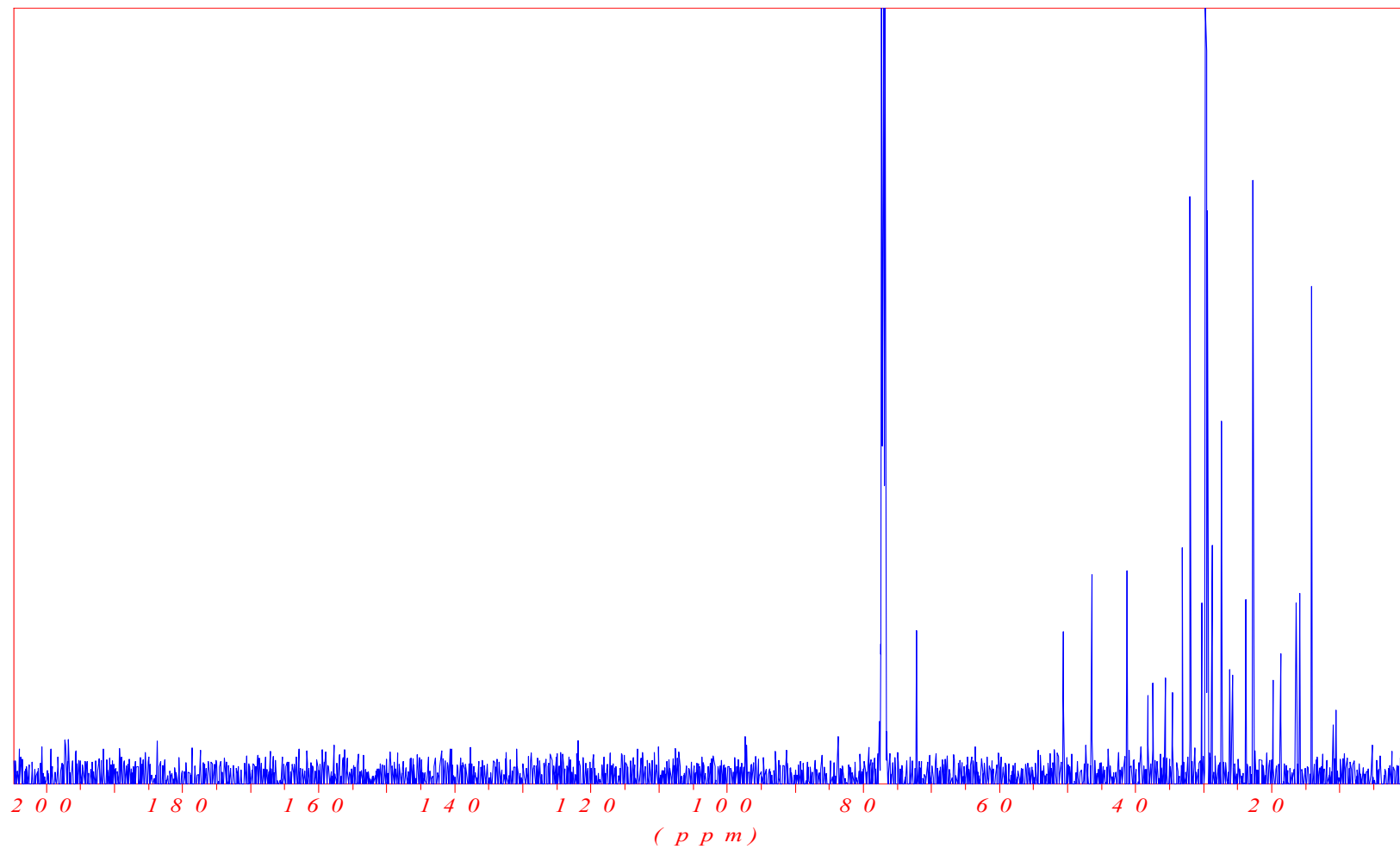




Figure 7: Carbon NMR of purified Ket-MA



References

- 1 **Castiglioni A.** 1933. History of Tuberculosis. Medical life. Froben Press. New York.
- 2 **Bloom B. R. and C. J. L. Murray.** 1992. Tuberculosis: commentary on a re-emergent killer. *Science*. **257**: 1055-1073
- 3 **Villemin J. A.** 1868. Studies on Tuberculosis. J. - B. Ballie `LMBO and Wire. Paris
- 4 **Koch R.** 1882. Reports of the Bavarian land institution for water research. 1932. English translation in American reviews in Tuberculosis and Pulmonary Diseases. **25**: 285
- 5 **Russel D. G.** 2007. Who puts the tubercle in tuberculosis? *Nat Rev Microbiol*. **5**: 39- 47
- 6 **Grange J. M.** 1988. Mycobacteria and human disease. Edward Arnold Ltd publishers. Bedford Square. London
- 7 **Glickman M. S. and W. R. Jacobs.** 2001. Microbial pathogenesis of *Mycobacterium tuberculosis*: Dawn of a discipline. *Cell*. **104**: 477-485
- 8 **Arora V. K., K. Gowrinath, and R. S. Rao.** 1995. Extrapulmonary involvement in HIV with special reference to tuberculosis cases. *Indian J. Tuberculosis*. **42**: 27-32
- 9 **Wells W. F.** 1955. Airborne Contagion and Air Hygiene. Harvard University Press. Cambridge
- 10 **Nardell E.** 1993. Pathogenesis of tuberculosis. In: Lung biology in health and disease. (Eds. L. B. Reichman, and E. Hirschfield). Marcel Dekker, Inc. New York. 103-123
- 11 **Capuano S. V., D. A. Croix, S. Pawar, A. Zinovik, A. Myers, P. L. Lin, S. Bissel, C. Fuhrman, E. Klein, and J. L. Flynn.** 2003. Experimental *Mycobacterium tuberculosis* infection of Cynomolgus Macaques closely resembles the various manifestations of human *M. tuberculosis* infection. *Infect Immun*. **71**: 5831–5844
- 12 **Ulrichs T. and S. H. E. Kaufmann.** 2002. Mycobacterial persistence and Immunity. *Front Biosci*. **7**: 458-469
- 13 **Schmitt E., G. Meuret, and L. Stix.** 1977. Monocyte recruitment in tuberculosis and sarcoidosis. *Br J Haematol*. **35**: 11-17

-
- 14 **Suter E.** 1952. The multiplication of tubercle bacilli within normal phagocytes in tissue culture. *J Exp Med.* **96**: 137
- 15 **Zhang Y.** 2004. Persistent and dormant tubercle bacilli and latent tuberculosis. *Front Biosci.* **9**: 1136-1156
- 16 **Brock I., M. Ruhwald, B. Lundgren, H. Westh, L. R. Mathiesen, and P. Ravn.** 2006. Latent tuberculosis in HIV positive , diagnosed by the *M. tuberculosis* specific interferon- γ test, *Respir Res.* **7**: 56
- 17 **American Thoracic Society.** 1999. Diagnostic standards and classification of tuberculosis in adult and children, an official statement adopted by the ATS Board of Directors, *Am J Respir Crit Care Med.* **161**: 1376-1395
- 18 **WHO report.** 2007. Fact sheet, HIV/ AIDS global and regional figures by end 2007
- 19 **WHO report.** 2007. Global tuberculosis control, the eleventh annual report. WHO/HTM/TB/2007.376
- 20 **WHO report.** 1994. Tuberculosis Programme: framework for effective tuberculosis control. WHO/TB/94.179
- 21 **Resolution WHA44.8.** 1993. Tuberculosis control programme. In: Handbook of resolutions and decisions of the World Health Assembly and the Executive Board. III. (1985-1992). World Health Organisation. Geneva. WHA44/1991/REC/1
- 22 **WHO report.** 2006. The Stop TB Strategy, Building on and enhancing DOTS to meet the TB-related Millennium Development Goals. WHO/HTM/TB/2006.368
- 23 **Frieden T. R., T. R Sterling, S. S Munsiff, C. J Watt, and C. Dye.** 2003. Tuberculosis. *Lancet.* **362**: 887-899
- 24 **Verschoor J. A. and P. Onyebujo.** 1999. The menace of the AIDS-tuberculosis combo: any solutions? *BioEssays.* **21**: 365-366
- 25 **Kremer L. and G. S. Besra.** 2002. Re-emergence of tuberculosis: strategies and treatment. *Expert Opin Drug Discovery.* **11**: 153-157
- 26 **Centre for Disease Control.** 2007. Fact sheet: Multidrug-Resistant Tuberculosis. Division of tuberculosis elimination. National centre for HIV/ AIDS, Viral Hepatitis, STD and TB prevention

-
- 27 **Murcia-Aranguren M. I.** 2001. Frequency of tuberculous and non-tuberculous mycobacteria in HIV infected patients from Bogota, Colombia. *BMC Infect Dis.* **1**:21
- 28 **Santoro-Lopes G., A. M. de Pinho, L. H. Harrison, and M. Schechter.** 2002. Reduced risk of tuberculosis among Brazilian patients with advanced human immunodeficiency virus infection treated with highly active antiretroviral therapy. *Clin Infect Dis.* **34**: 543–46
- 29 **Girardi E., G. Antonucci, P. Vanacore, M. Libanore, I. Errante, A. Matteelli, G. Ippolito, and the “Gruppo Italiano di Studio Tubercolosi e AIDS” (GISTA).** 2000. Impact of combination antiretroviral therapy on the risk of tuberculosis among persons with HIV infection. *AIDS.* **14**: 1985–991
- 30 **Lawn S. D., L. Bekker, and R. F. Miller.** 2005. Immune reconstitution disease associated with mycobacterial infections in HIV-infected individuals receiving anti-retroviral. *Lancet Infect Dis.* **5**: 361–73
- 31 **Gibson S. K., B. Mulder, A. J. A. M. van der Ven, N. Sam, M. J. Boeree, A. van der Zanden, and W. M. V. Dolmans.** 2007. Laboratory diagnosis of pulmonary tuberculosis in TB and HIV endemic settings and the contribution of real time PCR for *M. tuberculosis* in bronchoalveolar lavage fluid. *Trop Med Int Health.* **12**: 1210–1217
- 32 **Toossi Z.** 2003. Virological and immunological impact of tuberculosis on human immunodeficiency virus type 1 disease. *J Infect Dis.* **188**: 1146–55
- 33 **Schutze S., T. Machleidt, and M. Kronke.** 1992. Mechanisms of tumor necrosis factor action. *Sem Oncology.* **19**: 16–24
- 34 **Vicenzi E., M. Alfano, S. Ghezzi, A. Gatti, F. Veglia, A. Lazzarin, S. Sozzani, A. Mantovani, and G. Poli.** 2000. Divergent regulation of HIV-1 replication in PBMC of infected individuals by CC chemokines: suppression by RANTES, MIP-1alpha, and MCP-3, and enhancement by MCP-1. *J Leukoc Biol.* **68**: 405–12
- 35 **Pai M., L. W. Riley, and J. M. Colford, Jr.** 2004. Interferon- γ assays in the immunodiagnosis of tuberculosis: a systematic review, *Lancet Infect Dis.* **4**: 761-767
- 36 **Gennaro M. L.** 2000. Immunologic diagnosis of tuberculosis. *Clin Infect Dis.* **30**: S 243-246

-
- 37 **Dannenberg A. M., Jr.** 1989. Immune mechanisms in the pathogenesis of pulmonary tuberculosis. *Rev Infect Dis.* **11**: S369-378
- 38 **Watterson S. A. and F. A. Drobneiwski.** 2000. Modern laboratory diagnosis of mycobacterial infections. *J Clin Pathol.* **53**: 727-732
- 39 **Jackett P. S., G. H. Bothamley, H. V. Batra, A. Mistry, D. B. Young, and J. Iavanyi.** 1988. Specificity of antibodies to immunodominant mycobacterial antigens in pulmonary tuberculosis. *J Clin Microbiol.* **26**: 2313-2318
- 40 **Cheng A. C. C., W. W. Yew, and K. Y. Yuen.** 2005. Molecular diagnostics in tuberculosis. *Eur J Clin Microbiol Infect Dis.* **24**: 711-720
- 41 **Kalantri S., M. Pai, L. Pascopella, L. Riley, and A. Reingold.** 2000. Bacteriophage-based tests for the detection of *Mycobacterium tuberculosis* in clinical specimens: a systematic review and meta-analysis. *BMC Infect Dis.* **5**: 59
- 42 **Pounder J. I., W. K. Aldous, and G. L. Woods.** 2006. Comparison of real-time polymerase chain reaction using the Smart Cycler and the Gen-Probe amplified *Mycobacterium tuberculosis* direct test for detection of *M. tuberculosis* complex in clinical specimens. *Diagn Microbiol Infect Dis.* **54**: 217-222
- 43 **Pottumarthy S., V. C. Wells, and A. J. Morris.** 2000. A comparison of seven tests for serological diagnosis of tuberculosis. *J Clin Microbiol.* **38**: 2227-2231
- 44 **Shenai S., C. Rodrigues, and A. P. Mehta.** 2002. Evaluation of a new phage amplification technology for rapid diagnosis of tuberculosis. *Indian J Med Microbiol.* **20**: 194-199
- 45 **McNerney R.** 1999. TB: The return of the phage. A review of fifty years of mycobacteriophage research. *Int J Tuberc Lung Dis.* **3**: 179-184
- 46 **McNerney R., B. S. Kambashi, J. Kinkese, R. Tembwe, and P. Godfrey-Faussett.** 2004. Development of a bacteriophage phage replication assay for diagnosis of pulmonary tuberculosis. *J Clin Microbiol.* **42**: 2115-2120
- 47 **Tsicopoulos A., Q. Hamid, V. Varney, S. Ying, R. Moqbel, S. R. Durham, and A. B. Kay.** 1992. Preferential messenger RNA expression of Th1-type cells (IFN-gamma+, IL-2+) in classical delayed-type (tuberculin) hypersensitivity reactions in human skin. *J Immunol.* **148**: 2058-2061

-
- 48 **Daniel T. M.** 1980. The immunology of tuberculosis. *Clin Chest Med.* **1**: 189-201
- 49 **Shinnick T. M.** 2000. Diagnostic test needs for evaluating anti-tuberculosis vaccines. *Clin Infect Dis.* **30**: S276–8
- 50 **Lyashchenko K., C. Manca, R. Colangeli, A. Heijbel, A. Williams, and M. Laura.** 1998. Use of *Mycobacterium tuberculosis* complex-specific antigen cocktails for a skin test specific for tuberculosis. *Infect Immun.* **66**: 3606–3610
- 51 **Dewan P. K., J. Grinsdale, and L. M., Kawamura.** 2007. Low sensitivity of a whole-blood interferon- γ release assay for detection of active tuberculosis. *Clin Infect Dis.* **44**: 69-73
- 52 **Brock I., K. Welding, T. Lillebaek, F. Follmann, and P. Andersen.** 2004. Comparison of Tuberculin Skin Test and new specific blood test in tuberculosis contacts. *Am J Respir Crit Care Med.* **170**: 65–69
- 53 **Dogra S., P. Narang, D. K. Mendiratta, P. Chaturvedi, A. L. Reingold, J. M. C. Jr, L. W. Riley, and M. Pai.** 2007. Comparison of a whole blood interferon-g assay with tuberculin skin testing for the detection of tuberculosis infection in hospitalized children in rural India. *Journal of Infection.* **54**: 267-276
- 54 **Liebeschuetz S., S. Bamber, K. Ewer, J. Deeks, A. Pathan, and A. Lalvani.** 2004. Diagnosis of tuberculosis in South African children with a T-cell-based assay: A prospective cohort study. *Lancet.* **364**: 2196-2203
- 55 **Chapmana A. L. N., M. Munkantab, K. A. Wilkinson, A. A. Pathana, K. Ewera, H. Aylesb, W. H. Reecea, A. Mwingab, P. Godfrey-Faussettb, and A. Lalvania.** 2002. Rapid detection of active and latent tuberculosis infection in HIV-positive individuals by enumeration of *Mycobacterium tuberculosis*-specific T cells. *AIDS.* **16**: 2285-2293
- 56 **Grange J. M.** 1984. The humoral immune response in tuberculosis: its nature, biological role, and diagnostic usefulness. *Adv Tuberc Res.* **21**: 1-78
- 57 **WHO GMP.** 1997. WHO tuberculosis diagnostic workshop: product development guidelines. Cleveland. Ohio: 1-20.

-
- 58 **Ongut G., D. Ogunc, F. Gunseren, C. Ogus, L. Donmez, D. Colak, and M. Gultekin.** 2006. Evaluation of the ICT Tuberculosis test for the routine diagnosis of tuberculosis. *BMC Infect Dis.* **6**: 37
- 59 **Simmoney N., J. M Molina, M. Molimard, E. Oksenhendler, and P. H.Lagrange.** 1996. Circulating immune complexes in human tuberculosis sera: demonstration of specific antibodies against *Mycobacterium tuberculosis* glycolipids (DAT, PGLTb1, LOS) antigens in isolated circulating immune complexes. *Eur J Clin Invest.* **27**: 128-134
- 60 **Kawamura M., N. Sueshige, K. Imayoshi, I. Yano, R. Maekura, and H. Kohno.** 1997. Enzyme Immunoassay to detect anti-tuberculous glycolipid antigen (anti-TBGL antigen) antibodies in serum for diagnosis of tuberculosis. *J Clin Lab Anal.* **11**: 40–145
- 61 **Sekanka G., M. Baird, D. E. Minnikin, and J. Grooten.** 2007. Mycolic acids for the control of tuberculosis. *Expert opinion on Therapeutic Patents.* **17**: 315-331
- 62 **Maekura R., Y. Okuda, M. Nakagawa, T. hiraga, S. Yokota, M. M. Ito, I. Yano, H. Oakikohno, M. Wada, C. Abe, T. Toyoda, T. Kishimoto, and T. Ogura.** 2001. Clinical evaluation of anti-tuberculous glycolipid immunoglobulin G antibody assay for rapid serodiagnosis of pulmonary tuberculosis. *J Clin Microbiol.* **39**: 3606-3608
- 63 **Fujita Y., T. Doi, K. Sato, and I. Yano.** 2005. Diverse humoral immune responses and changes in IgG antibody levels against mycobacterial lipid antigens in active tuberculosis. *Microbiology.* **151**: 2065-2074
- 64 **Schleicher G. K., C. Feldman, Y. Vermaak, and J. A. Verschoor.** 2002. Prevalence of Anti-mycolic acid antibodies in patients with pulmonary tuberculosis co-infected with HIV. *Clin Chem Lab Med.* **40**: 882-87
- 65 **Sada E., P. J. Brennan, T. Herrera, and M. Torres.** 1990. Evaluation of lipoarabinomannan for the serological diagnosis of tuberculosis. *J Clin Microbiol.* **28**: 2587-2590
- 66 **Talbot E. A., D. C. H. Burgess, N. M. Hone, M. F. Iademarco, M. J. Mwasekaga, H. J. Moffat, T. L. Moeti, R. A. Mwansa, P. Letsatsi, N. T Gokhale, T. A.**

-
- Kenyon, and C. D. Wells.** 2004. Tuberculosis serodiagnosis in a predominantly HIV–infected population of hospitalized patients with cough, Botswana. *Clin Infect Dis.* **39**: 1–7
- 67 **Sada E., D. Aguilar, M. Torres, and T. Herrera.** 1992. Detection of lipoarabinomannan as a diagnostic test for tuberculosis. *J Clin Microbiol.* **30**: 2415-2418
- 68 **Boehmea C., E. Molokova, F. Minja, S. Geis, T. Loscher, L. Maboko, V. Koulchin, and M. Hoelscher.** 2005. Detection of mycobacterial lipoarabinomannan with an antigen-capture ELISA in unprocessed urine of Tanzanian patients with suspected tuberculosis. *Trans R Soc Trop Med Hyg.* **99**: 893-900
- 69 **Nabeshima S., M. Murata, K. Kashiwagi, M. Fujita, N. Furusyo, and J. Hayashi.** 2005. Serum antibody response to tuberculosis-associated glycolipids antigen after BCG vaccination in adults, *J Infect Chemotherapy.* **11**: 256-258
- 70 **Kitada S., R. Maekura, N. Toyoshima, T. Naka, N. Fujiwara, M. Kobayashi, I. Yano, M. Ito, and K. Kobayashi.** 2005. Use of a glycopeptidolipid core antigen for serodiagnosis of *Mycobacterium avium* complex pulmonary disease in immunocompetent patients. *Clin Diagn Lab Immunol.* **12**: 44-51
- 71 **Siko G. D. R.** 2002. Mycobacterial mycolic acids as immunoregulatory lipid antigens in the resistance to tuberculosis. PhD thesis in the Faculty of Natural and Agricultural Sciences Department of Biochemistry. University of Pretoria
- 72 **Thanyani S. T., V. Roberts, D. G. R. Siko, P. Vrey, and J. A. Verschoor.** 2008. A novel application of affinity biosensor technology to detect antibodies to mycolic acid in tuberculosis patients. *J Immunol Methods.* **332**: 61-72
- 73 **Minnikin D. E., S. M. Minnikin, J. H. Parlett, M. Goodfellow, and M. Magnusson.** 1984. Mycolic acid patterns of some species of *Mycobacterium*. *Arch Microbiol.* **139**: 225-231
- 74 **Fenton M. J. and M. W. Vermeulen.** 1996. Immunopathology of tuberculosis: Roles of Macrophages and Monocytes. *Infect Immun.* **64**: 683-690
- 75 **Brennan P. J. and H. Nikaido.** 1995. The envelope of mycobacteria. *Annu Rev Biochem.* **64**: 29-63.

-
- 76 **McNeil M., M. Daffé, and P. J. Brennan.** 1991. Location of the mycolyl ester substituents in the cell walls of mycobacteria. *J Biol Chem.* **266**: 13217-13223
- 77 **Boshoff H. I. and C. E. Barry.** 2006. Is the mycobacterial cell wall a hopeless drug target for latent tuberculosis? *Drug Discov Today: Disease Mechanisms.* **3**: 237-245
- 78 **Rastogi N., C. Frehel, and H. L. David.** 1986. Triple-layered structure of mycobacterial cell wall: Evidence for the existence of a polysaccharide-rich outer layers in 18 mycobacterial species. *Curr Microbiol.* **13**: 237-242
- 79 **Daffé M. and G. Etienne.** 1999. The capsule of *Mycobacterium tuberculosis* and its implications for pathogenicity. *Tubercle Lung Dis.* **79**: 153–169
- 80 **Minnikin D. E. and M. Goodfellow.** 1980. Lipid composition in the classification and identification of acid-fast bacteria. *Soc Appl Bacteriol Symp Ser.* **8**: 189–256
- 81 **Kartman B., S. Stengler, and M. Niederweis.** 1999. Porins in the cell wall of *Mycobacterium tuberculosis*. *J Bacteriol.* **181**: 6543–6546
- 82 **Hoffmann C., A. Leis, M. Niederweis, J. M. Plitzko, and H. Engelhardt.** 2008. Disclosure of the mycobacterial outer membrane: Cryo-electron tomography and vitreous sections reveal the lipid bilayer structure. *PNAS.* **105**: 3963–3967
- 83 **Imaeda T., F. Kanetsuma, and B. Galindo.** 1968. Ultrastructure of cell walls of genus *Mycobacterium*. *J Ultrastruct Res.* **25**: 46-63
- 84 **Klegermann M. E., P. O. Devadoss, J. and L. Garrido, H. R. Reyes, and M. J. Groves.** 1996. Chemical and ultrastructural investigations of *Mycobacterium bovis* BCG: applications for the molecular structure of the mycobacterial cell envelope. *FEMS Immunol Med Microbiol.* **15**: 213-222
- 85 **Faller M., M. Niederweis, and G. E. Schulz.** 2004. The structure of a mycobacterial outer-membrane channel. *Science.* **303**: 1189 – 1192
- 86 **Minnikin, D.E.** 1982. Lipids: complex lipids, Their chemistry, biosynthesis and roles. In *The Biology of the Mycobacteria*. 1. Ratledge, C., and Stanford, J. (eds). London: Academic Press. 95–185.
- 87 **Ortalo-Magne A., A. Lemassu, M.-A. Laneelle, F. Bardou, G. Silve, P. Gounon, G. Marchal, and M. Daffe.** 1996. Identification of the surface-exposed lipids on the

-
- cell envelopes of *Mycobacterium tuberculosis* and other mycobacterial species. J Bacteriol. **178**: 456-461
- 88 **Puech V., M. Chami, A. Lemassu, M.-A. Laneelle, B. Schiffler, P. Gounon, N. Bayan, R. Benz, and M. Daffe.** 2001. Structure of the cell envelope of corynebacteria: importance of the noncovalently bound lipids in the formation of the cell wall permeability barrier and fracture plane. Microbiol. **147**: 1365-1382
- 89 **Liu J., E. Y. Rosenberg, and H. Nikaido.** 1995. Fluidity of the lipid domain of cell wall from *Mycobacterium chelonae*. PNAS. **92**: 11254-11258
- 90 **Wang L., R. A. Slayden, C. E. Barry III, and J. Liu.** 2000. Cell wall structure of a mutant of *Mycobacterium smegmatis* defective in the biosynthesis of mycolic acids. J Biol Chem. **275**: 7224-7229
- 91 **Villineuve M., M. Kawai, H. Kanashima, M. Watanabe, D. E. Minnikin, and H. Nakahara.** 2005. Temperature dependence of the langmuir monolayer packing of mycolic acids from *Mycobacterium tuberculosis*. Biochim Biophys Acta. **1715**: 71-80
- 92 **Hasegawa T., J. Nishijo, and M. Watanabe.** 2000. Conformational characterization of α -mycolic acid in a monolayer film by the Langmuir-Blodgett technique and Atomic Force Microscopy. Langmuir. **16**: 7325-7330
- 93 **Christensen H., N. J. Garton, R. W. Horobin, D. E. Minnikin, and M. R. Barer.** 1999. Lipid domains of mycobacteria studied with fluorescent molecular probes. Mol Microbiol. **31**: 1561-1572
- 94 **Dover L. G., A. M. Cerdeno-Tarraga, M. J. Pallen, J. Parkhill, and G. S. Besra.** 2004. Comparative cell wall core biosynthesis in the mycolated pathogens, *Mycobacterium tuberculosis* and *Corynebacterium diphtheriae*. FEMS Microbiol Rev. **28**: 225-250
- 95 **Wiker H. G. and M. Harboe.** 1992. Antigen 85 complex: a major secretion product of *Mycobacterium tuberculosis*. Microbiol Rev. **56**: 648-661
- 96 **Bukhary Z. A.** 2007. Evaluation of anti-A60 antigen IgG enzyme linked immunosorbant assay for serodiagnosis of pulmonary tuberculosis. Ann Thorac Med. **2**: 47-51

-
- 97 **Lee B-Y., S. A. Hefta, and P. J. Brennan.** 1992. Characterisation of the major membrane protein of virulent *Mycobacterium tuberculosis*. *Infect Immun.* **60**: 2066-2074
- 98 **Dhiman N. and G. K. Kuller.** 1997. Immunoprophylactic properties of 71-kDa cell wall-associated protein antigen of *Mycobacterium tuberculosis* H37Ra. *Med Microbiol Immunol.* **186**: 45-51
- 99 **Britton W. J., L. Hellqvist, A. Basten, and R. L. Raison.** 1985. *Mycobacterium leprae* antigens involved in human immune responses: Identification of 4 antigens by monoclonal antibodies. *J Immunol.* **135**: 4171 – 4179
- 100 **Katti M. K.** 2001. Immunodiagnosis of tuberculous meningitis: rapid detection of mycobacterial antigens in cerebrospinal fluid by reverse passive hemagglutination assay and their characterization by Western blotting. *FEMS Immunol Med Microbiol.* **31**: 59-64
- 101 **Hirschfield G. R., M. McNeil, and P. J. Brennan.** 1990. Peptidoglycan-associated polypeptides of *Mycobacterium tuberculosis*. *J Bacteriol.* **172**: 1005-1013
- 102 **Yeruva V. C., S. Duggirala, V. Lakshmi, D. Kolarich, F. Altmann, and M. Sritharan.** 2006. Identification and characterization of a major cell wall-associated iron-regulated envelope protein (Irep-28) in *Mycobacterium tuberculosis*. *Clin Vac Immunol.* **13**: 1137–1142
- 103 **Jackson M., G. Stadthagen, and B. Gicquel.** 2007. Long-chain multiple methyl-branched fatty, acid-containing lipids of *Mycobacterium tuberculosis*: Biosynthesis, transport, regulation and biological activities. *Tuberculosis.* **87**: 78–86
- 104 **Munoz M., M-A. Lanéelle, M. Luquin, J. Torrelles, E. Julián, V. Ausina, and M. Daffé.** 1997. The occurrence of an antigenic triacyl trehalose in clinical isolates and reference strains of *Mycobacterium tuberculosis*. *FEMS Microbiol Lett.* **157**: 251-259
- 105 **Minnikin D. E., G. Dobson, M. Goodfellow, P. Draper, M. Magnusson.** 1985. Quantitative comparison of the mycolic and fatty acid compositions of *Mycobacterium leprae* and *Mycobacterium goodsonae*. *J Gen Microbiol.* **131**: 2013–2021

-
- 106 **Daffé M., F. Papa, A. Laszlo, and H. L. David.** 1989. Glycolipids of recent clinical isolates of *Mycobacterium tuberculosis*: Chemical characterization and immunoreactivity. *J Gen Microbiol.* **135**: 2759-2766
- 107 **Baer H. H.** 1993. The structure of an antigenic glycolipid (SL-IV) from *Mycobacterium tuberculosis*. *Carbohydr Res.* **240**: 1-22
- 108 **Tórtola M. T., M. A. Lanéle, and N. Martín-Casabona.** 1996. Comparison of two 2,3-diacyl trehalose antigens from *Mycobacterium tuberculosis* and *Mycobacterium fortuitum* for serology in tuberculosis patients. *Clin Diagn Lab Immunol.* **3**: 563–566
- 109 **Cruaud P., J. T. Yamashita, N. M. Casabona, F. Papa, and H. David.** 1990. Evaluation of a novel 2,3-diacyl-trehalose-2'-sulphate (SL-IV) antigen for case finding and diagnosis of leprosy and tuberculosis. *Res Microbiol.* **141**: 679-694
- 110 **Gilleron M., S. Stenger, Z. Mazorra, F. Wittke, S. Mariotti, G. Böhmer, J. Prandi, L. Mori, G. Puzo, and G. De Libero.** 2004. Diacylated sulfoglycolipids are novel mycobacterial antigens stimulating CD1-restricted T cells during infection with *Mycobacterium tuberculosis*. *J Exp Med.* **199**: 649-659
- 111 **Ortalo-Magné A., M-A. Dupont, A. Lemassu, B. Andersen, P. Goudon, and M. Daffé.** 1995. Molecular composition of the outermost capsular material of the tubercle bacillus. *Microbiol.* **141**: 1609–1620
- 112 **Lemaire G., G. P. Tenu, and J. F. Petit.** 1986. Natural and synthetic trehalose diesters as immunomodulators. *Med Res Rev.* **6**: 243-274
- 113 **Bekierkunst A., I. S. Levij, E. Yarkoni, E. Vilkas, A. Adam, and E. Lederer.** 1969. Granuloma formation induced in mice by chemically defined mycobacterial fractions. *J Bacteriol.* **100**: 95-102
- 114 **Guidry T. V., Hunter R. L. Jr, and J. K. Actor.** 2007. Mycobacterial glycolipid trehalose 6,6'-dimycolate-induced hypersensitive granulomas: contribution of CD4+ lymphocytes. *Microbiol.* **152**: 3360-3369
- 115 **Fujita Y., T. Doi, R. Maekura, M. Ito, and I. Yano.** 2006. Differences in serological responses to specific glycopeptidolipid-core and common lipid antigens in

-
- patients with pulmonary disease due to *Mycobacterium tuberculosis* and *Mycobacterium avium* complex. J Med Microbiol. **55**: 189-199
- 116 **Fujiwara N., J. Pan, K. Enomoto, Y. Terano, T. Honda, and I. Yano.** 1999. Production and partial characterization of anti-cord factor (trehalose-6, 6'-dimycolate) IgG antibody in rabbits recognizing mycolic acid subclasses of *Mycobacterium tuberculosis* or *Mycobacterium avium*. FEMS Immun Med Microbiol. **24**: 141-149
- 117 **Dinadayala P., F. Laval, C. Raynaud, A. Lemassu, M-A. Lanéelle, G. Lanéelle, and M. Daffé.** 2003. Tracking the putative biosynthetic precursors of oxygenated mycolates of *Mycobacterium tuberculosis*. J Biol Chem. **278**: 7310-7319
- 118 **Liu J., C. E. Barry III, G. S. Besra, and H. Nikaido.** 1996. Mycolic acid structure determines the fluidity of the mycobacterial cell wall. J Biol Chem. **271**: 29545–29551
- 119 **Beckman E. M., S. A. Porcelli, C. T. Morita, S. M. Behar, S. T. Furlong, and M. B. Brenner.** 1994. Recognition of lipid antigen by CD1-restricted $\alpha\beta^+$ T-cells. Nature. **372**: 691-694
- 120 **Porcelli S. M., C. T. and M. B. Brenner.** 1992. CD1b restricts the response of human CD 4– 8– T lymphocytes to a microbial antigen. Nature. **360**: 593-597
- 121 **Pan J., N. Fujiwara, S. Oka, R. Maekura, T. Ogura, and I. Yano.** 1999. Anti-cord factor (trehalose 6,6'-dimycolate) IgG antibody in tuberculosis patients recognizes mycolic acids subclasses. Microbiol Immunol. **43**: 863-69
- 122 **Bhatt A., N. Fujiwara, K. Bhatt, S. S. Gurcha, L. Kremer, B. Chen, J. Chan, S. A. Porcelli, K. Kobayashi, G. S. Besra, and W. R. Jacobs, Jr.** 2007. Deletion of kasB in *Mycobacterium tuberculosis* causes loss of acid-fastness and subclinical latent tuberculosis in immunocompetent mice. Microbiol. **104**: 5157–5162
- 123 **Stodola F. H., A. Lesuk, and R. J. Anderson.** 1938. The chemistry of the lipids of tubercle bacilli. J Biol Chem. **54**: 505-513
- 124 **Asselineau J. and E. Lederer.** 1950. Structure of the mycolic acids of mycobacteria. Nature. **166**: 782-3

-
- 125 **Asselineau C. and J. Asselineau.** 1966. Stereochemistry of the corynomycolic acids. *Bulg Soc Chem.* 6: 1992-1999
- 126 **Barry C. E., R. E. Lee, K. Mdluli, A. E. Sampson, B. G. Schroeder, R. E. Slayden, and Y. Yuan.** 1998. Mycolic acids: Structure, biosynthesis and physiological functions. *Prog Lipid Res.* 37: 43-179
- 127 **Watanabe M., Y. Aoyagi, M. Ridell, and D. E. Minnikin.** 2001. Separation and characterization of individual mycolic acids in representative mycobacteria. *Microbiol.* 147: 1825-183
- 128 **Watanabe M., Y. Aoyagi, H. Mitome, T. Fujita, H. Naoki, M. Ridell and D. E. Minnikin.** 2002. Location of functional groups in mycobacterial meromycolate chains; the recognition of new structural principles in mycolic acids. *Microbiol.* 148: 1881-1902
- 129 **Minnikin D. E. and N. Polgar.** 1967. The methoxymycolic and ketomycolic acids from human tubercle bacilli. *Chem Commun.* 1172-1174
- 130 **Yuan Y., D. C. Crane, J. M. Musser, S. Sreevatsan, and C. E. Barry, III.** 1997. MMAS-1, the branch point between *cis*- and *trans*-cyclopropane containing oxygenated mycolates in *Mycobacterium tuberculosis*. *J Biol Chem.* 272: 10041-10049
- 131 **Shui G., A. K. Bendt, K. Pethe, T. Dick, and M. R. Wenk.** 2007. Sensitive profiling of chemically diverse bioactive lipids. *J Lip Res.* 48: 1976-1984
- 132 **Yuan Y., Y. Zhu, D. D. Crane, and C. E. Barry III.** 1998. The effect of oxygenated mycolic acid composition on cell wall function and macrophage growth in *Mycobacterium tuberculosis*. *Mol Microbiol.* 29: 1449-1458
- 133 **Hasegawa T. and R. M. Leblanc.** 2003. Aggregation properties of mycolic acid molecules in monolayer films: a comparative study of compounds from various acid-fast bacterial species. *Biochim Biophys Acta.* 1617: 89-95
- 134 **Dubnau E., J. Chan, C. Raynaud, V. P. Mohan, M-A. Lan elle, K. Yu, A. Que mard, I. Smith, and M. Daff .** 2000. Oxygenated mycolic acids are necessary for virulence of *Mycobacterium tuberculosis* in mice. *Mol Microbiol.* 36: 630-637

-
- 135 Yuan Y., R. E. Lee, G. S. Besra, J. T. Belisle, and C. E. Barry, III. 1995. Identification of a gene involved in the biosynthesis of cyclopropanated mycolic acids in *Mycobacterium tuberculosis*. PNAS. **92**: 6630-6634
- 136 George K. M., Y. Yuan, D. R. Sherman, and C. E. Barry, III. 1995. The biosynthesis of cyclopropanated mycolic acids in *Mycobacterium tuberculosis*. Identification and functional analysis of CMAS-2. J Biol Chem. **270**: 27292–27298
- 137 Koch M., V. S. Stronge, D. Shepherd, S. D. Gadola, B. Mathew, G. Ritter, A. R. Fersht, G. S. Besra, R. R. Schmidt, E. Y. Jones, and V. Cerundolo. 2005. The crystal structure of human CD1d with and without α -galactosylceramide. Nature Immunol. **6**: 819-826
- 138 Moody D. B., M. Sugita, P. J. Peters, M. B. Brenner, and S. A. Porcelli. 1996. The CD1-restricted T-cell response to mycobacteria. Res Immunol. **67**: 550-559
- 139 Grant E. P., E. M. Beckman, S. M. Behar, M. Degano, D. Frederique, G. S. Besra, I. A. Wilson, S. A. Porcelli, S. T. Furlong, and M. B. Brenner. 2002. Fine specificity of TCR complementarity-determining region residues and lipid antigen hydrophilic moieties in the recognition of a CD1-lipid complex. J Immunol. **168**: 3933-3940
- 140 Rosat J-P., E. P. Grant, E. M. Beckman, C. C. Dascher, P. A. Sieling, D. Frederique, R. L. Modlin, S. A. Porcelli, S. T. Furlong, and M. B. Brenner. 1999. CD1-restricted microbial lipid antigen-specific recognition found in the CD8⁺ $\alpha\beta$ T cell pool. J Immunol. **162**: 366-371
- 141 Goodrum M. A., D. G. R. Siko, T. Niehues, T. Eichelbauer, and J. A. Verschoor. 2001. Mycolic acids from *Mycobacterium tuberculosis*: Purification by countercurrent distribution and T-cell stimulation. Microbios. **106**: 55-67
- 142 Sieling P. A., M.-T. Ochoa, D. Jullien, D. S. Leslie, S. Sabet, J.-P. Rosat, A. E. Burdick, T. H. Rea, M. B. Brenner, S. A. Porcelli, and R. L. Modlin. 2000. Evidence for human CD41 T cells in the CD1-restricted repertoire: derivation of mycobacteria-reactive T cells from leprosy lesions. J Immunol. **164**: 4790-4796

-
- 143 **Sugita M., D. B. Moody, R. M. Jackman, E. P. Grant, J. P. Rosat, S. M. Behar, P. J. Peters, S. A. Porcelli, and M. B. Brenner.** 1998. CD1-A new paradigm for antigen presentation and T cell activation. *Clin Immun Immunopathol.* **87**: 8-14
- 144 **Schluger N. W.** 2001. Recent advances in our understanding of human host responses to tuberculosis. *Respir Res.* **2**: 157–163
- 145 **Alving C. R. and G. M. Swartz.** 1990. Antibodies to cholesterol, cholesterol conjugates, and liposomes: Implications for atherosclerosis and autoimmunity. *Crit Rev Immunol.* **10**: 441-453
- 146 **Sebatjane S. I.** 2003. Anti-tuberculosis drug design based on a possible mimicry between host and pathogen lipids. MSc dissertation. Faculty of Natural and Agricultural Sciences. University of Pretoria
- 147 **Deysel M.** 2007. Structure function relationships of mycolic acids in tuberculosis. PhD in the Department of Biochemistry. Faculty of Natural and Agricultural Sciences. University of Pretoria
- 148 **Benadie Y.** 2007. Amphotericin B as a mycolic acid specific targeting agent in tuberculosis. MSc dissertation. Faculty of Natural and Agricultural Sciences. University of Pretoria
- 149 **Brajtburg A., W. G. Powderly, G. S. Kobayash, G. Medoff.** 1990. Amphotericin: Current understanding of mechanisms of action. *Antimicrob Agents Chemother.* **34**: 183-188
- 150 **Dmetriéve B. A., S. Ehlers, E. T. Rietschel, and P. J. Brennan.** 2000. Molecular mechanics of the mycobacterial cell wall: From horizontal layers to vertical scaffolds. *Int J Med Microbiol.* **3**: 251-258
- 151 **Sheriff S., E. W. Silverton, E. A. Padlan, G. H. Cohen, S. J. Smith-Gill, B. C. Finzel, and D. R. Davies.** 1987. Three-dimensional structure of an antibody-antigen complex. *PNAS.* **84**: 8075-8079
- 152 **Swartz G. M., M. K. Gentry, L. M. Amende, E. J. Blanchette-Mackie, and C. R. Alving.** 1988. Antibodies to cholesterol. *PNAS.* **85**: 1902-1906
- 153 **Horvath A., G. Fust, I. Horvath, G. Vallus, J. Duba, P. Harcos, Z. Prohaszka, E. Rajnavolgyi, L. Janoskuti, M. Kovacs, A. Csaszar, L. Romics, and I. Karadi.**

-
2001. Anti-cholesterol antibodies (ACHA) in patients with different atherosclerotic vascular diseases and healthy individuals. Characterization of human ACHA. *Atherosclerosis*. **156**: 185-192
- 154 **Dijkstra J., G. M. Swartz Jr, J. J. Raney, J. Anigolu, L. Toro, C. A. Nacy, and S. J. Green.** 1996. Interactions of anti-cholesterol antibodies with human lipoproteins. *J Immunol*. **157**: 2006-2013
- 155 **Bíró A., L. Cervenak, A. Balogh, A. Lőrincz, K. Uray, A. Horváth, L. Romics, J. Matkó, G. Füst, and G. László.** 2007. Novel anti-cholesterol monoclonal immunoglobulin G antibodies as probes and potential modulators of membrane raft-dependent immune functions, *J Lipid Res*. **48**: 19-29
- 156 **Goodrum M. A., D. G. R. Siko, T. Neihust, D. Eichelbauer, and J. A. Verschoor.** 2001. Mycolic acids from *Mycobacterium tuberculosis*: Purification by countercurrent distribution and T-cell stimulation. *Microbios*. **106**: 55-67
- 157 **Al Dulayymi J. R., M. S. Baird, and E. Roberts.** 2003. The synthesis of a single enantiomer of a major alpha-mycolic acid of *Mycobacterium tuberculosis*. *Chem Commun* **2**: 228-229
- 158 **Stolz A. C.** 2002. Immunological properties of mycolic acids, the major lipid cell wall component of *Mycobacterium tuberculosis*. PhD thesis in Faculty of Health Science. University of Pretoria. Pretoria
- 159 **Sackman E.** 1996. Supported membranes: scientific and practical applications, *Science*. **271**: 43-48
- 160 **Almeida R. F. M., A. Federov, and M. Prieto.** 2003. Sphingomyelin/phosphatidyl choline/cholesterol phase diagram: Boundaries and composition of lipid rafts, *Biophys J*. **85**: 2406-2416
- 161 **Benadie Y., M. Deysel, D. G. R. Siko, V. V. Roberts, S. Van Wyngaardt, S. T. Thanyani, G. Sekanka, A. M. C. Ten Bokum, L. A. Collett, J. Grooten, M. S. Baird, and J. A. Verschoor.** 2008. Cholesteroid nature of free mycolic acids from *M. tuberculosis*. *Chem Phys Lipids*. **152**: 95-103

-
- 162 **Thanyani S. T.** 2005. A novel application of affinity biosensor technology to detect antibodies to mycolic acid in tuberculosis patients. MSc. dissertation. Faculty of Natural and Agricultural Sciences. University of Pretoria
- 163 **Brown R. M.** 2003. Lipoarabinomannan-Reactive human secretory immunoglobulin A responses induced by mucosal Bacille Calmette-Guérin vaccination. *J Infect Dis.* **187**: 513–517
- 164 **Okuda Y., R. Maekura, A. Hirotsu, S. Kitada, K. Yoshimura, T. Hiraga, Y. Yamamoto, M. Itou, T. Ogura, and T. Ogihara.** 2004. Rapid serodiagnosis of active pulmonary *Mycobacterium tuberculosis* by analysis of results from multiple antigen-specific tests. *J Clin Microbiol.* **42**: 1136–1141
- 165 **Sousa A. O., A. Wagnier, Y. Poinson, N. Simonney, F. Gerber, F. Lavergne, J. L. Herrmann, and P. H. Lagrange.** 2000. Kinetics of circulating antibodies, immune complex and specific antibody-secreting cells in tuberculosis patients during 6 months of antimicrobial therapy. *Tubercle Lung Dis.* **80**: 27–33
- 166 **Boggian K., W. Fierz, and P. L. Vernazza.** 1996. Infrequent detection of lipoarabinomannan antibodies in human immunodeficiency virus-associated mycobacterial disease. Swiss HIV Cohort. *J Clin Microbiol.* **34**: 1854-1855
- 167 **Gustafson I.** 2003. Phospholipid membranes in biosensor applications. PhD thesis. Department of Biochemistry. Umea University. Sweden
- 168 **Brian A. and H. McConnel.** 1984. Allogeneic stimulation of cytotoxic T cells by supported planar membranes. *PNAS.* **81**: 6159-6163
- 169 **Puu G. and I. Gustafson.** 1997. Planar lipid bilayers on solid supports from liposomes-factors of importance for kinetics and stability. *Biochim Biophys Acta.* **1327**: 149–16
- 170 **Dimitrova M. N., H. Matsumura, N. Terezova, and V. Neytchev.** 2001. Binding of globular proteins to lipid membranes studied by isothermal titration calorimetry and fluorescence. *Colloids Surf. B.* **24**: 53-61
- 171 **Ibdah J. A. and M. C. Phillips.** 1988. Effects of lipid composition and packing on the adsorption of apolipoprotein A-I to lipid monolayers. *Biochem.* **27**: 7155-7162

-
- 172 **Nicholson J. P., M. R. Wolmerans, and G. R. Park.** 2000. The role of albumin in critical illness. *Br J Anaesth.* **85**: 599-610
- 173 **Ledford A. S., R. B. Weinberg, V. R. Cook, R. R. Hantgan, and G. S. Shelness.** 2006. Self-association and lipid binding properties of the lipoprotein initiating domain of apolipoprotein B. *J Biol Chem.* **281**: 8871-8876
- 174 **Eliasson M., R. Andersson, A. Olsson, H. Wigzell, and M. Uhlen.** 1989. Differential IgG-binding characteristics of staphylococcal protein A, streptococcal protein G, and a chimeric protein AG. *J Immunol.* **142**: 575-581
- 175 **Vermaak Y.** 2005. Properties of anti-mycolic acid antibodies in human tuberculosis patients. MSc dissertation. Department of Biochemistry in the faculty of Natural and Agricultural Sciences. University of Pretoria. Pretoria
- 176 **Sepälä I., M. Kaartinen, S. Ibrahim, and O. Makela.** 1990. Mouse IgG coded by Vh families S107 or J606 bind to Protein A. *J Immunol.* **145**: 2989-2993
- 177 **Ey P.L., E. P Prowse, and S. J. Jenkins.** 1978. Isolation of pure IgG1, IgG2a, and IgG2b immunoglobulins from mouse serum using protein A-Sepharose. *Immunology.* **15**: 429
- 178 **Liang M., S. L. Klakamp, C. Funelas, H. Lu, B. Lam, C. Herl, A. Umble, A. W. Drake, M. Pak, N. Ageyeva, R. Pasumarthi, and L. K. Roskos.** 2007. Detection of high- and low-affinity antibodies against a human monoclonal antibody using various technology platforms. *Assay and Drug Development Technologies.* **5**: 655-661
- 179 **Goding J. W.** 1978. Use of staphylococcal protein A as an immunological reagent. *J Immunol Methods.* **20**: 241-253
- 180 **Klasen I. S., J. H. C. Göertz, G. A. S. van de Wiel, C. M. R. Weemaes, J. W. M van der Meer, and J. P. H. Drenth.** 2001. Hyper-Immunoglobulin A in the Hyperimmunoglobulinemia D Syndrome. *Clin Diagn Lab Immunol.* **8**: 58-61
- 181 **Arakawa T., J. S. Philo, K. Tsumoto, R. Yumioka, and D. Ejima.** 2004. Elution of antibodies from a Protein-A column by aqueous arginine solutions. *Protein Expr Purif.* **36**: 244-248

-
- 182 **Ejima D., R. Yumioka, K. Tsumoto, and T. Arakawa.** 2005. Effective elution of antibodies by arginine and arginine derivatives in affinity column chromatography. *Anal Biochem.* **345**: 250–257
- 183 **Wang J., H. Qiang, C. Zhang, X. Liu, D. Chen, and S. Wang.** 2003. Detection of IgG-bound lipoprotein (A) immune complexes in patients with coronary heart disease. *Clin Chim Acta.* **327**: 15–122
- 184 **Pangborn M.** 1941. A new serologically active phospholipid from beef heart. *Proc Soc Exp Biol Med.* **48**: 484-486
- 185 **Kolb C., R. Di Pauli, and E. Weiler.** 1974. Induction of IgG by Lipid A in the newborn mouse. *J Exp Med* **139**: 467-478
- 186 **Asselineau J. and E. Lederer.** 1951. The constitution of the mycolic acids from two virulent *Mycobacterium tuberculosis* human strains. *Biochem Biophys Acta.* **7**: 126-145
- 187 **Minnikin D. E., S. M. Minnikin, and G. Dobson.** 1983. Mycolic acid patterns of four vaccine strains of *Mycobacterium bovis* BCG. *J Gen Microbiol.* **129**: 889-891
- 188 **Villeneuve M., M. Kawai, M. Watanabe, Y. Aoyagi, Y. Hitotsuyanagi, K. Takeya, H. Gouda, S. Hirono, D. E. Minnikin, and H. Nakahara.** 2007. Conformational behaviour of oxygenated mycobacterial mycolic acids from *Mycobacterium bovis* BCG. *Biochem Biophys Acta.* **1768**: 1717–1726
- 189 **Dinadayala P., F. Laval, C. Raynaud, A. Lemassu, M-A. Lanéelle, G. Lanéelle, and M. Daffé.** 2003. Tracking the putative biosynthetic precursors of oxygenated mycolates of *Mycobacterium tuberculosis*. *J Biol Chem.* **278**: 7310- 7317
- 190 **Laval F., M-A. Lanéelle, C. Deon, B. Monsarrat, and M. Daffé.** 2001. Accurate molecular mass determination of mycolic acids by MALDI-TOF Mass Spectroscopy. *J Anal Chem.* **73**: 4537-4544
- 191 **Watanabe M., A. Ohta, S. Sasaki, and D. E. Minnikin.** 1999. Structure of a new glycolipid from *Mycobacterium avium-Mycobacterium intracellulare* complex. *J Bacteriol.* **181**: 2293-2297
- 192 **Uenishi Y., Y. Fujita, N. Kusunose, I. Yano, and M. Sunagawa.** 2008. Comprehensive analysis of mycolic acid subclass and molecular species composition

-
- of *Mycobacterium bovis* BCG Tokyo 172 cell wall skeleton (SMP-105). *J Microbiol Methods*. **72**: 149-156
- 193 **Glynn J. R.** 1998. Resurgence of tuberculosis and the impact of HIV infection. *Br Med Bull*. **54**: 579-593
- 194 **Corbett E. L., C. J. Watt, N. Walke, D. Maher, B. G. Williams, M. C. Raviglione, and C. Dye.** 2003. The growing burden of tuberculosis. Global trends and interactions with the HIV epidemic. *Arch Intern Med*. **163**: 1009–1021
- 195 **Harries A. D., N. J. Hargreaves, J. Kemp, A. Jindani, D. A. Enarson, D. Maher, and F. M. Salaniponi.** 2001. Deaths from tuberculosis in sub-Saharan African countries with a high prevalence of HIV-1. *Lancet*. **357**: 1519–1523
- 196 **McMurray D.** 2001. Disease model: pulmonary tuberculosis. *Trends in Molecular Medicine*. **7**: 135-137
- 197 **Mendelson M.** 2007. Diagnosing tuberculosis in HIV-infected patients: challenges and future prospects. *Br Med Bull*. **81**: 149–165
- 198 **Sieling P. A., D. Chatterjee, S. A. Porcelli, T. I. Prigozy, R. J. Mazzaccaro, T. Soriano, B. R. Bloom, M. B. Brenner, M. Kronenberg, and P. J. Brennan.** 1995. CD1-restricted T cell recognition of microbial lipoglycan antigens. *Science*. **269**: 227–30
- 199 **Sosroseno W., P. S. Bird, E. Gemmell, and G. J. Seymour.** 2006. The role of CD4⁺ and CD8⁺ T cells on antibody production by murine Peyer's patch cells following mucosal presentation of *Actinomyces viscosus*. *Oral Microbiol Immunol*. **21**: 411–414
- 200 **Chmielowski B., R. Pacholczyk, P. Kraj, P. Kisielow, and L. Ignatowicz.** 2002. Presentation of antagonist peptides to naive CD4-T cells abrogates spatial reorganization of class II MHC peptide complexes on the surface of dendritic cells. *PNAS*. **99**: 15012-15017
- 201 **Mizusawa M., M. Kawamura, M. Takamori, T. Kashiya, A. Fujita, M. Usuzawa, H. Saitoh, Y. Ashino, I. Yano, and T. Hattori.** 2008. Increased synthesis of anti-tuberculous glycolipid immunoglobulin G (IgG) and IgA with cavity formation in patients with pulmonary tuberculosis. *Clin Vac Immunol*. **15**: 544–548

-
- 202 **Simonney N., P. Chavanet, C. Perronne, M. Leportier, F. Revol, J. L. Herrmann, and P. H. Lagrange.** 2007. B-cell immune responses in HIV positive and HIV negative patients with tuberculosis evaluated with an ELISA using a glycolipid antigen. *Tuberculosis*. **87**: 109–122
- 203 **Lawn S. D., E. H. Frimpong, and E. Nyarko.** 2004. Evaluation of a commercial diagnostic kit incorporating lipoarabinomannan in the serodiagnosis of pulmonary tuberculosis in Ghana. *Trop Med Int Health*. **2**: 978-981
- 204 **Turner M., J. P. Van Vooren, J. Nyabenda, F. Legros, A. Lecomte, J. Thiriaux, E. Serruys, and J. C. Yernault.** 1988. The humoral immune response after BCG vaccination in humans: Consequences for the serodiagnosis of tuberculosis. *Eur Respir J*. **1**: 589-593
- 205 **Goodfellow M. and D. E. Minnikin (eds.).** 1985. Chemical methods in bacterial systematics. Academic press. London. 237-262
- 206 **Hawkins C. C., J. W. Gold, E. Whimbey, T. E. Kiehn, P. Brannon, R. Cammarata, A. E. Brown, and D. Armstrong.** 1986. *Mycobacterium avium* complex infections in patients with the acquired immunodeficiency syndrome. *Ann Intern Med*. **105**: 184-188
- 207 **Gatfield J. and J. Pieters.** 2000. Essential role for cholesterol in entry of mycobacteria into Macrophages. *Science*. **288**: 1647-1650
- 208 **De Chastellier C. and L. Thilo.** 2006. Cholesterol depletion in *Mycobacterium avium*-infected macrophages overcomes the block in phagosome maturation and leads to the reversible sequestration of viable mycobacteria in phagolysosome-derived autophagic vacuoles. *Cell Microbiol*. **8**: 242–256
- 209 **Van der Geize R., K. Yam, T. Heuser, M. H. Wilbrink, H. Hara, M. C. Anderton, E. Sim, L. Dijkhuizen, J. E. Davies, W. W. Mohn, and L. D. Eltis.** 2007. A gene cluster encoding cholesterol catabolism in a soil actinomycete provides insight into *Mycobacterium tuberculosis* survival in macrophages. *PNAS*. **104**: 1947–1952
- 210 **Ordway D., M. Henao-Tamayo, I. M. Orme, and M. Gonzalez-Juarrero.** 2005. Foamy macrophages within lung granulomas of mice infected with *Mycobacterium*

tuberculosis express molecules characteristic of dendritic cells and anti-apoptotic markers of the TNF receptor-associated factor family. *J Immunol.* **175**: 3873–3881

- 211 **Horváth A., D. Bánhegyi, A. Bíró, E. Ujhelyi, A. Veres, L. Horváth, Z. Prohászka, A. Bácsi, V. Tarján, L. Romics, I. Horváth, F. D. Tóth, G. Füst, and I. Karádi.** 2001. High level of anti-cholesterol antibodies (ACHA) in HIV patients. Normalization of serum ACHA concentration after introduction of HAART. *Immunol.* **203**: 756-768